Dynamic Operation of an Integrated Direct Air Capture and CO_2 Compression System

Kunal Vidyarthi

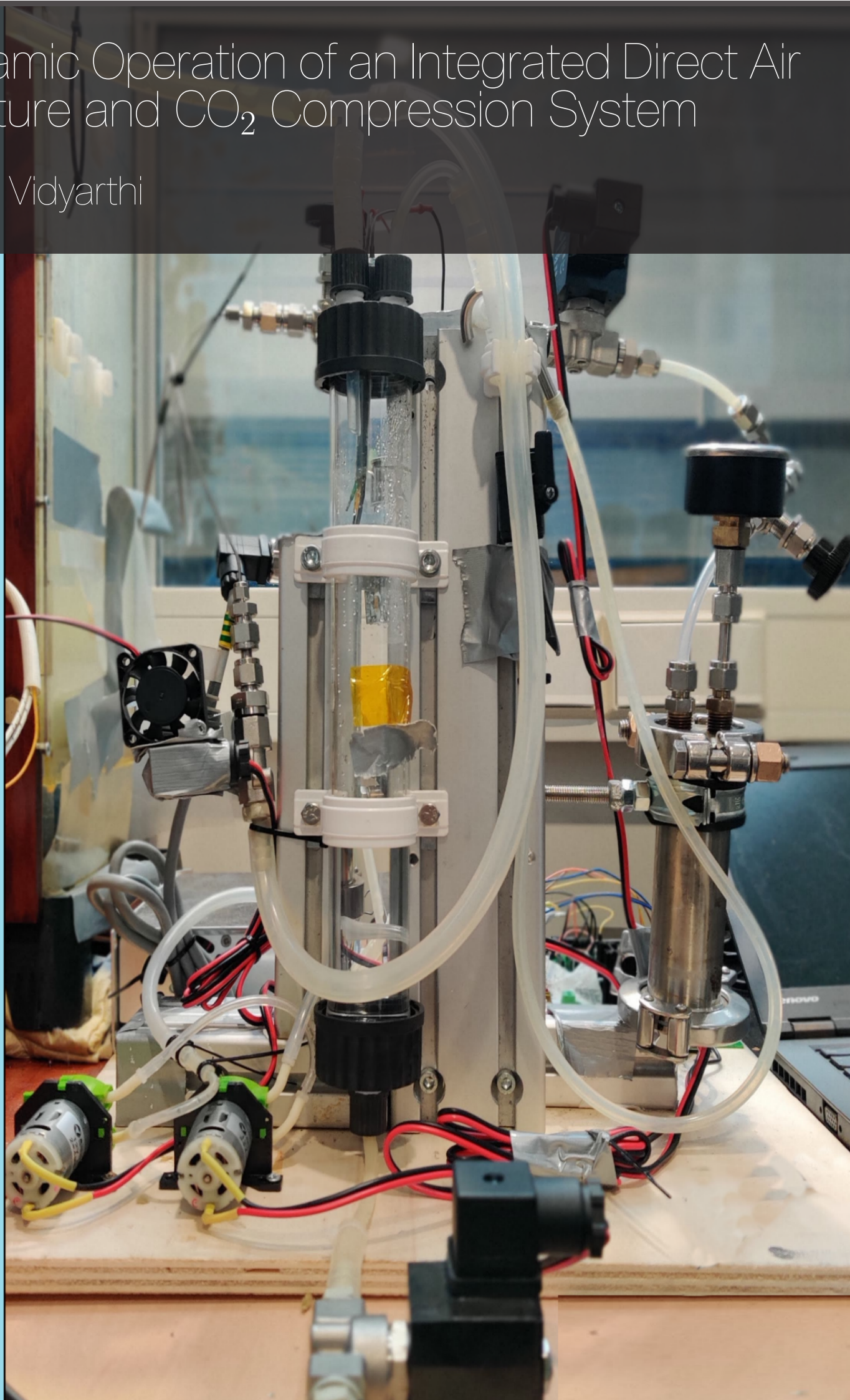

Delft University of Technology

Dynamic Operation of an Integrated Direct Air Capture and CO_2 Compression System

by

Kunal Vidyarthi

to obtain the degree of Master of Science at the Delft University of Technology, to be defended publicly on August 26, 2022 at 09:00 AM.

Student Number:	5351502
Project Duration:	December 2021 - August 2022
Supervisor:	Prof. dr. ir. E Goetheer, TU Delft
Daily Supervisor:	Ir. M. Sinha, ZEF BV
Thesis committee:	Prof. dr. ir. E Goetheer, TU Delft, Chairman Prof. dr. ir. W De Jong, TU Delft Dr. H.B Eral, TU Delft Ir. M. Sinha, ZEF BV

TU Delft

Abstract

CO_2 concentration in the atmosphere has soared since the industrial era owing to the rapid and unabated increase in fossil fuel consumption globally. This has resulted in an increase in global average temperature by $\approx 1.1\ ^{o}C$ in this period; and has sparked the concern of climate disaster events across the globe. In order to tackle the issue of climate change, research into Carbon dioxide removal (CDR) technology such as Carbon Capture and Storage (CCS) and Carbon Capture and Utilization (CCU) has gained prominence.

Zero Emission Fuels (ZEF) B.V is a technology startup based in Delft, working on the CCU pathway for CDR. ZEF is developing micro plants to capture CO_2 and H_2O from the atmosphere using Direct Air Capture (DAC) system. The captured CO_2 is then compressed to 50bar using compressor system (FM) while H_2O is split electro-chemically to H_2 at 50bar. This high pressure CO_2 and H_2 are then used to produce methanol. The energy for the whole process is derived from the sun, making the entire process sustainable and emission free.

ZEF's micro-plant will derive its raw materials i.e. CO_2 and H_2O, from the environment. Thus, variation in the environmental conditions, i.e., humidity, temperature and solar radiation (external disturbances for the system), will affect the overall system output. Current work focused on design of control scheme for the integrated DAC and CO_2 compression system, which will be able to meet ZEF's performance target. The effect of variation in solar radiation was not considered for this work.

At first the performance parameters for the various sub-systems of integrated DAC+FM system were identified. With this information, the operating scenarios and the process constraints for the system were identified.

Then, models for the sub-systems of the DAC and compressor system, i.e., Absorber, sump, desorber, flash tank and compressor system were developed. Parts of the model, i.e., the desorber and flash tank, were validated using experimental setup developed by integrating the existing DAC prototype at ZEF with a representative compression system.

The main target of the experimental setup was to develop control scheme to maintain the pressure of the flash tank to required target levels. Through multiple iterations, the final layout and control system for the integrated setup was identified which was able to control the pressure of the flash tank at the target level.

Finally, a control scheme for DAC production control was developed based on the steady-state output from the desorber model. Through this, the feed and power (heat) input to the desorber is varied to control the production of CO_2 and H_2O.

The system model developed as part of this work can be further used as a tool by ZEF to integrate different sub-systems, test the performance of different sorbents, and assess the viability of different control schemes for the integrated system.

Acknowledgement

It feels surreal to be writing this with the realization that a journey that began with a set of happy coincidences, is finally reaching its conclusion. This journey of the past 2 years at TU Delft has been humbling, and enriching and has helped me rediscover the joy of learning. I have grown immensely during my time at Delft and none of this would have been possible without the help and support of the people who made this possible, to quote Sir Isaac Newton:

"If I have seen further it is by standing on the shoulders of Giants"

First and foremost, I would like to thank ZEF for giving me the opportunity to work on my thesis in such an amazing and inspiring workplace. The 1 year I spent here is going to be the most cherished memory of my entire MSc and I will forever be grateful for this opportunity.

I would like to thank Dr. Earl Goetheer for being my supervisor and thesis chair. Your support and encouragement throughout the project were immensely helpful. Thanks for being patient with me and always reminding me to look at the bigger picture. I would also like to thank the thesis committee members for taking the time to assess my work.

Also, this work would have not been possible without support and guidance from Jan van Kranendonk and Mrigank Sinha. Jan is probably the best engineer and problem solver I have and will ever come across and the only thing that surpasses your knowledge is your humility. Thanks for always answering my questions with so much patience and having faith in me even when I lacked self-belief.
Mrigank's work ethic, formidable knowledge, and the energy he brings to every task are awe-inspiring and his positive attitude rubs off on you. I am really happy I got the opportunity to work and interact with you almost daily through this project. Thanks for being an amazing mentor and for your motivating "short speeches" which pushed me to keep striving for more during the thesis.

Ulrich Starke, Paul Vroegindeweij Faculty: and Hessel Jongebreur. I would like to thank all of you for making me feel a part of the ZEF team. Friday evening drinks and chat were always great and made the whole thesis phase a lot more fun and memorable.

I would like to give a special shout-out to my ZEF thesis buddies Alex and Blas for their constant support and encouragement. Our daily interactions, coffee breaks, after-office drinks, and especially the Utrecht and Ijsselstein trip will always be special for me. I would also like to thank all the students, I worked with at ZEF for making the ZEF a place where everyone comes together and "get it done".

I would also like to thank my whole family. Your support and love have shaped me into what I am today. Finally and most importantly I want to thank Pooja, who joined me on this journey to the unknown. Your presence is what makes everything worth it.

Kunal Vidyarthi
Delft, August 2022

Contents

Nomenclature

Abbreviations

Abbreviation	Definition
AEC	Alkaline Electrolysis
AMP	Adenosine monophosphate
CAT	Climate Action Tracker
CCS	Carbon Capture and Storage
CCU	Carbon Capture and Utilisation
DAC	Direct Air Capture
DEA	Diethanolamine
DS	Distillation
FM	Fluid Machinery
MEA	Monoethanolamine
MTZ	Mass Transfer Zone
MS	Methanol Synthesis
PEG	Polyethylene glycol
PV	Photo-Voltaic
RH	Relative Humidity
rpm	rotations per minute
STY	Space Time Yield
TEPA	Tetraethylenepentamine
VLE	Vapour Liquid Equilibrium
ZEF	Zero Emission Fuels

Symbols

Symbol	Definition	Unit
c	Number of components in the mixture	[-]
c_{gas}	Solubility of gas	[mol m^{-3}]
D	Diffusivity	[m^2 s^{-1}]
$\frac{d_{ca}}{dz}$	molar concentration gradient	[mol m^{-4}]
F	Feed flow rate into DAC Flash Tank	[mol s^{-1}]
f	Number of degrees of freedom	[-]
f_{leak}	Leakage factor	[-]
g	Acceleration due to gravity	[ms^{-2}]
h	height of fluid	[m]
H_{gas}	Henry's constant	[Pa]
J	Diffusion Flux	[mol m^{-2} s^{-1}]
L	Vapour flow rate out of DAC Flash Tank	[mol s^{-1}]
k_B	Boltzmann Constant	[J K^{-1}]
K	Ratio of y_i and x_i	[-]
$\dot{m}_{des}$	Mass flow into desorber	[kg s^{-1}]
$\dot{m}_{cmpr}$	Compressor mass flow rate	[kg s^{-1}]
mw_{suction}	Molecular mass of fluid at suction	[kg mol^{-1}]
$\dot{n}_{cmpr}$	Compressor mole flow rate	[mol s^{-1}]
N_{rpm}	Compressor speed	[rpm]
P	Pressure	[Pa]
P_{Tot}	Total system pressure	[Pa]

Symbol	Definition	Unit
p	Number of phases in co-existence	[-]
P_d	Compressor discharge Pressure	[Pa]
p_{gas}	Partial pressure of gas	[Pa]
P_i^{sat}	Saturation Pressure	[Pa]
P_s	Compressor suction Pressure	[Pa]
Q_{sens}	Sensible Heat	[W]
r	Radius of spherical particle	[m]
T	Temperature	[K]
T_{abs}	Temperature of rich sorbent entering desorber from absorber	[K]
T_{des}	Desired Temperature of desorber	[K]
V	Liquid flow rate out of DAC Flash Tank	[mol s^{-1}]
$\dot{V}_{cmpr}$	Compressor volume flow rate	[m^3 s^{-1}]
V_{cc}	Cubic capacity of compressor	[m^3]
x_i	Mass fraction of component i in liquid phase	[-]
y_i	Mass fraction of component i in gas phase	[-]
z_i	Mass fraction of component i in feed inlet to DAC Flash Tank	[-]
η_{cmpr}	Compressor efficiency	[-]
η_{vol}	Volumetric efficiency	[-]
μ	Dynamic viscosity	[Pa-s]
ρ	Density of fluid	[kg m^{-3}]
ρ_{suction}	Density of fluid at compressor suction	[kg m^{-3}]
γ_c	Polytropic coefficient	[-]
γ_i^L	Liquid Activity coefficient	[-]
ϕ_i^V	Fugacity co-efficient	[-]

Molecular Structure

Abbreviation	Definition
CO_2	Carbon Dioxide
CH_3OH	Methanol
H_2	Hydrogen
H_2O	Water
KOH	Potassium Hydroxide
LiCl	Lithium Chloride
NOx	Nitrogen oxides
O_2	Oxygen
SOx	Sulphur Oxides

List of Figures

List of Tables

1 Introduction

In this chapter, the issue of global warming and climate change is briefly explained including the major causes and their consequences. This is followed by short description of some mitigation strategies and through them the motivation for this thesis is discussed. Lastly, the research objectives and scope is defined and the chapter concludes with the research methodology and outline.

1.1. Climate Change

Earth's climate has undergone many changes throughout its history with alternating periods of cold and hot weather. This cyclic change which occurs over time scale spanning thousands of years is attributed to small changes in earth's orbit which affects how much solar radiation earth receives[1]. However, since the late 18^{th} century, there has been constant warming up of earth's atmosphere and the rate of increase is unprecedented [2]. This rise in global temperatures, has altered the earth's climate adversely resulting in warming up of land, air and oceans. Apart from global warming, other catastrophic events such as shrinking of glacial ice covers, ocean acidification and extreme weather events are also being observed more frequently all around the globe.

There is unequivocal evidence that this rise in temperature is directly linked to increase in greenhouse gas emissions with CO_2 being the major contributor[3]. The same is shown in Figure [1.1a] and [1.1b] below.

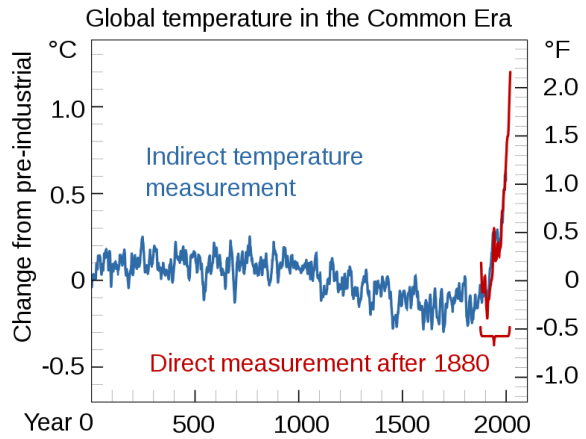

(a) Global Temperature Rise [2]

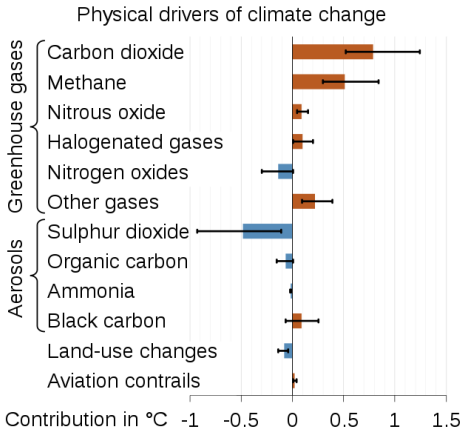

(b) CO_2 is the main driver of climate change [3]

Figure 1.1: Climate Change and contribution of CO_2

1.2. Combating Climate Change

In the last decade, since the effects and threat of global warming has become more and more evident, global concerted efforts to tackle the issue have gained momentum. Paris Climate accord was the landmark agreement signed by 192 countries in 2015 [4], where the countries around the globe pledged

to take concrete steps to limit the temperature rise to 1.5^{o}C as compared to pre-industrial levels. As per this agreement, a reduction in CO_2 emissions by 45% to 2010 level will be accomplished by 2030, followed by a net zero CO_2 emission target by 2050.

1.2.1. Mitigation

In order to meet the Paris Agreement targets, a plethora of technology needs to deployed concurrently. Carbon Dioxide Removal(CDR) or Carbon Capture, is one such technology which can gained a lot of popularity in the recent years.

- **Carbon Capture Technology**
  - **Carbon Capture and Storage (CCS)** involves capturing CO_2 and then transporting & storing it at suitable geological location such as underground pits or ocean beds so that it doesn't re-enter the atmosphere.
  - **Carbon Capture and Utilisation (CCU)** involves converting the captured CO_2 into other useful products such as fuel or raw material for other chemical process. Synthesis of Methanol, linear and cyclic carbonates, carboxylic acid etc., are some of the popular applications of captured CO_2 [5].

Recent study by Kleijne et al.[6] has showed that very few CCU technologies are currently compatible with requirements of Paris climate accord. Although CO_2 captured in CCU and CCS are same, the emissions involved in CCS are lower than most CCU technologies, because the CO_2 captured by CCU is ultimately released back (at different time scales depending on product). The main takeaway from this study is that for CCU domain, focus should be on the development of technology which can achieve net zero carbon emissions.

Direct Air Capture (DAC) coupled with utilisation and powered by renewable energy is one potential solution which checks all the boxes for an ideal carbon capture technology. The current thesis, being undertaken at Zero Emission Fuels (ZEF) will focus in this direction.

1.3. Zero Emission Fuels (ZEF) B.V

ZEF is working on developing modular chemical plants which will take up CO_2 and H_2O from the atmosphere and convert it into Methanol using solar energy.

The ZEF micro-plant is split into 5 sub-system as shown in Figure 1.2 below:

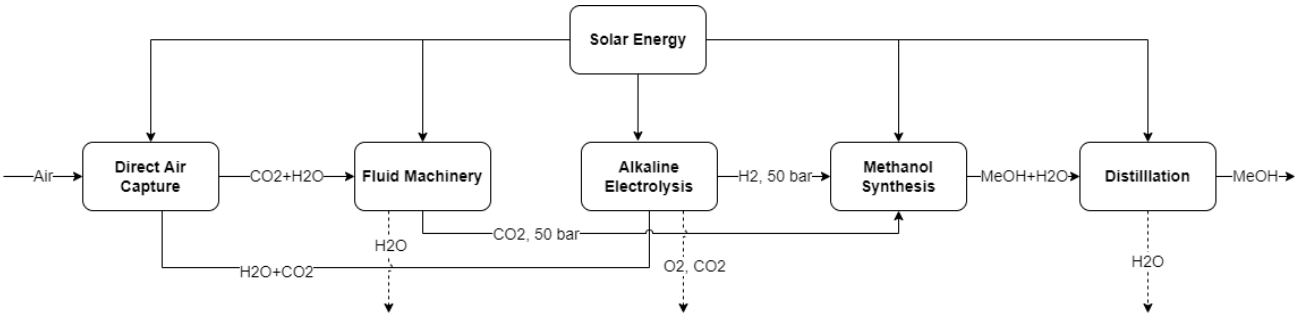

Figure 1.2: ZEF: Micro Plant

The current thesis pertains to designing a control system for dynamic, safe and efficient operation of the DAC+FM system. In the next section, the performance specifications for the DAC and FM system is discussed which will give an insight into the research objectives for the project.

1.3.1. Direct Air Capture System

The main goal at ZEF is to develop micro-plants capable of producing 2000g of methanol/day. However, the system being powered through Solar power has an inherent limitation of intermittent power availability of $\sim$ 7 sun-hours per day.

After extensive research on multiple DAC configurations, ZEF has developed an absorption based continuous DAC process using liquid amine as sorbent. The current system has two main sections, absorber and desorber. In the absorber, air flows counter-current to vertically falling liquid amine sorbent through which CO_2 and H_2O are absorbed in the sorbent. This sorbent then goes to the desorber column, where it is heated up to release the captured CO_2 and H_2O. The desorbed sorbent is recycled back to the absorber to complete the continuous process. Figure 1.3 shows a representative schematic of the current DAC system at ZEF.

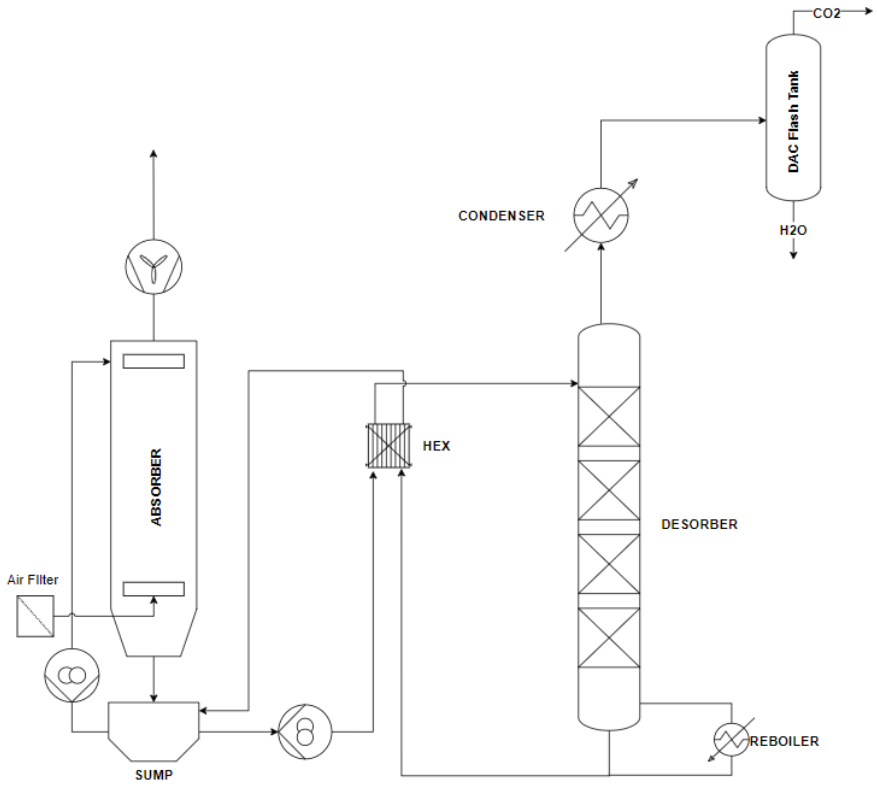

Figure 1.3: Schematic of DAC setup at ZEF

The desorbed CO_2 and H_2O from the desorber, then go to the DAC Flash tank. In the flash tank, the CO_2 leaves at the top as vapour and goes to the FM, while the liquid H_2O goes to the AEC sub-system.

For the Methanol synthesis reaction 1.1, to produce 1 mol of Methanol, 1 mole of CO_2 and 3 mole of H_2 is required. While the electrolysis of 1 mol H_2O 1.2, produces 1 mol H_2. This forms the target for CO_2 and H_2O to be captured by the DAC system 1.1.

$$CO_2 + 3H_2 \rightleftharpoons CH_3OH + H_2O \tag{1.1}$$

$$2H_2O(l) \rightarrow O_2(g) + 4H^+(aq) + 4e^- \tag{1.2}$$

Product Specification

The target performance specifications for the ZEF DAC sub-system are given in Table 1.1:

Table 1.1: DAC Design Specification

Parameter	Design Specification		Remarks
Methanol Production	2000 g/day	62.5 mol/day	ZEF Target
Production Rate of CO_2	2750 g/day	62.5 mol/day	For 2000g Methanol production
Production Rate of H_2O	3375 g/day	187.5 mol/day	
Optimum CO_2:H_2O ratio	1:3		Ratio of CO_2:H_2O
Desorber Operating Pressure	Atmospheric Pressure ($\sim$ 1bar)		Operation at atmospheric condition
Desorber Operating Temperature	≤ 120 °C		Sorbent thermal degradation limits
Energy consumption	<400 kJ/mol CO_2*		ZEF Target

*The current energy target for CO_2 capture at ZEF is comparable to existing DAC technology across the globe. Climeworks and Global Thermostat are DAC companies that use solid sorbent-based DAC systems. The energy consumption per mol of CO_2 captured, is $\sim$ 360kJ and $\sim$ 250 kJ for Climeworks and Global Thermostat respectively [7],[8]. Carbon Engineering, on the other hand, uses a liquid sorbent (KOH) DAC system which consumes $\sim$300 kJ energy for every mol of CO_2 captured [9].

1.3.2. Fluid Machinery System

FM sub-system at ZEF performs two main functions, dehumidification of CO_2 stream and compression of dried CO_2 to 50 bar. A schematic representation of the FM sub-system at ZEF is shown in Figure [1.4] below (in the figure only 1 compressor is shown, although in the final design more than 1 compressor may be implemented):

Dehumidification :
CO_2 captured through the DAC sub-system is sent to the FM section through the DAC Flash tank. This CO_2 stream can contain a significant fraction of water (up to $\sim$ 5% depending on operating temperature [10]), which can be detrimental to the lifetime of pipelines, compressors, and lubricants used in compressors. Currently, the drying system based on cooling separation and silica gel-based adsorption separation is under investigation at ZEF. Based on the results of prototype testing the final configuration will be decided.

Compression System:
The dried CO_2 stream is then sent to the compressor system, which compresses it to the pressure of 50-55 bar. The compressed CO_2 is stored in the buffer tank, through which it is supplied to the MS sub-system.

The target performance specifications for the ZEF FM sub-system and specifications for the compressor being used at ZEF are given in Table 1.2 and 1.3 below:

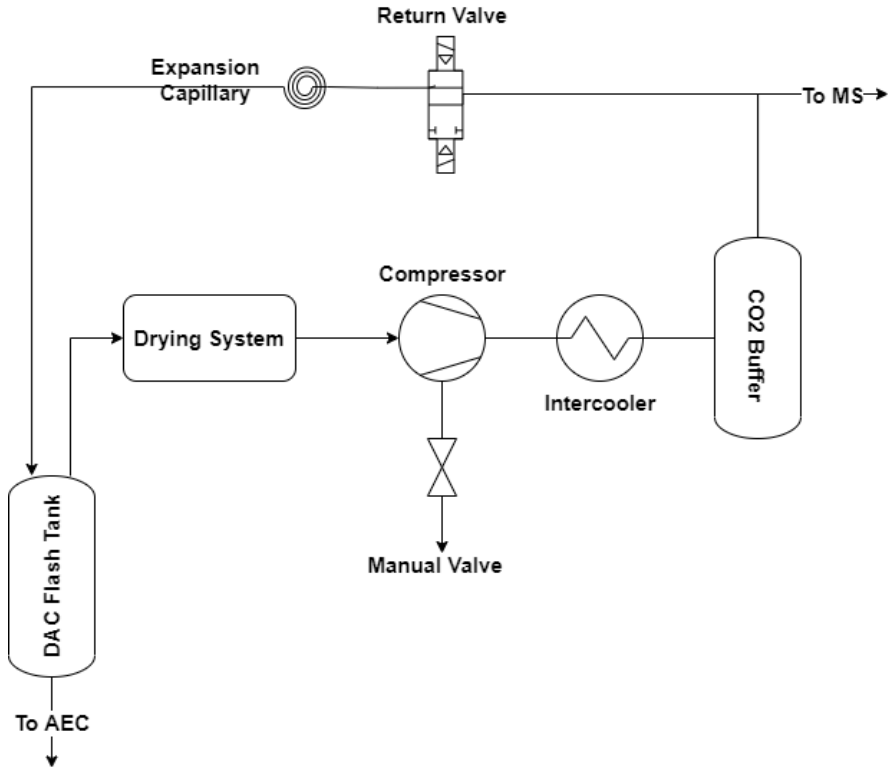

Figure 1.4: Schematic of FM sub-system at ZEF

Table 1.2: FM Design Specification

Parameter	Design Specification	Remarks
CO_2 Flow rate	2750 g/day	ZEF Target
CO_2 Pressure	50 bar	ZEF Target
Water Content	<2% RH	Lubricant Safety requirement
Energy consumption: Compression	<1.06 MJ/kg CO_2	ZEF Target

Table 1.3: Compressor specification

Parameter	Description	Value	Unit
$\mathbf{V}_{cmpr}$	Compressor Cubic Capacity	2.8E-6	[$m^3 stroke^{-1}$]
$\mathbf{N}_{min}$	Minimum compressor speed	1800	[rpm]
$\mathbf{N}_{max}$	Maximum compressor speed	4500	[rpm]

1.4. Aim of the Thesis

The main objectives of the thesis can be split into the following parts:

- Identification of parameters that will affect the input and performance of the integrated DAC+FM system at ZEF.
- Identification of operating scenarios and the associated process constraints for the integrated system.
- Developing a model and simulation environment for the integrated system to design control schemes for efficient operation of the system.
- Experimentally validate the identified control schemes on the integrated experimental setup being developed at ZEF.

1.5. Research Questions

The main research question for the thesis is as below:

1. ***What is the optimum control strategy for the operation of DAC+FM system which meets the ZEF's requirements?***

   In order to answer this research question, the following sub-questions were identified which will help answer the main research question.

   (a) What parameters influence the performance of the DAC+FM system and their effect on each sub-system?

   (b) What control strategies can be used to ensure ZEF target performance levels are met for the operating scenarios identified above?

   (c) What is the optimum control strategy for the operation of the DAC+FM system which meets the ZEF's requirements?

1.6. Thesis Approach

1.6.1. Research Scope

The field of DAC and work being done at ZEF is novel and thus the research areas can be endless. Hence it is essential to define the scope of this research.

- The control schemes developed will focus on the dynamic behaviour of DAC and FM sub-system only and the effect on other sub-systems will not be considered.
- The technology to be used for the drying system for CO_2 captured by the DAC system is still evolving at ZEF. Hence for this thesis, the effects and dynamics of the drying system will not be covered. Further, for the integrated system model which will be developed as part of this thesis, the CO_2 captured by the DAC system will be assumed to be completely dry before it enters the compression system.
- ZEF's DAC desorber section will be operating at atmospheric pressure. Hence control schemes involving pressure control of DAC section will be limited to atmospheric pressure.
- The sorbent used in DAC system is determined by sorbent selection team at ZEF to meet the performance targets. The sorbent used for the system modelling and experimental validation will use the composition decided by ZEF. Similarly, the Compressor system used for CO_2 compression, will be decided by ZEF and their selection will not be a part of the thesis.
- For this work, the impact of variation in solar power on system dynamics has not been covered.

- Lifetime and cost analysis of the system will not be covered in this thesis.

1.6.2. Methodology

The thesis approach is depicted in 1.5. In order to design a control scheme for efficient operation under dynamic operating conditions, it was necessary to first understand the unit operation of each part of the sub-systems. To this end, a review of existing literature was done for liquid amine-based Direct Air Capture systems and CO_2 compression system.

Through this literature review the first research question will be answered and the necessary background knowledge for modelling the integrated system will be acquired.

Post this, modelling and setting up the workable simulation model of the integrated system will be done. For this, a model of individual sub-components will be made on SIMULINK and the same will be then integrated to get the final model. This work will be used to answer the second research question and will also help to design the experiments to validate the developed model.

The experiments to validate the integrated model will be performed. Once the model is validated, then system performance through the model will be simulated for the dynamic operating conditions and through this control schemes will be developed.

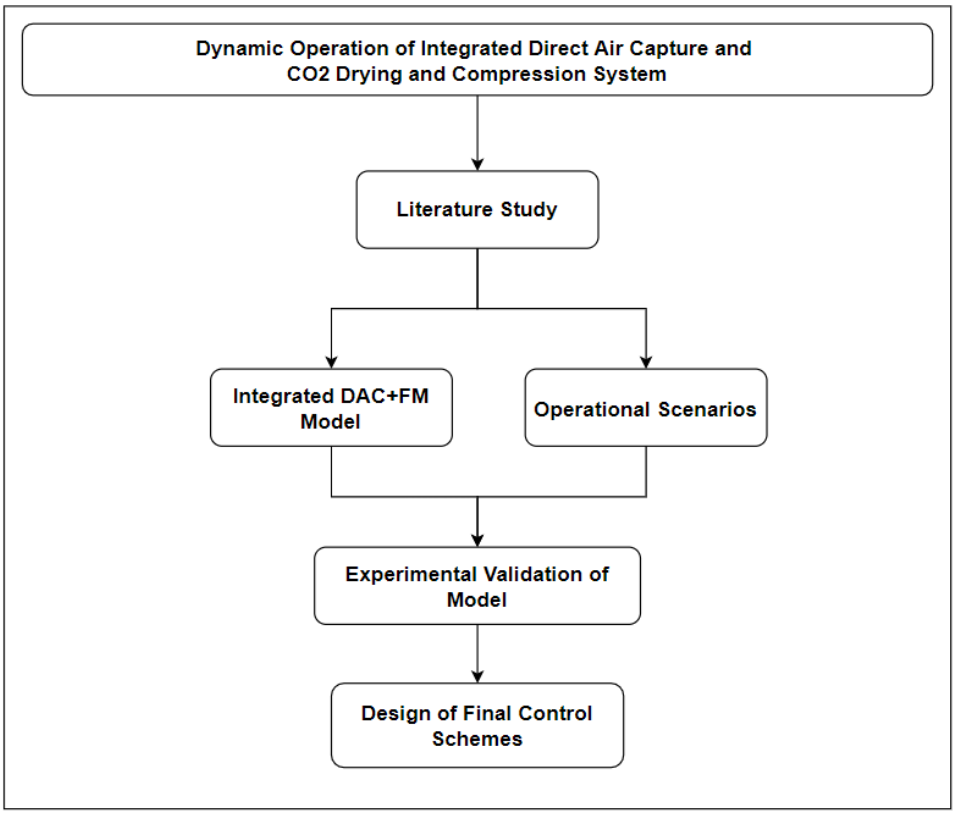

Figure 1.5: Thesis Overview

2

Background

This chapter covers the background information which was required to bring the entire project to its fruition. In the first section, an overview of carbon capture technology is provided which is followed by description of DAC in the next section. In the next section, Dehumidification system is discussed, which includes drying requirement for the system, CO_2 drying technologies and lastly rolling piston compressors, their working, dynamics and modelling requirements are discussed.

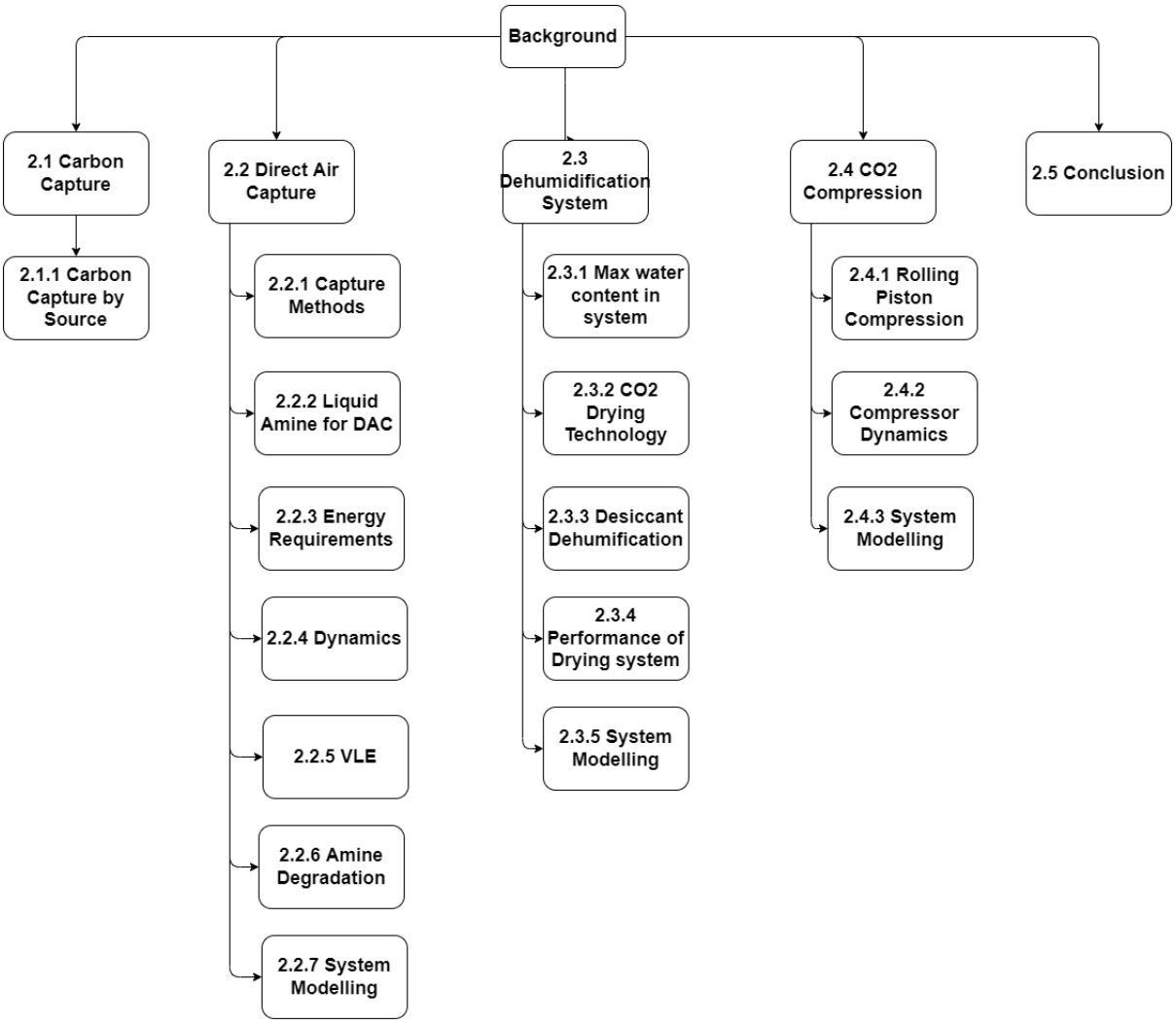

Figure 2.1: Schematic of the Background chapter

2.1. Carbon Capture

Carbon capture technologies can be sub-divided on the basis of source of carbon capture and the end use of the captured carbon. The latter was discussed in section 1.2.1. On the basis of source of carbon capture, it can be classified into two broad areas as shown in Figure [2.2] below. The current thesis will focus on the DAC technology.

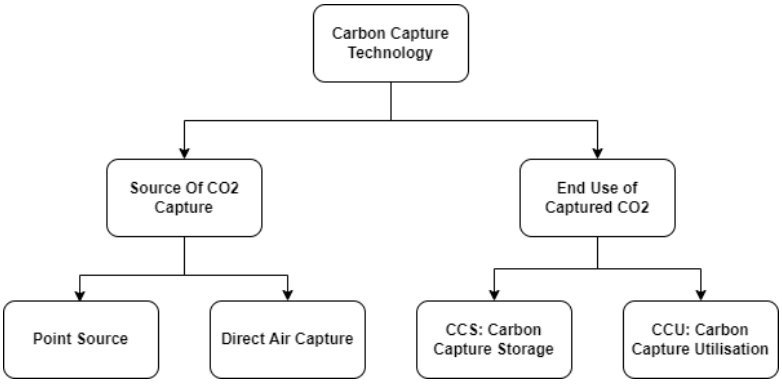

Figure 2.2: Carbon Capture Technology can be classified into Point source and Direct Air Capture on the basis of source of Carbon Capture

Point source carbon capture involves capturing CO_2 directly from the source of emission, where the concentration of CO_2 in flue gases is high ($\sim$ 10-15%). This makes the overall process less energy intensive than DAC technology where concentration of CO_2 is very low. [11]. However, point source capture technology cannot capture CO_2 from distributed sources such as transport, buildings etc., which contributes $\sim$ 52% to total global emissions.

2.2. Direct Air Capture

Direct Air Capture (DAC) removes CO_2 directly from the atmosphere and enables CO_2 capture irrespective of the source of emission. However, the low concentration of CO_2 in air ($\sim$0.04%) makes it challenging to develop an economical DAC process which can ensure high CO_2 capture.

2.2.1. Carbon Capture Method

The most prominent methods for direct air capture of CO_2 are Adsorption and Absorption. However, the most efficient method can vary based on scale of emission, pressure, temperature etc.,[12]. The same is shown in Figure [2.3] below.

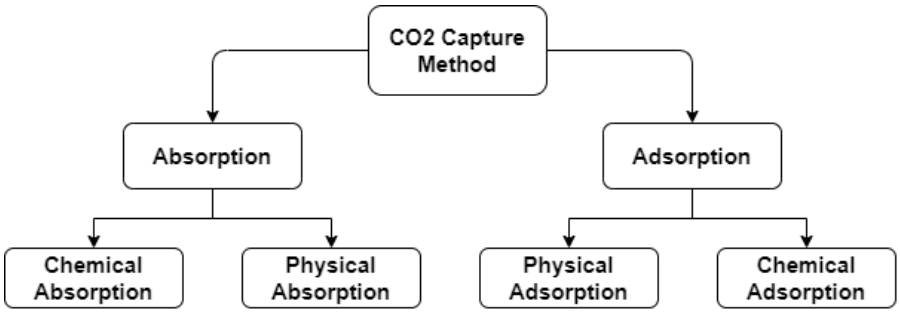

Figure 2.3: CO2 separation Methods

Most DAC technology are based on chemical absorption or adsorption to capture CO_2. Atmospheric

air is made to flow through sorbents usually impregnated with amines or other sorbents which can capture CO_2. DEA (Diethanolamine), KOH (Potassium Hydroxide) etc., are some of the commonly used sorbents used in DAC systems across the globe [7].

DAC technology based on chemical absorption can be further sub-divided into two main groups based on the type of sorbent being used as shown in Figure [2.4] below. Current work will focus on liquid amine based chemical absorption system for capture of CO_2 from atmosphere.

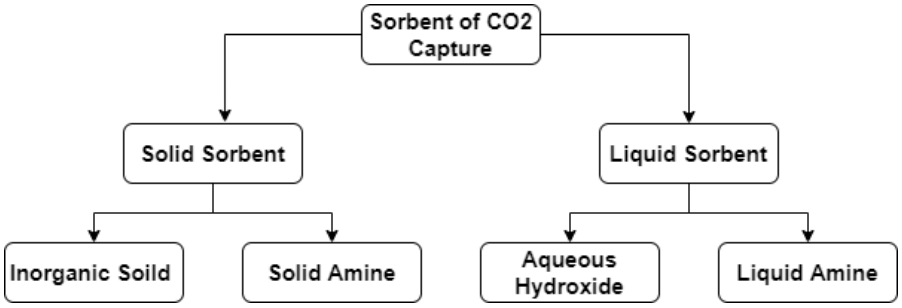

Figure 2.4: Sorbent used for Carbon capture can be further classified into Solid and Liquid Sorbents

2.2.2. Liquid Amines for Carbon Capture

Amines are organic derivatives of ammonia. They are classified as primary, secondary, or tertiary depending on whether one, two, or three of the hydrogen atoms of ammonia have been replaced by organic groups [13]

Absorption of CO_2 in Amines

In order to design the control scheme for the desorber, it is also necessary to understand the absorption process so that the dynamics of sorbent loading is known.

Absorption of CO_2 in liquid amines in an exothermic process and thus is more favourable at lower temperatures. The absorption process can be described in the following steps [14] below:

1. Diffusion of CO_2 from the bulk of the gas to the gas-liquid amine interface. The same can be described by Fick's law of diffusion as given in equation 2.1 below.

$$J = -D\frac{dc_a}{dz} \tag{2.1}$$

where:

J:	Diffusion Flux
D:	Diffusivity
$\frac{dc_a}{dx}$:	Concentration of gradient of species 'a' along length x

2. Physical dissolution of CO_2 in the amine. The same can be explained using Henry's law as given in equation 2.2 below.

$$H_{gas} = \frac{c_{\text{gas}}}{p_{\text{gas}}} \tag{2.2}$$

where:

H_{gas}: Henry's constant
c_{gas}: Solubility of gas
p_{gas}: Partial pressure of gas

3. Reaction of CO_2 with the amine. Primary and secondary amines react with CO_2 to form carbamate via zwitter ion formation while tertiary amines react with CO_2 to form bicarbonate. For the reaction of CO_2 with primary and secondary amines, 2 moles of amine are required per mole of CO_2 while for tertiary amine the 1 mole of amine absorbs 1 mole of CO_2. The heat of regeneration of CO_2 from primary amine is higher than for tertiary amines; this is because the heat of reaction of bicarbonate formation is lower than carbamate formation [15].

4. Diffusion of reacted CO_2 with the amine. The same can be described by Stokes-Einstein equation which in given in equation 2.3 below. This equation is valid for fluid with low Reynolds number [16].

$$D = \frac{k_B T}{6\pi\mu r} \tag{2.3}$$

where:

D: Diffusivity
k_B: Boltzmann constant
T: Temperature of fluid(K)
μ: Dynamic viscosity
r: Radius of particle

The DAC system at ZEF uses a tertiary amine, TEPA (Tetraethylenepentamine) as the sorbent. It was selected after extensive research and experimentation on the basis of its high carbon absorption rate, equilibrium solubility of CO_2 and viscosity [17],[18].

Desorption of CO_2

Desorption of CO_2 is an endothermic process and thus is more favourable at higher temperatures. Previous work by Ovaa et al. [18] showed that desorption of CO_2 from liquid amine (TEPA) is more favourable at higher temperature and lower pressure. However, in the current thesis, the desorber operation will be performed at atmospheric pressure. Operating at atmospheric pressure reduces the usage of valves and purge systems to maintain system pressure which greatly simplifies the overall system operation.

The desorption of CO_2 from the amine can be described as the inverse process of absorption as described in section 2.2.2. At first, the bicarbonate/carbamate formed during absorption is converted back to CO_2 and the amine is regenerated. Then, the CO_2 diffuses to the interface of sorbent-gas due to concentration gradient. Once the latent heat required to vaporise CO_2 is reached, CO_2 escapes into vapour phase and the desorption process is completed. [14]

2.2.3. Energy Requirement for Desorption

The energy target for CO_2 capture in ZEF system is $\leq$400 kJ/mol of CO_2 [1.1]. Hence a model which accurately predicts the dynamic energy requirement of the desorber is essential to optimally control the desorber system. For the same, knowledge of all energy demands of the system is essential. The energy requirements of the desorber can be sub-divided as shown below.

- **Sensible Heat:** It is the energy required to heat the rich sorbent entering the desorber to target desorber temperature. It is calculated as below 2.4

$$Q_{\text{sens}} = \dot{m} \cdot c_p \left(T_{\text{des}} - T_{feed}\right) \tag{2.4}$$

where:

Q_{sens}:	Sensible heat
$\dot{m}$:	Feed flow rate
c_p:	Specific heat
T_{des}:	Desorber temperature
T_{feed}:	Feed temperature

- **Energy for desorption:** The energy required for desorption can be further split into the heat of desorption of CO_2 and H_2O from the sorbent.

  Dowling et al. [19] estimated the heat of desorption of CO_2 using the Clausius-Clapeyron relation [20]. The experimental data for different CO_2 and H_2O loadings in TEPA were used to obtain the heat of absorption using equation 2.5 below. The heat of absorption of H_2O can be determined in similar manner.

$$\ln\left(\frac{P_2}{P_1}\right) = \frac{\Delta H_{absorption}}{R}\left(\frac{1}{T_2} - \frac{1}{T_1}\right) \tag{2.5}$$

  where:

P_i:	Pressure at state i
T_i:	Temperature at state i (K)
H_{abs}:	Heat of absorption
R:	Universal gas constant

- **Heat of Vapourisation:** This is the energy required to vapourise H_2O from the sorbent. Previous work by Sinha et al. [17] determined the heat of vaporisation of H_2O for different TEPA loadings. The heat of vapourisation of TEPA-H_2O mixture was found to be higher than for pure water.

- **Energy for water reflux:** The ratio of H_2O to CO_2 in vapour form, obtained from the desorber can also be varied by introducing reflux of water back to the desorber. Increasing reflux increases the water content in the desorber and thus will increases the sensible heat and vapourisation heat demand. This will increase the overall energy consumption of the desorber and hence the same needs to be modelled in the energy demand for the desorber.

- **Heat Losses:** Depending on the size and thermal gradient in the desorber column, the heat losses to surrounding can be significant. The same needs to be described in the system model to make sure energy demand is accurately determined.

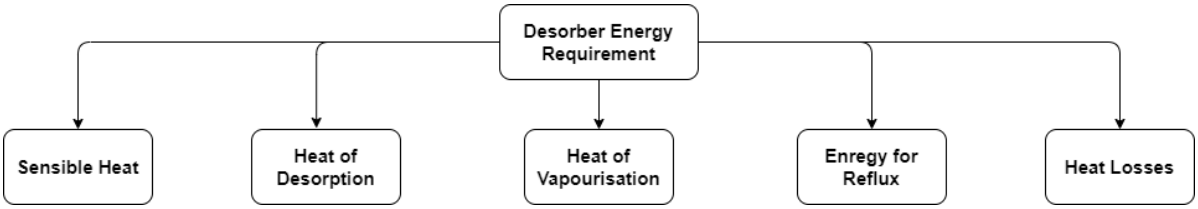

Figure 2.5: Energy requirement in the desorber consists of 5 components: sensible heat, heat of desorption, heat of vaporisation, energy for reflux and heat losses from desorber

2.2.4. VLE

In order to model the desorption of CO_2 and H_2O from the desorber and subsequent separation in the flash tank, understanding the vapour-liquid behaviour of the system is required. The interaction of CO_2 and H_2O in gas and liquid phase in the system can be described using the concept of Vapour-Liquid Equilibrium.

The co-existence of liquid and vapor phase of a pure substance or a mixture in equilibrium with one another is referred to as Vapour Liquid Equilibrium (VLE). For a mixture of two components, using the phase rule [20] given in equation 2.6 below we get that we have two degrees of freedom, i.e., for any given Temperature (T) and Pressure (P) the liquid mixture will be in equilibrium with the vapour mixture and thus the composition of the mixture can be calculated.

$$f = c - p + 2 \tag{2.6}$$

Where f=Degree of freedom, c=Number of components and p=Number of phases

For an ideal mixture, the equilibrium between the liquid and vapour phase can be defined using the Raoult's law [20] given below (2.7

$$y_i \cdot P_{Tot} = x_i \cdot P_i^{sat} \tag{2.7}$$

where:

y_i:	Vapour fraction of component i
x_i:	Liquid fraction of component i
P_{Tot}:	Total system pressure
P_i^{sat}:	Saturation pressure of component i

To further describe the system behaviour, concept of phase-equilibrium ratio, also called the K value is defined as equation 2.8 below is used. The K value of the species, expresses the tendency of the component to vapourise. For ideal mixtures, equation 2.7 can be written as equation 2.8 below.

$$K_i = \frac{y_i}{x_i} = \frac{P_i^{sat}}{P_{Tot}} \tag{2.8}$$

Where K_i = K value of component i

Here, K value only depends on P_i^{sat} and P_{Tot} and thus is a function of only T and P_{Tot}. However for the non-ideal mixture, K value also depends on the composition of the mixture and is given by the following equation 2.9 [20]:

$$K_i = \frac{\gamma_i^L}{\phi_i^V} \frac{P_i^{sat}}{P_{Tot}} \tag{2.9}$$

Where:

γ_i^L:	Liquid phase activity coefficient component i
ϕ_i^V:	Vapour fugacity coefficient of i

VLE for TEPA-H_2O-CO_2 mixture

The desorber of the DAC system at ZEF involves desorption of CO_2 and H_2O from the mixture of TEPA-CO_2-H_2O mixture. So, in order to understand the behaviour of the system, Dowling et al.[19] performed VLE experiments on the mixture. Further, using the experimental results, Dowling et al. [19]

built a model to predict the VLE behaviour of TEPA-H_2O-CO_2 mixture for different Temperature and Pressure conditions. Figure 2.6 shows the model vs experimental results for the VLE of TEPA-H_2O-CO_2 mixture.

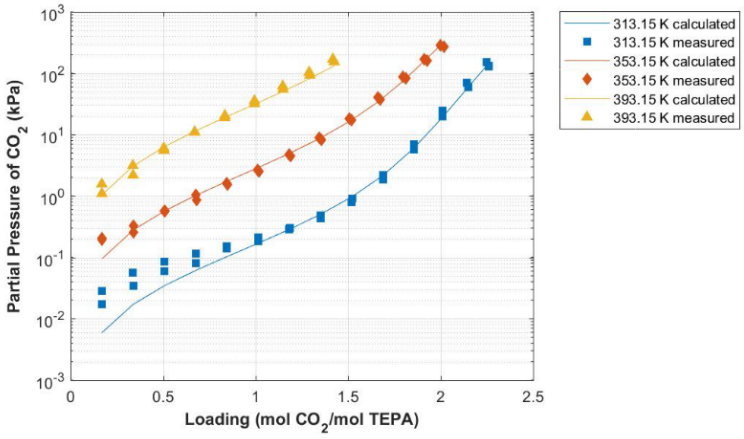

Figure 2.6: Experimental VLE data of the equilibrium CO2 absorption in an aqueous solution of 30 wt% TEPA at 313.15, 353.15 and 393.15 K versus the ternary TEPA-H2O-CO2 model prediction [19]

The model developed by Dowling et al.[19], uses on Special Ion interaction Theory (SIT) which works on activity co-efficient theory and is an extension of Debye-Huckel law [19]. The decision to choose SIT to build the VLE model was based on the work of Puxty et al. [21] which showed that SIT described the VLE behaviour of amines such as MEA, AMP etc., even for high concentrations (10 Molar) in a very good manner, at par with much more complex models such as e-NRTL and e-UNIQUAC [21].

Vapour Curve for H_2O-TEPA mixture

Dowling et al.[19] also performed experiments to determine the VLE behaviour of H_2O-TEPA mixture. The experiments results were then used to develop a VLE model of H_2O-TEPA mixture using modified Raoult's law and Wilson activity co-efficient equation. Figure 2.7 shows the comparison between model and experiment results for H_2O-TEPA mixture.

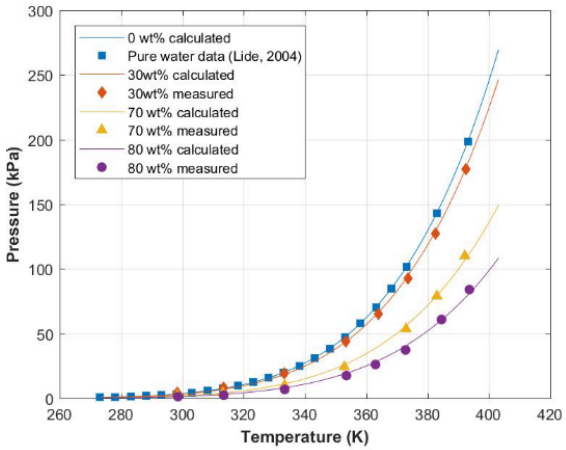

Figure 2.7: Comparison of experimentally obtained equilibrium pressure of binary mixtures of TEPA and H_2O 30, 70 and 80 wt% TEPA and pure water as a function of temperature, to the prediction of the H_2O-TEPA VLE model [19]

Using the VLE models of TEPA-H_2O-CO_2 and H_2O-TEPA mixture described in section 2.2.4 above,

the cyclic loading of desorber for given pressure and temperature at absorber and desorber can be predicted.

2.2.5. Dynamics of DAC Desorber

In order to design a control system for efficient and safe operation of the system, it is imperative to understand the parameters which impact the system performance. As briefly discussed in section 1.4, the environmental fluctuations in temperature, humidity and solar radiation greatly influence the system productivity and efficiency. Moreover, the transient behaviour of the desorber column during system operation such as Start-up, shut-down and desorption kinetics also impact the system performance.

Broadly, the dynamics of the desorber can be split into two main sub-sections:

- **External Disturbances** This includes fluctuations in environmental conditions like Ambient temperature, humidity, solar radiation etc. These variations can directly impact the system performance as described below:

    1. **Ambient Temperature:** Absorption of CO_2 into liquid amine is an exothermic process and thus is will be favourable at low temperatures [22], [23]. In order to determine the temperature dependence of CO_2 absorption in TEPA, Dowling et al. [19] performed VLE experiments and developed a model to determine the rich loading of CO_2 in the absorber section of DAC for different operating temperatures and TEPA loading.
    Moreover, viscosity of the sorbent is also affected by the temperature and CO_2 loading in the sorbent. With increase in temperature the viscosity goes down while with higher CO_2 loading the viscosity goes up [24],[25].
    Viscosity of the sorbent impacts the power required to pump the sorbent in the system and also impacts the mass transfer rate, as can be seen from equation 2.1 and2.3. This affects the overall system efficiency.

    2. **Humidity:** The humidity level in the atmosphere, directly impacts the H_2O loading in the sorbent. Mulder et al. [26] found that the equilibrium water loading in the sorbent increases with increase in absolute humidity in the atmosphere. Further, increase in H_2O loading in the sorbent, also reduces the sorbent viscosity which as mentioned previously affects the power requirement and mass transfer rate in the sorbent.

    3. **Solar Power:** The power required to drive ZEF's micro-plant is derived from Sun. Hence, any fluctuation is solar power input will affect the plant performance. Figure[2.8] below shows the hourly variation in solar power for a week for different months of year 2020 over Bechar, Algeria [27] (representative of Sahara climate). It can be seen from the graph that variation in solar radiation has both daily and seasonal component and hence the same needs to be factored in while designing the control scheme for the plant. Moreover, the different sub-systems of ZEF 1.2 have different power requirements 2.9 and hence based on the availability, the distribution of power across sub-systems will have to be optimised for maximum efficiency of the plant.

- **Internal variables:** This includes factors which affect the system performance but are internal to the DAC system. Some of these factors such as Desorber temperature, Reflux ratio etc., are process variables which can be varied as an input variable while other factors such as Sump volume, Number of stages in the desorber are fixed design parameters which cannot be varied as part of control scheme for the system.

    1. **Desorber Temperature:** Lean loading of CO_2 in the desorber will decrease with temperature. This implies that higher desorber temperature will increase the amount of CO_2 desorbed at the desorber. However, the temperature cannot be increased indiscriminately as thermal degradation of sorbent 2.2.6 needs to be kept in consideration. [C]

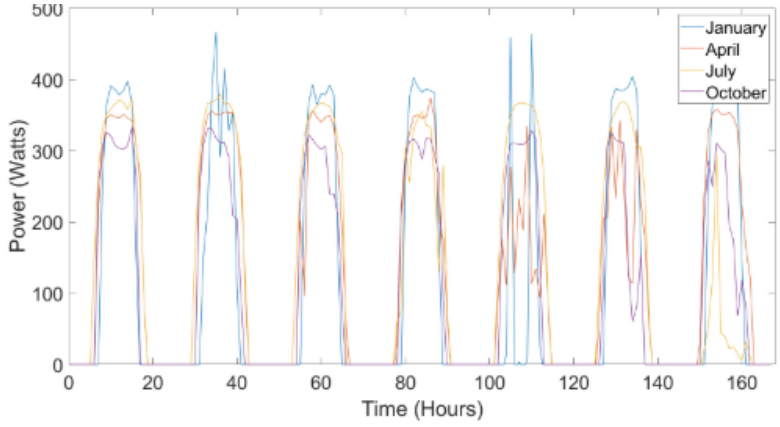

Figure 2.8: Variation in Solar power available at Bechar, Algeria (Sahara climate) for a week over different months in 2020. [27]

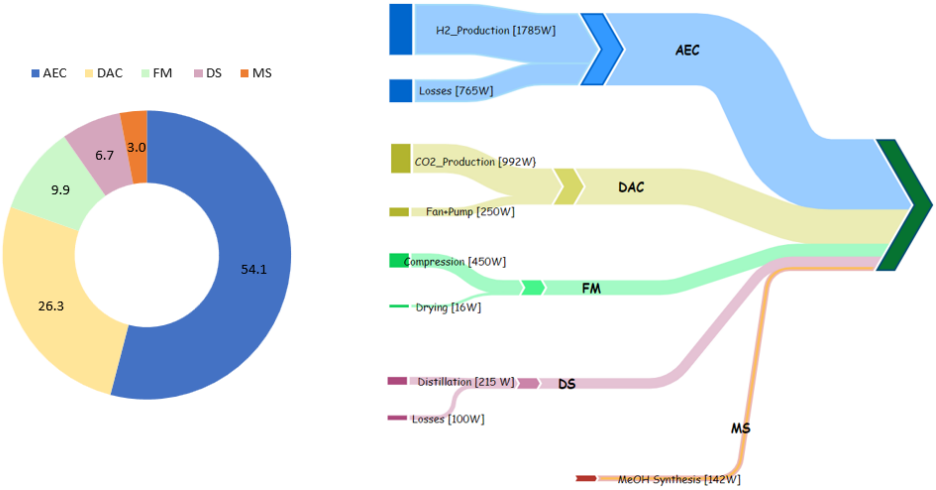

Figure 2.9: Power requirement of different sub-systems at ZEF

2. **Desorber Pressure** The partial pressure of H_2O in the desorber depends on the desorber temperature and sorbent loading. Hence, assuming a constant temperature in desorber, the variation in pressure will impact the CO_2 desorbed and thus will impact the production and efficiency of the system. [C]

3. **Reflux Ratio:** The reflux ratio can be altered to vary the H_2O outlet from the desorber. Increasing the reflux will increase the H_2O in the outlet from the desorber, however the energy demand also increases as more water needs to be vapourised in the desorber. Hence an optimisation of the reflux is required if and when the same is used.

4. **Start-up of Desorber** The entire micro-plant works on solar power and hence the entire system needs to be shutdown when the solar energy is not available after sunset. This implies that the energy and time required to startup the desorber determines how quickly the production can be started the next day and how the power available needs to be distributed to ensure system can be efficiently switched on. Previous work by Dubhashi et al. [27] estimated the effect of external disturbances on startup requirement of the desorber column. Figure[2.10] shows the time and energy fraction required for desorber startup for two different climatic conditions, Sahara and Mediterranean over different months of the year. While designing the control scheme for the integrated system, the dynamics for desorber startup will be incorporated.

5. **Desorption Kinetics:** Other parameters which affect the dynamic behaviour of the desorber

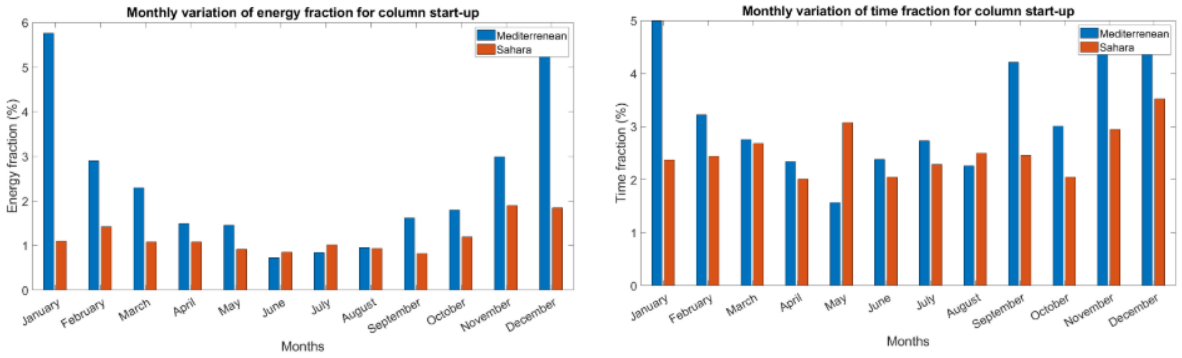

(a) Energy fraction required for desorber column startup

(b) Time fraction required for desorber column startup

Figure 2.10: Monthly energy and time fraction required for Desorber startup for different climatic conditions [27]

column output is the kinetics of desorption reaction. The time required to desorb CO_2 and H_2O from the rich sorbent to the target lean concentrations affects the system output and efficiency. Previous work by Poll et. al [26] showed how the hold-up time, which is defined as the time a reactant/substance spends in the reactor expressed as given in 2.10 required to reach different lean loading for different operating conditions. [C]

$$\text{Hold-up Time} = \frac{\text{Volume of vessel } (m^3)}{\text{Net volume flow rate from vessel } (m^3/s)} \tag{2.10}$$

2.2.6. Amine Degradation

Amine degradation in the presence of O_2, CO_2 etc., are a major deterrent in chemical absorption process for CO_2 capture. Degradation of amines results in the formation of a range of compounds that inhibit the carbon capture capacity of the amine and decreases the overall efficiency of the DAC process [28]. The target at ZEF is to ensure that the sorbent degradation should not reduce CO_2 output by $\geq$ 20% of the target output over a period of 4 years.

Amine degradation in DAC systems is primarily of 3 types as shown in Figure [2.11] below.

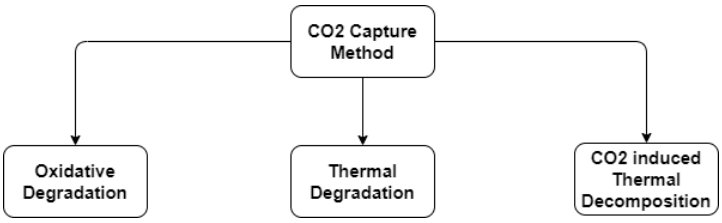

Figure 2.11: Amine degradation can be broadly classified in oxidative, CO_2 induced thermal degradation and thermal decomposition

1. **Thermal Decomposition:** becomes prominent at temperature $\geq 200^oC$ and hence will not affect the current system where the maximum temperature in the DAC will be limited to 120^oC in the desorber [1.1].

2. **Oxidative Degradation** Based on literature review [28], [29] and ongoing research at ZEF, the parameters which affect oxidative degradation are described below. The same is also shown in Figure [2.12]:

   - **Temperature:** Higher temperature → Higher rate of degradation

- **CO_2 concentration:** Presence of CO_2 reduces the degradation; however the degradation is not affected by the concentration of CO_2. At 0% CO_2, degradation is maximum.

  For the current system, oxidative degradation is relevant as interaction of amine with O_2 in the absorber section is not avoidable.

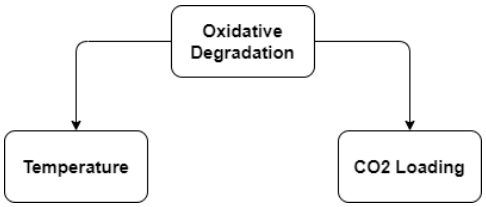

Figure 2.12: Oxidative Degradation in affected by CO_2 loading in the amine and Temperature

3. **CO_2 induced thermal degradation** is impacted by the following parameters [30],[31] which are also shown in Figure [2.13] below:

   - **CO_2 loading:** Degradation increases linearly with CO_2 concentration. However, in case of no CO_2 in the sorbent, there is no thermal degradation even at 140 ^{o} C [32].

   - **Temperature:** Degradation increases exponentially with temperature; however the effect becomes prominent only at temperature $>$ 100 ^{o} C.

   - **Water/Diluent Loading:** It is expected that presence of water/diluent in the sorbent should reduce the degradation. However, current research at ZEF was not conclusive on its impact of on degradation, thus more research is required to conclusively determine effect of water/diluent loading on amine degradation.

   - **Residence Time:** The amount of time the sorbent spends in the desorber, where it is exposed to higher temperature will also impact the degradation. Longer the exposure time to high temperature, higher will be the degradation.

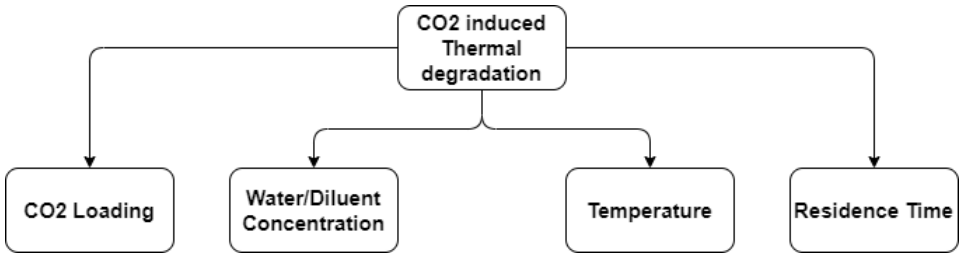

Figure 2.13: Thermal Degradation in affected by CO_2 loading, Temperature and Water/Diluent content in the Amine

2.3. Dehumidification System

2.3.1. Dehumidification requirement

Dehydration of CO_2 is required to lower the water content which may be detrimental for the CO_2 pipelines and compressors [33]. However, at present there is no consensus on the maximum limit of water level in CO_2 stream to avoid corrosion of downstream components [34],[35]. This is mainly because the solubility of water in CO_2 will depend on the concentration of the other impurities. [36]. Hence at the outset, it is essential to first determine the maximum water content which can be allowed in the ZEF FM system. The same is covered in the next section.

2.3.2. Maximum H_2O content in system

CO_2 and H_2O which is desorbed by the desorber in DAC, are required to be separated out to ensure purity of CO_2 gas which will be used for further processing in units downstream to DAC. This separation is achieved using a Flash tank as the fluids and the separated vapor is then sent to the FM sub-system for further processing as seen in Figure 1.4 in section 1.3.2.

If this vapor from DAC flash tank is sent directly to the compressors and compressed to 50 bar pressure, then it can result in condensation of this water (depending on the fraction of H_2O in the vapour). The system was simulated in COCO simulator for feed with fixed H2O:CO2 ratio od 3:1, to estimate the fraction of water in the flash tank vapour. The simulation results are shown Figure 2.14 below respectively.

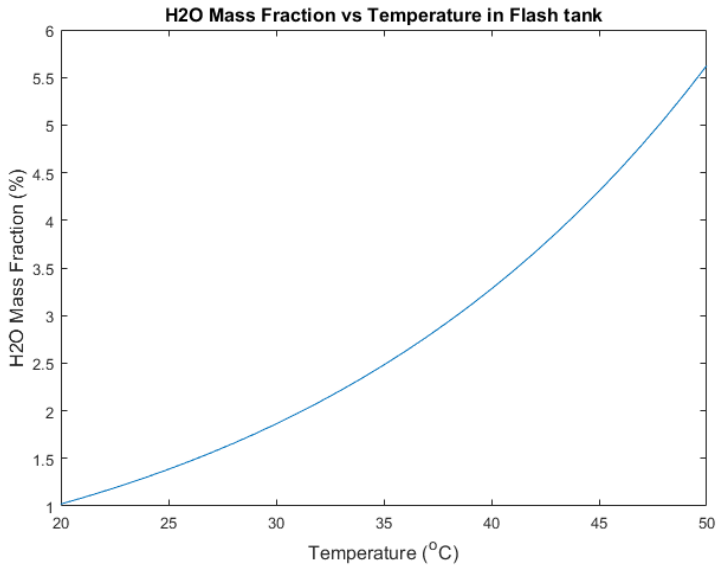

Figure 2.14: COCO simulation results showing variation in the fraction of water in vapor phase of DAC Flash tank with temperature

It can be seen from the simulation results in Figure [2.14], that for flash tank operation at 1bar and 20-50^{o}C, water fraction can be as high as $\sim$ 5% of total mass fraction. This mixture when compressed to 50 bar will result in condensation of water.

This condensed water can be harmful for the FM and subsequent downstream systems in the following ways:

- It can lead to corrosion of pipelines and the compressor components.
- It can combine with the lubrication oil of the compressor to form emulsion which will be adversely effect the lifetime of the compressor.
- It can form CO_2 hydrate which can clog the pipelines and affect plant operations.

The maximum water content of the CO_2 stream depends on the factors described in section 2.3.2 below.

Corrosion Resistance of transportation pipes and compressor components:

Based on literature focusing on CO_2-H_2O system for corrosion performance was reviewed. Based on

the review, H_2O concentration $\leq$ 1000 ppm in CO_2 rich phase (CO_2-H_2O system), is sufficient to limit corrosion in Carbon steel pipelines and components to $\leq$ 100 μm/year [37],[33].

Thus, for Corrosion prevention in pipelines, ≤1000ppm H_2O in CO_2 is sufficient

Hydrate Formation Prevention:

Hydrates are solid crystalline compounds which can form in the presence of both free and dissolved water. CO_2 in the presence of water, can form structure type I hydrates in pure CO_2 and structure type II hydrates in a gas mixture [38].

For temperature $\geq$ -5^{o}C, hydrate formation is possible for water content $\geq$ 1000 ppm (C). This implies that in terms of hydrate formation prevention, water content limit for FM system is $\leq$ 1000ppm.

Lubrication Water content

The lubricant used in compressor has its absolute water content, which is the maximum solubility of the water in the lubrication oil. If water concentration, exceeds this value, then 'free' water will be present in the system which can combine to form emulsion with the lubricant. ZEF's compressor uses the Hydraulic oil DIN 51524 HVLP (manufactured by Kroon Oil B.V). For this particular lubricant, absolute water content is 500ppm [39] , which means that maximum water content to maintain lubricant lifetime is $\leq$ 500ppm.

Thus, the maximum water content in the CO_2 stream for the current setup is limited by **Lubrication Oil Limit** and should be $\leq$ 500 ppm.

In the ZEF system, the water content is measured in terms of Relative Humidity (RH). So, for different operating temperatures, the water content for different RH values is calculated [40] and plotted as shown in Figure[2.15] below. It can be inferred from the graph for operating temperature below 100^{o}C, RH value of $\leq$ 2% , is sufficient to meet the system requirements of $\leq$ 500 ppm water content.

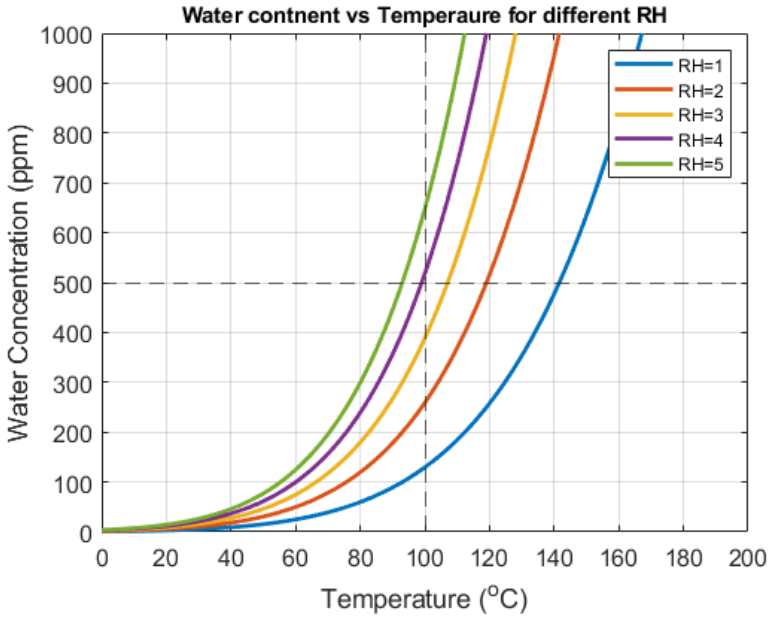

Figure 2.15: Water Content (ppm) vs Temperature for different RH values. RH value of $\leq$ 2% is sufficient to meet the system requirements of $\leq$500ppm water content

2.3.3. CO_2 Drying Technology

In order to dehumidify the CO_2 different types of technology are available as shown in Figure [2.16] below.

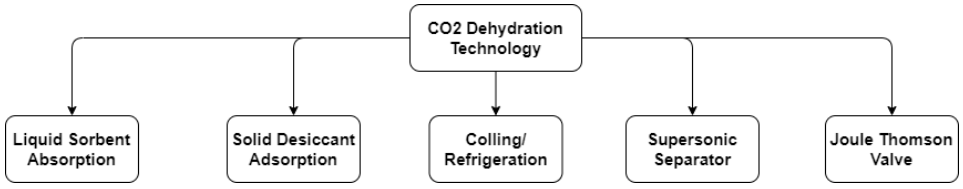

Figure 2.16: Technology used for CO_2 drying

Drying using Cooling/Refrigeration, Supersonic separator and Joule Thompson valve are not suitable for current system as their operation is complex and they involve large pressure drop and also prone to hydrate formation due to low temperature operation.

Liquid Sorbent absorption with glycol as the sorbent, is used in many systems across the world for Natural gas dehydration. However, glycol's higher affinity for CO_2 makes the system operation more complicated and poses a risk of failure of CO_2 production.

The solid desiccant based systems are simple to operate and work on adsorption of H_2O on micro-porous adsorbate such as Silica gel, Zeolites etc. Currently ZEF is in the process of finalising the technology to be used for the drying system with prototype testing in progress; hence for this thesis drying system has not been considered.

2.4. CO_2 Compression

CO_2 gas after processing by the dehumidification system then goes to the Compression system where it is compressed to 50-55 bar pressure (see Figure [1.4] for FM system schematic of ZEF system). The pressurized CO_2 is stored in the CO_2 buffer from where it is supplied to the MS reactor for Methanol synthesis.

One of the major challenge in the design of the CO_2 compression system at ZEF is the high pressure ratio (PR(Pressure ratio)=50) coupled with low mass flow of CO_2 (m_{CO_2}=$\sim$392 g/h). In order to meet this demand, previous research to determine the most optimum CO_2 compression system was done by Konning et al. [41]. The research concluded that compression system without lubrication was the most suitable option for the system followed by an oil lubricated system. However, as no lubrication free compressor system was commercially available, it was decided to proceed with oil lubricated system. Further, for the mass flow rate and PR required, an oil lubricated rolling piston compressor was the only option available in market. The current research will also focus on this compressor system. Figure[2.17] shows cross-sectional view of a rolling piston compressor.

2.4.1. Rolling piston compressor

Rolling piston compressors have been around since the 1960s and is most widely used in room air conditioner (RAC) systems [43]. The working of a rolling piston compressor can be seen in Figure[2.18] below.

2.4.2. Compressor Dynamics

Compressor Leakages
The output and efficiency of compressor is largely affected by internal leakages due to clearances in the compressor. Review of literature review on internal leakages and volumetric efficiency of rolling

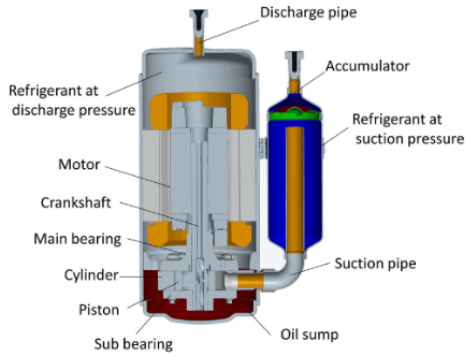

Figure 2.17: Cross-sectional view of a rolling piston compressor [42]

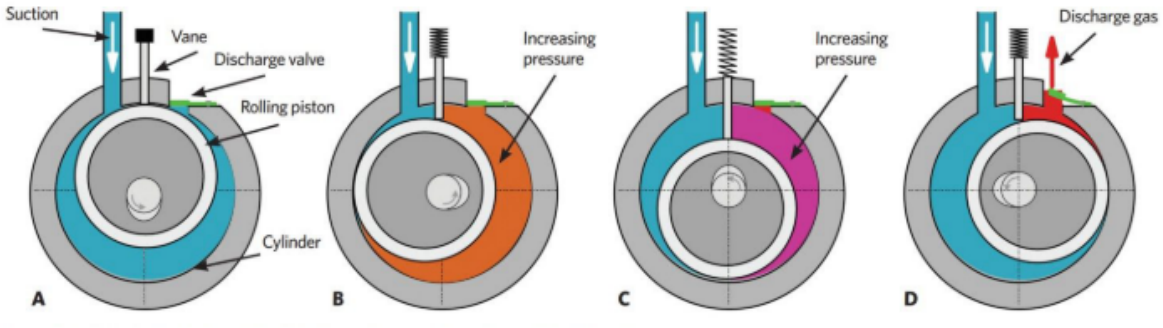

Figure 2.18: Working of rolling piston compressor. As the roller turns in clockwise direction, compressor starts suction of refrigerant. At the same time, the pressure in the next section increases and once the discharge pressure is reached, then discharge valve opens and high pressure refrigerant flows out. [44]

piston compressors [45], [46], [47] provided many insights into the leakage mechanisms and the overall leakages that are present in rolling piston compressors.

Leakages: The internal leakages in a rolling piston compressor can be broadly attributed to the following factors [46]:

- **Radial leakage:** This comprises of the leakage through the radial clearance between rolling piston wall and cylinder wall. This is the major source of losses in the compressor and ∼60% of total losses can be attributed to radial losses.
- **Piston Face leakage:** This includes the losses due to clearance between face of rolling piston and head walls of the cylinder. This type of losses contributes ∼35% of total losses.
- **Sliding vane leakage:** Leakage through sliding vane can be from two clearances, one from the clearance between sliding vane face and head walls cylinder and second through the leakage between sides of sliding vane and side walls of chutes inside the cylinder.

The leakages described above can be seen the Figure[2.19] below:

Further work by Gashe et al. [47], found the total leakage losses to be ∼12-14% of the total mass flow through the compressor. Based on these factors, for the purpose of this thesis, the leakage factor will be considered to be 15% and the same will be used for the compressor modelling.

Compressor Response Time:

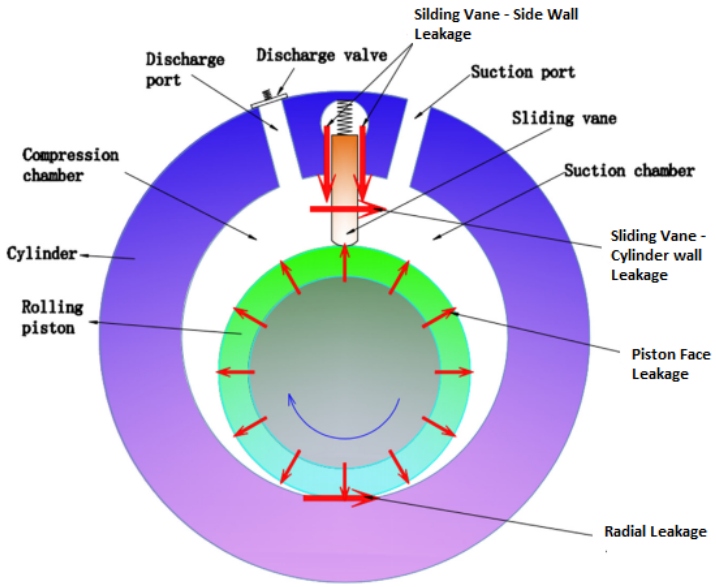

Figure 2.19: The main leakage paths in a rolling piston compressor (Marked with red arrow in the figure). Radial Leakage and Piston face leakage contribute ∼95% of total leakage losses in the compressor. Adapted from work by Cai et al. [46]

Compressor response time can be described as the time taken by the compressor to reach the defined set-point speed. This is the physical lag which will be present in the system due to its inertia. The same will be determined through experimentation on the ZEF test setup and will be incorporated in the compressor model to account for the dynamic change in speed and in turn the volume, mass and mole flow rate of the compressor.

2.5. Dynamics of integrated system:

Based on the system dynamics of DAC, drying and compression system as discussed in section 2.2.5 and 2.4.2, some of the main operating scenarios for the integrated system can be described as below:

- **High Production:** This would include operating scenarios in which the CO_2 and/or H_2O production rate is higher than the target (as described in 1.1) such as during ramp-up of production, increase in CO_2/H_2O loading in the sorbent etc. The possible operating scenarios and effect of the operation on the system is shown in Table 2.8 below:

Table 2.8: Possible operating scenario for Integrated DAC+FM system: Higher production than target (1.1). The vapour flow into DAC flash tank will be higher and thus the operation of drying and compression system will have to be adjusted to match this increase in output from desorber

Scenario	Possible operating conditions	Effect of operation
High desorber output than target	High mass flow into desorber	High vapour flow in DAC flash tank
	High H_2O in sorbent: High humidity	
	High CO_2 in sorbent: Low ambient temp.	
	High desorber temperature	

- **Low Production:** This would include operating scenarios in which the CO_2 and/or H_2O production rate is lower than the target (as described in 1.1) such as during ramp-down of production,

during start-up/shut-down of system etc. The possible operating scenarios and effect of the operation on the system is shown in Table 2.9 below:

Table 2.9: Possible operating scenario for Integrated DAC+FM system: Lower production than target (1.1). The vapour flow into DAC flash tank will be lower and thus the operation of drying and compression system will have to be adjusted to match this reduction in output from desorber

Scenario	Possible operating conditions	Effect of operation
Low desorber output than target	Low mass flow into desorber	Low vapour flow in DAC flash tank
	Low H_2O in sorbent: Low humidity	
	Low CO_2 in sorbent: High ambient temp.	
	Low desorber temperature	

- **System behaviour after shutdown:** Once the system is shutdown for instance at night, the sorbent in the desorber will cool down. The CO_2 and H_2O desorbed after the system shutdown will be again re-absorbed in the sorbent. This will reduce the vapour pressure in the desorber. Resulting operational scenarios are shown in Table 2.10 below:

Table 2.10: After system shutdown sorbent in the desorber will cool down which will result in re-absorption of CO_2 and H_2O desorbed after shut-down. This will reduce vapour pressure in the desorber which can result in drawing of air or sorbent into desorber depending on whether the system is leak tight or not.

Scenario	Effect of Operation	
System shutdown	If no leakage in system: Suction pressure in desorber	Sorbent drawn into Desorber: Worst case spill-over to Flash Tank
	If leakage in system: Air drawn in desorber	CO_2 purity will be affected in subsequent operation

- Other operating scenarios include variation in availability of solar power and optimising the same to ensure efficient plant operation. Such scenarios will be simulated on the integrated system model which will be developed in the current work.

2.5.1. Control Schemes

The main aim of this thesis is the design of control schemes for efficient and safe operation of the integrated DAC+FM system. The integrated system will be subjected to dynamic operating conditions as seen in the dynamics of DAC (2.2.5), compressor (2.4.2) and the integrated system (2.5).

Some of the major control requirements identified by ZEF for the operation of the integrated system under the dynamic conditions are summarised below:

- Pressure in the DAC flash tank should be maintained at atmospheric pressure ($\sim$1 bar)
- The temperature of the re-boiler and sorbent in the desorber should not exceed 120^{o}C.

For various process parameters such flash tank pressure, re-boiler temperature etc., different types of controllers (C) can be used. The same will be decided based on simulation of operational scenarios in the integrated system model to be developed in the current work.

2.6. Summary

- Through the literature research and previous work at ZEF [27],[10],[48], parameters which affect the dynamic behaviour of the DAC desorber 2.2.5 and Compression 2.4.2 system were identified.

Current thesis will build up on these findings to describe the dynamics of the integrated system.

- The modelling approach and the assumptions to describe the dynamic behaviour of the individual sub-systems were researched and the approach to be used for the system modelling were identified. Experiments will be planned to validate the developed model and their underlying assumptions.

- The interaction of the different sub-systems will result in different operational scenarios. Some of the operating scenarios and possible control schemes for the same were discussed. Based on the interaction of the DAC and FM system, more operational scenarios will be encountered. Such operating scenarios and possible control schemes for the same will be identified through this thesis.

3
Modelling

This chapter covers the modelling work performed in this work. At first the DAC system model, which consists of Absorber, Sump, Desorber and Flash Tank model are presented. Post this the FM system model, which consists of Compressor model is described. In the final section, the integrated DAC+FM system model is presented.

3.1. DAC Model

The working of the DAC sub-system has been explained in section 1.3.1 in Chapter 1. The next task in the thesis was to develop a representative model of the same, so that the performance of the DAC system can be simulated for various system disturbances (as described in section 2.2.5). For the same, the DAC system model was split into micro-models of different sections of DAC and these micro-models will be integrated to get the final DAC model.

The various micro-models of the DAC are explained in the next sections of the chapter.

3.1.1. Absorber Model

The absorber model used in the current work is based on model used in the previous work at ZEF by Dubhashi et al.[27]. The model does not delve deep into the mass transfer of CO_2 and H_2O into the sorbent and uses experimentally obtained Space Time Yield (STY) curves for absorption of H_2O and CO_2 into the sorbent. The schematic of the model is shown in Figure 3.1 below:

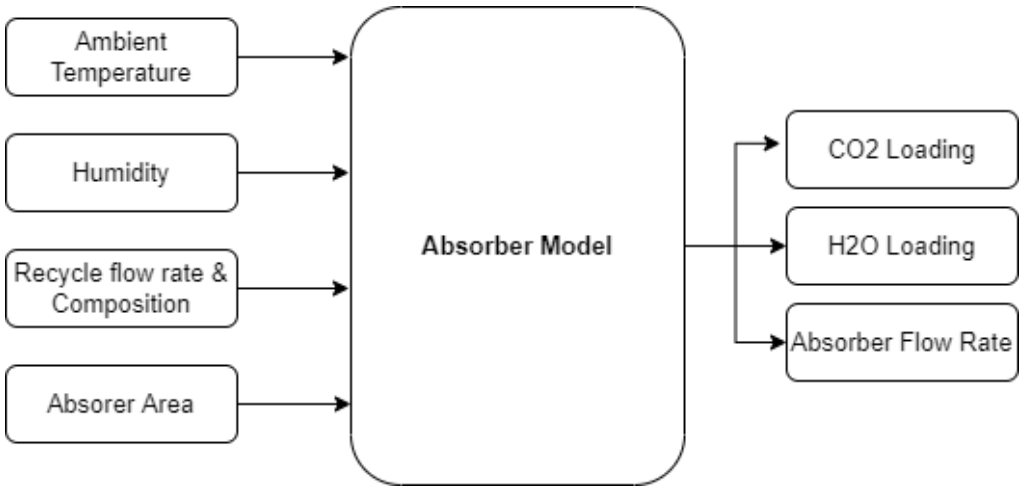

Figure 3.1: DAC Absorber Model

Model Assumptions

The assumptions used in the Absorber model are as below:

1. It is assumed that the viscosity does not affect the STY of CO_2 and H_2O in the sorbent. The viscosity is impacted by sorbent loadings which in turn will affect the mass transfer of CO_2 and H_2O in the sorbent.

2. For the STY curve of CO_2, it has been assumed that Clausius-Clapeyron [20] relation can be applied to determine vapour pressure of CO_2 at VLE loadings for different temperatures. Further it has been assumed that the variation of loading with vapour pressure of CO_2 in the sorbent is same for all temperatures. More experimental data is required to accurately determine the effect of temperature on CO_2 STY curve.

3. The sorbent flow rate into the absorber column and the residence time of the sorbent in the absorber is assumed to be constant.

Model Inputs and Outputs

The inputs used for the model as shown in Figure[3.1] are described below:

- **Ambient Temperature and humidity:** The ambient temperature and relative humidity values are taken as input for calculating the Space time yield (STY) of CO_2 and H_2O.

- **Recycle flow rate and composition:** Recycle feed flow rate and composition of the feed from the sump (described in section 3.1.2 below), is used as an input to determine CO_2 and H_2O entering the absorber.

- **Absorber area:** Absorber area is the user defined input for the area of the column over which the sorbent flows and CO_2, H_2O are absorbed into it.

Symbol	Input Parameter	Unit
T_{amb}	Ambient Temperature	[^oC]
H	Humidity	[%]
F_{rec}	Recycle flow rate	[mol/s]
z_{rec}	Recycle flow composition	[-]
L_{abs}	Length of absorber	[m]

The outputs obtained from the absorber model are described below:

- **CO_2 Loading:** Based on the feed composition of sorbent entering the absorber, the area of absorber and using the experimentally obtained STY curve for CO_2, the loading of CO_2 in the outlet stream of the absorber is determined.

- **H_2O Loading:** Similar to CO_2 loading, the H_2O loading in the outlet of the absorber is determined using the existing loading of H_2O in recycle stream, STY curve of H_2O (which is an experimentally derived function of temperature and relative humidity) and length of absorber, the final H_2O loading in the absorber outlet is determined.

- **Absorber Outlet flow rate:** Based on the CO_2 and H_2O outlet loading and feed flow rate entering the absorber, the outlet flow rate from the absorber is calculated.

Symbol	Output Parameter	Unit
F_{abs}	Absorber outflow rate	[mol s^{-1}]
z_{abs}	Absorber outflow composition	[-]
CO_{2abs}	CO_2 Loading	[molCO_2.kgTEPA^{-1}]
H_2O_{abs}	H_2O Loading	[molH_2O.kgTEPA^{-1}]

The above outputs are used to calculate the rich loading in the sump (described in section 3.1.2 below) which is then used as input for the Absorber and Desorber model (3.1.3).

Model Description
Recycle flow and composition:

At first, from the feed entering the absorber from the sump, the loading of CO_2 and H_2O is determined. This is done as the mole fraction of CO_2, H_2O, TEPA and PEG_{200} in the feed is known from the sump model (3.1.2).

STY CO_2:

The Space time yield (STY) curve for CO_2 is determined by extrapolation of experimentally obtained VLE data through previous works at ZEF [26].

The procedure used for determining STY function for CO_2 is described in Appendix B

STY H_2O:

The STY curve for H_2O used in this work, is a function of absolute humidity and H_2O loading in the sorbent. The function used has been carried over from previous work at ZEF by Dubhashi et al.[27].

Using the above STY curves and recycle stream flow rate and composition, the flow rate and composition of the absorber outlet stream is determined and is used for calculation of concentration of sorbent in the sump model (3.1.2).

The working of the model is described using the flow-chart 3.2 below:

3.1.2. Sump Model

The sorbent for DAC system is present in the sump through which it is sent to the absorber and desorber via pumps. The overflow from the absorber and desorber flows back into the sump and thus the cycle is completed. The sump also acts as the dampener for fluctuations in sorbet loading due to mixing of rich and lean sorbent from absorber and desorber respectively. Therefore, it is essential to model the behaviour of the sump in order to be able to sorbent loading which is the input for both Absorber and Desorber section. The schematic of the sump model is shown in Figure[3.3] below.

Model Assumptions

The main assumptions used in modelling the sump are as below:

1. The sump is modelled as continuously stirred tank [49] with two sorbent outlet streams (one to absorber and desorber each) and two sorbent inlet streams (one each from absorber and desorber) and the net sorbent in the sump is well mixed.

2. It is assumed that the mixing of sorbent streams of different temperatures does not alter the sump temperature and it remains in thermal equilibrium with the surroundings. The assumption holds as the flow rate from the absorber and desorber is very small compared to the sorbent mass in the sump.

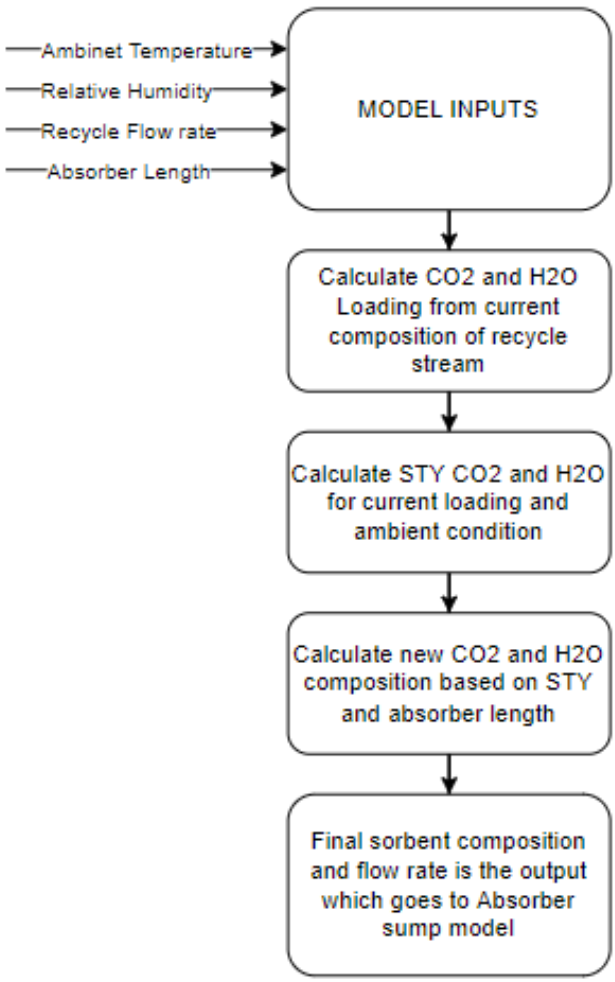

Figure 3.2: DAC Absorber Model working

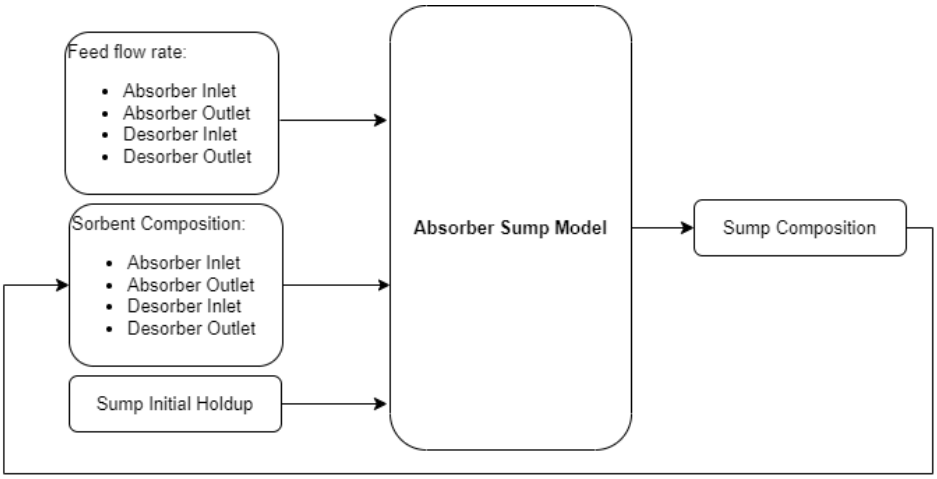

Figure 3.3: DAC sump model

3. It is assumed that no chemical reaction takes place in the sump. The assumption is valid since the absorption of CO_2 and H_2O into the sorbent in sump will be negligible since it is not in direct contact with air.

Model Inputs and Outputs

The below inputs used in the sump model to determine the sorbent composition in the sump.

- **Feed flow rate:** The feed flow rate from absorber and desorber inlet and outlet.
- **Sorbent composition:** The composition of the sorbent streams from absorber and desorber input and output.
- **Sump Holdup:** The sump holdup is the initial mass and concentration of the sorbent which is present in the sump at the start of the simulation.

Symbol	Input Parameter	Unit
F_{rec}	Absorber inlet flow rate	[mol s^{-1}]
F_{abs}	Absorber outflow rate	[mol s^{-1}]
F_{rich}	Desorber inlet flow rate	[mol s^{-1}]
F_{lean}	Desorber outflow rate	[mol s^{-1}]
z_{rec}	Absorber inlet flow composition	[-]
z_{abs}	Absorber outflow composition	[-]
z_{rich}	Desorber inlet flow composition	[-]
z_{lean}	Desorber outflow composition	[-]
N_{sump}	Initial Sump holdup	[mol]

Sump composition: The output of the sump model is sump composition, which is calculated using above input parameters. This sump composition is then used as input composition for the feed streams to absorber and desorber.The model output results for the absorber and sump model are presented in Appendix B.

Symbol	Output Parameter	Unit
z_{sump}	Sump composition	[-]

Model Description

The equation 3.1 below determines the rate of change of moles for each component in the sump, which is then integrated over time to find the total sump mass and final sump composition. The working is described in the flowchart 3.4 below.

$$\frac{dM}{dt} = Fabs.zabs + Flean.zlean - Frec.zrec - Frich.zrich \tag{3.1}$$

Where:

$\frac{dM}{dt}$	Rate of change of moles in the sump
F_{abs}	Feed flow rate absorber outlet
z_{abs}	Sorbent composition absorber outlet
F_{lean}	Feed flow rate lean sorbent from desorber
z_{lean}	Sorbent composition lean sorbent from desorber
F_{rec}	Feed flow rate absorber inlet
z_{rec}	Sorbent composition absorber inlet
F_{rich}	Feed flow rate rich sorbent to desorber
z_{rich}	Sorbent composition rich sorbent to desorber

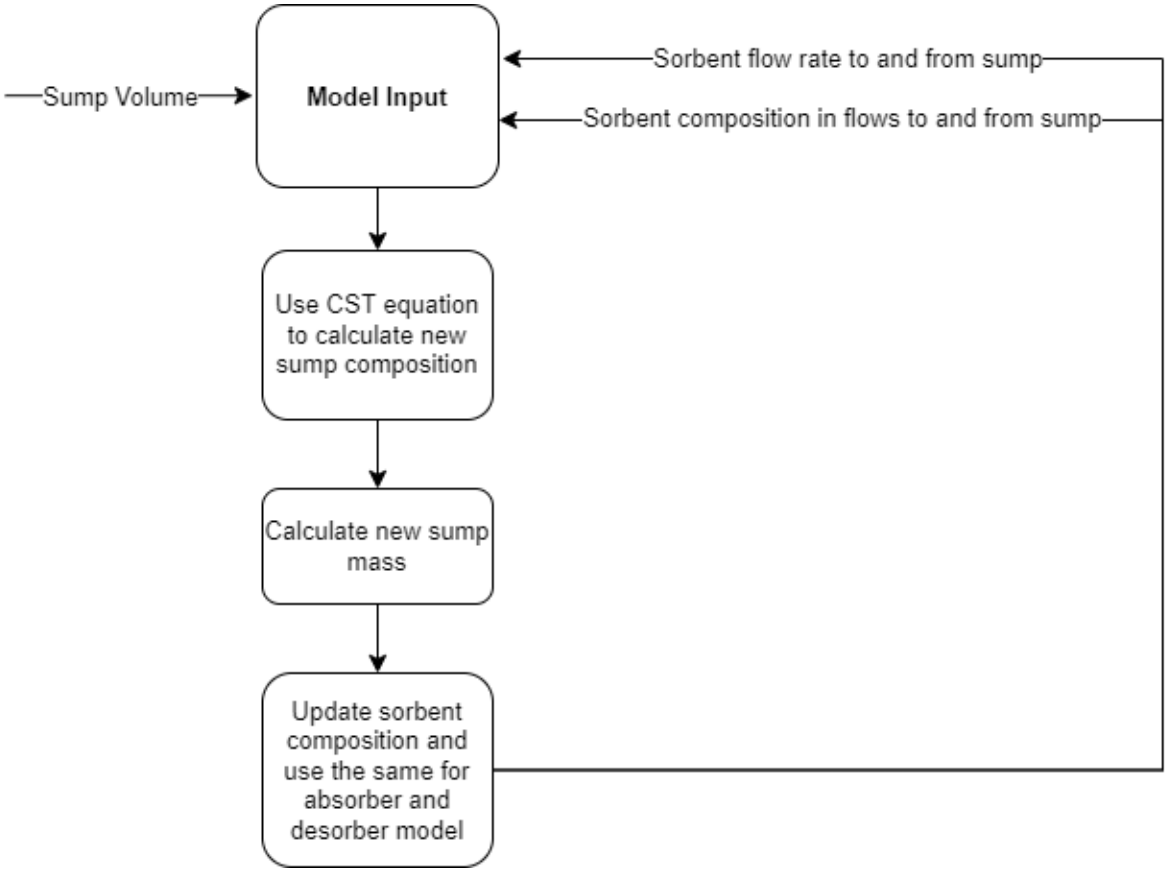

Figure 3.4: DAC sump model working

3.1.3. Desorber Model

The desorber model serves as the main element of the integrated DAC+FM system model developed in this thesis. The desorption column is modelled as a trayed column with multiple stages and was developed to describe the dynamic behaviour of the system. In the next sections, the main assumptions, working and limitations of the desorber model are explained. The schematic of a single stage of the desorber model is shown in Figure[3.5] below.

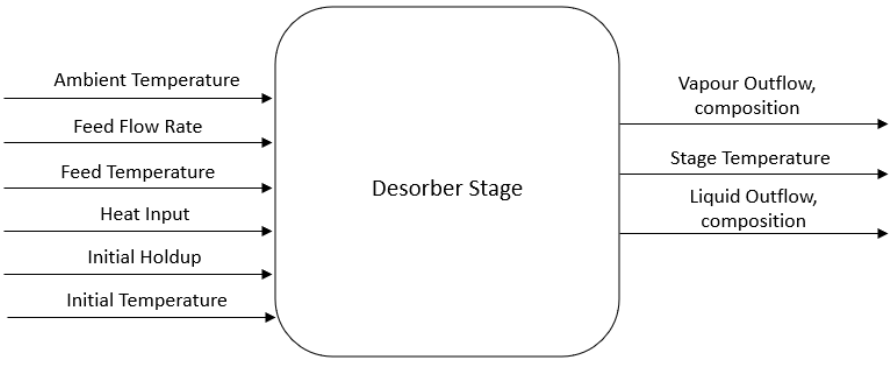

Figure 3.5: Schematic of a single stage of the desorber model

Model Assumptions

The main assumptions used in the model are as below:

1. The column is assumed to operate at equilibrium i.e., the vapour curves used in the model assume the system to be at vapour liquid equilibrium (VLE).

2. Each stage of the desorber column is assumed to be a lumped mass, with uniform temperature and the liquid/vapour exiting the stage is at the same temperature as the calculated stage temperature.

3. It is assumed that in the sorbent mixture, TEPA and PEG are non-volatile components and the vapour phase only contains CO_2 and H_2O.

4. Specific heat and heat of desorption of different components is assumed to remain constant.

5. It is assumed that the desorption of CO_2 and H_2O are independent of each other.

6. It is assumed that the pressure of each stage of the desorber is same i.e., there is no pressure drop within the desorber and the stage pressure is same as the pressure in the flash tank.

Model Inputs and Outputs

The various inputs used for the model are mentioned below:

- **Feed** The flow rate, composition and temperature of the liquid and vapour feed entering the stage is needed to calculation of each stage outputs.

- **Ambient and Initial stage temperature:** The ambient and initial stage temperature is needed to calculate the heat loss and current stage temperature.

- **Heat Input:** Heat input (if any) to the stage is a required input for energy balance and calculation of current stage parameters.

- **Holdup:** The initial stage holdup is a required input for the mass balance and determining the stage parameters.

- **Pressure:** The stage pressure is a required input, which is calculated in the flash tank model as described in section 3.1.4.

Symbol	Input Parameter	Unit
F_{rich}	Desorber inlet flow rate	[mol s^{-1}]
z_{rich}	Desorber inlet flow composition	[-]
T_{amb}	Ambient Temperature	[^{o}C]
$T_{initial}$	Initial stage temperature	[^{o}C]
$\acute{Q}_{in}$	Heater Power Input to desorber	[W]
-	Stage Holdup	[mol]
P_{Des}	Desorber pressure	[Pa]

The outputs from the desorber model are described below:

- **Vapour and Liquid outlet:** For each stage the liquid and vapour outflow and composition is determined with dynamically changing input parameters.

- **Temperature:** For each stage the temperature of the stage is determined and the outflow, both liquid and vapour is considered to be at the same temperature as the stage temperature.

  The model output results are presented in Appendix B.

Symbol	Output Parameter	Unit
F_{lean}	Desorber liquid outflow rate	[mol s^{-1}]
z_{lean}	Desorber liquid outflow composition	[-]
T_{lean}	Temperature of lean sorbent out from desorber	[^oC]
V_{des}	Desorber vapour outlet flow	[mol s^{-1}]
y_{des}	Desorber liquid outlet flow composition	[-]
T_{des}	Temperature of vapour outlet from desorber	[^oC]

Model Description

In the following section the various aspects of the desorber model are explained in detail.

Mass Balance:

The mass balance block is used to calculate the total mass present in the stage. The total liquid and vapour inflows to the stage are added and the outflows are subtracted to get the rate of change in mass in the stage per time step. This rate of change is then integrated to get the current mass of components in the stage. The integration block is initiated using the holdup mass input to the stage. The same is depicted in Figure 3.6 below. The vapour and liquid outflow which is subtracted in the mass balance block is calculated using the Flash block which is described in section 3.1.4.

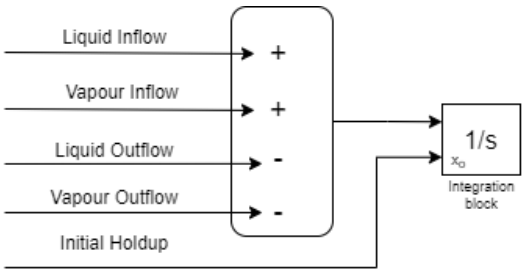

Figure 3.6: Mass balance block in each stage of desorber model

Energy Balance:

The energy balance block is used to calculate and account for all energy interactions that take place within the desorber stage.

- **Sensible Heat:** The energy from liquid and vapour inflow to the stage is calculated using equations 3.2 and 3.3 below.

$$\dot{Q}_{liq-in} = \dot{M}_{liq-in} \cdot Cp_{Liq} \cdot (T_{liq-in} - T_{Stage}) \tag{3.2}$$

$$\dot{Q}_{vap-in} = \dot{M}_{vap-in} \cdot Cp_{Vap} \cdot (T_{vap-in} - T_{Stage}) \tag{3.3}$$

Where:

$\acute{Q}_{liq-in}$:	Heat input from liquid entering stage
$\acute{M}_{liq-in}$:	Mass of liquid entering the stage
Cp_{Liq}:	Specific heat of liquid
$\acute{Q}_{vap-in}$:	Heat input from vapour entering stage
$\acute{M}_{vap-in}$:	Mass of vapour entering the stage
Cp_{Vap}:	Specific heat of vapour

T_{liq-in}: Temperature of liquid entering the stage
T_{vap-in}: Temperature of vapour entering the stage
T_{Stage}: Temperature of the stage

- **Heat of Desorption:** The heat of desorption removed from the stage due to desorption of vapour exiting the stage is subtracted while heat of desorption added to the stage by vapour entering the stage is added the energy balance block. The equations used to calculate the heat of desorption is given by equation 3.4 and 3.5 below.

$$\dot{Q}_{des-in} = \dot{M}_{vap-in} \cdot H_{des} \tag{3.4}$$

$$\dot{Q}_{des-out} = \dot{M}_{vap-out} \cdot H_{des} \tag{3.5}$$

Where:

$\acute{Q}_{des-in}$: Heat of absorption of vapour entering stage
$\acute{M}_{vap-in}$: Mass of vapour entering the stage
$\acute{Q}_{des-out}$: Heat of absorption of vapour exiting stage
$\acute{M}_{vap-out}$: Mass of vapour exiting the stage
H_{des}: Heat of desorption

- **Heat Loss:** Heat lost from the stage is subtracted from the energy balance block. The same is calculated using equation 3.6 below:

$$\dot{Q}_{loss} = UA \cdot (T_{Stage} - T_{Amb}) \tag{3.6}$$

Where:

$\acute{Q}_{loss}$: Heat loss from the stage
U: Overall heat transfer co-efficient
A: Total heat transfer area
T_{Stage}: Temperature of the stage
T_{Amb}: Ambient Temperature
H_{des}: Heat of desorption

The overall schematic of energy balance block is shown in Figure[3.7] below.

Flash Calculation:
For each stage, to determine the vapour and liquid fraction, pT flash calculation is performed at each time step for which the feed flow, temperature and pressure of the stage is the input. The calculation steps are described below:

- At first step, it is assumed that the liquid composition of the stage is same as the feed composition. Using this, the sorbent loading is calculated, which is then used to calculate the partial pressure of CO_2 and H_2O.

- For CO_2 the same is calculated by extrapolation of experimental VLE data of TEPA-PEG-CO_2-H_2O quaternary system available at ZEF. Using the fit of this data, Clausius-Clapeyron relation (2.5) is used to get the partial pressure of CO_2 at the current stage temperature and loading.

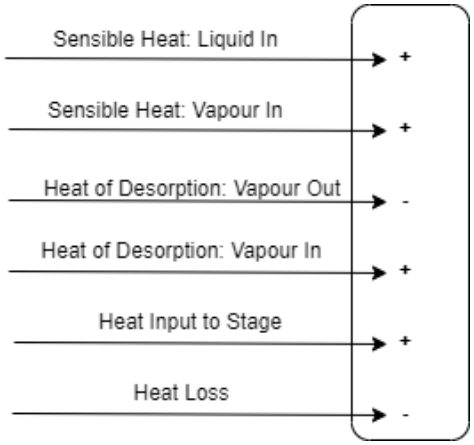

Figure 3.7: Energy balance block in each stage of desorber model

- For H_2O, the partial pressure is determined by using modified Raoult's law 2.9. The saturation pressure of pure water is calculated using Antoine's equation (shown in equation 3.13) and the activity coefficient is determined using Wilson's equation [50] (shown in equation 3.7).

$$\ln(\gamma_1) = -\ln(x_1 + \Lambda_{12}x_2) + x_2\left[\frac{\Lambda_{12}}{x_1 + \Lambda_{12}x_2} - \frac{\Lambda_{21}}{x_2 + \Lambda_{21}x_1}\right] \tag{3.7}$$

Where:

γ_i:	Activity coefficient component i
Λ_{ij}:	Wilson parameters
x_i:	mole fraction of component i

The development of these algorithms to calculate the partial pressure of CO_2 and H_2O was done previously at ZEF and the same have been incorporated in the current model.

- If the sum of the partial pressure of CO_2 and H_2O is lower than or equal to the stage pressure, then the stage composition is considered as a single phase liquid and the vapour liquid fraction ($\frac{V}{F}$) in the stage is set to 0 and the vapour composition is set as the ratio of calculated partial pressure of each component to sum of partial pressures in the stage.

- If the sum of partial pressure of CO_2 and H_2O is greater than stage pressure, then the K-value 2.8 for the step is calculated as ratio of vapour composition to the liquid composition, and first assumption is made for the $\frac{V}{F}$ value.

- In the next step, with the assumed $\frac{V}{F}$ and K value, the vapour composition and partial pressures of CO_2 and H_2O are re-calculated and the steps described earlier are repeated and new $\frac{V}{F}$ value is calculated. This iteration is repeated till difference between assumed and calculated $\frac{V}{F}$ value is small enough and then model converges and gives the final results. In this way the composition of liquid and vapour fraction of each stage is determined.

Stage Holdups:
In the model, each stage is assigned a maximum liquid and vapour holdup level is defined as the user input. When the total liquid level exceeds this maximum holdup limit, then the liquid starts to overflow to the next lower stage. Similarly when vapour level in the stage exceeds the maximum holdup level, vapour starts to overflow to the next upper stage.

As the liquid and vapour start to overflow to the next stages, this can result in fluctuations in solving the system numerically. So as a solution to this, a dampening factor is introduced to soften the liquid and vapour overflow from the stage. The value for this dampening factor was chosen so as to have smoother transition of liquid and vapour from one stage to the next.

The liquid and vapor which flow out from the stage are subtracted in the mass balance block as shown in Figure 3.6 to calculate the mass of components in the stage.

Temperature Calculation:
The desorber model also determines how the temperature of the stage changes dynamically. The same is calculated by solving the unsteady heat transfer equation 3.8 as given below:

$$\dot{M}Cp_{stage} \cdot \frac{dT}{dt} = \dot{Q}_{in} - \dot{Q}_{out} + \dot{Q}_{gen} \tag{3.8}$$

Where:

$\acute{M}Cp_{stage}$:	Total Thermal mass in the stage
$\acute{Q}_{in}$:	Heat input to the stage
$\acute{Q}_{out}$:	Heat out from the stage
$\frac{dT}{dt}$:	Rate of change in temperature with time
$\acute{Q}_{gen}$:	Heat generated in the stage

Thermal mass of the stage, $\dot{M}\text{Cp}_{stage}$ is calculated as below:

$$\dot{M}Cp_{stage} = M_{stage} \cdot Cp_{stage} + \dot{M}_{liq} \cdot Cpiq + \dot{M}_{vap} \cdot Cpvap \tag{3.9}$$

Using equation 3.8 and 3.9, the temperature of the stage is determined using equation 3.10 below which is initialised with initial stage temperature as the user input:

$$T_{stage} = \int \frac{Q_{net}}{\dot{M}Cp_{stage}} \cdot dt \tag{3.10}$$

Where:

$\acute{T}_{stage}$:	Stage temperature
$\acute{Q}_{net}$:	Net heat input to stage from energy balance block
$\acute{M}Cp_{stage}$:	Total Thermal mass in the stage

3.1.4. Flash Tank Model

The vapour output from the desorber (CO_2 and H_2O) is separated out into liquid and gaseous phase by flashing the mixture in the flash tank. The flash tank controls the gas and liquid input to the FM and the AEC sub-system respectively, and hence it was necessary to describe the working of the DAC flash tank. For the same, a model for the working of the flash tank was prepared and is explained in this section. The schematic of the flash tank and the model is shown in Figure3.8 below.

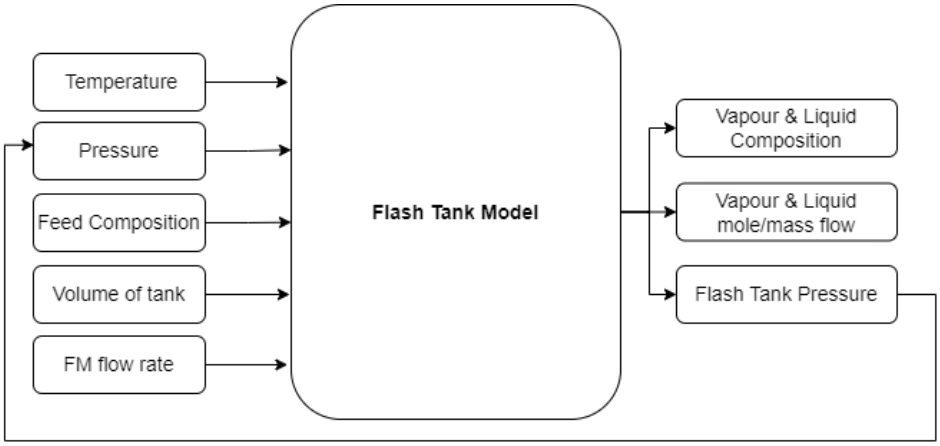

Figure 3.8: DAC Flash Tank Model

Model Assumptions

The main assumptions used for the flash tank model are as below:

- The flash tank is assumed to operate at equilibrium and the vapour curves used in the model assume the system to be at equilibrium .
- It is assumed that the vapour entering the flash tank is a binary mixture of CO_2 and H_2O only, and no sorbent (TEPA or PEG) is evaporated from the desorber.
- It is assumed that the gas mixture in the flash tank behaves as an ideal gas. Since the pressure in the flash tank remains close of atmospheric pressure (1̃bar), hence this assumption is valid.
- It is assumed that CO_2 and H_2O are in Vapour-Liquid equilibrium (VLE) in the flash tank.
- It is assumed the mixture in the flash tank is well mixed and the temperature of the flash tank is same as ambient temperature.

Model Inputs and Outputs

The inputs used for the DAC Flash tank model are as below:

- **Temperature:** The temperature of flash tank and its contents are assumed to be in equilibrium with the ambient as mentioned above. So, the ambient temperature is taken as the temperature of the flash tank.
- **Pressure:** The pressure in the flash tank is calculated based on the interaction of the flash tank output and compressor model (described in 3.2.1 below).
- **Feed Composition:** Vapour output of the desorber model (3.1.1) is taken as the feed input to the flash tank.
- **Volume of Tank:** Volume of the flash tank is a user defined input and is used for calculation of pressure in the flash tank.
- **FM model flow rate:** The net flow rate from the flash tank to FM from the FM model (3.2) is used as input along with feed from desorber and volume of the flash tank to calculate the flash tank pressure.

Symbol	Input Parameter	Unit
T_{amb}	Ambient Temperature	[^{o}C]
P_{flash}	Flash tank pressure	[Pa]
F_{flash}	Feed flow into flash from desorber	[mol s^{-1}]
V_{flash}	Flash tank volume	[m^3]
F_{FM}	Net flow rate FM subsection	[mol s^{-1}]

The outputs from Flash tank model are given below:

- **Liquid and Vapour flow rate:** The flow rate of liquid and vapour from the desorber feed after flashing in the DAC flash tank.
- **Liquid and Vapour fraction:** The composition of liquid and vapour fraction in the flash tank.
- **Pressure:** Flash tank pressure is calculated based on the net mole flow in flash tank and flash tank volume, assuming ideal gas behaviour in flash tank. The same pressure is also used as input to both Desorber and flash tank model itself for calculation of pT flash at each time step.

The model output results are presented in Appendix B.

Symbol	Output Parameter	Unit
V_{Flash}	Vapour flow into flash tank	[mol s^{-1}]
L_{Flash}	Liquid flow into flash tank	[mol s^{-1}]
z_{Flash}	Composition of mixture in flash tank	[-]
P_{flash}	Flash tank pressure	[Pa]

Model Description

The working of the model can be explained using the flowchart 3.9 below:

Saturation Pressure:

As stated in the assumption, mixture of H_2O and CO_2 is considered as a ideal mixture, which implies that Raoult's law is applicable and hence equation 3.11 holds.

$$y_i = f(T, P) = x_i \cdot P_i^{sat}/P \tag{3.11}$$

which can also be written as 3.12

$$K_i = P_i^{sat}/P \tag{3.12}$$

where:

y_i:	Mass fraction of component i in gas phase
x_i:	Mass fraction of component i in liquid phase
T:	Temperature
P:	Pressure
P_i^{sat}:	Saturation Pressure
K_i:	Ratio of y_i and x_i

For H_2O, saturation pressure is calculated using Antoine equation 3.13.

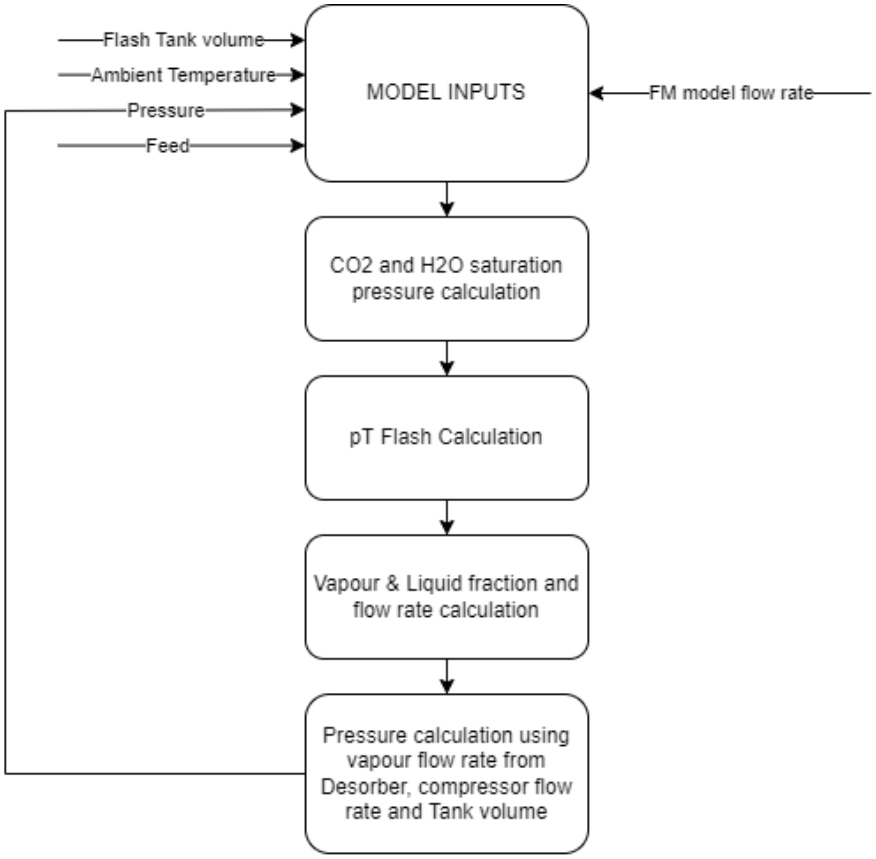

Figure 3.9: DAC Flash Tank Model working

$$P_{\text{sat}} = 10^{\left(A - \frac{B}{C+T}\right)} \tag{3.13}$$

where:

P_i^{sat}:	Saturation Pressure
A,B,C:	Antoine Constants
T:	Temperature

For CO_2 saturation pressure is calculated using interpolation of vapour pressure data. The data is valid till critical temperature (T_C) of CO_2 ($\tilde{3}1^oC$).For temperature higher than T_C, Henry's law 3.14 is used to calculate K_{CO2}.

$$y_i = \frac{H_i}{P} \cdot x_i \tag{3.14}$$

where:

y_i:	Mass fraction of component i in gas phase
H_i:	Henry's constant
P:	Pressure
x_i:	Mass fraction of component i in liquid phase

pT Flash:

Through mass balance and component balance, we get equation 3.15 and 3.16 as shown below:

$$F * z_i = L * x_i + V * y_i \tag{3.15}$$

$$\sum_i y_i - \sum_i x_i = 0 \tag{3.16}$$

Where:

F	Feed flow into flash tank
z_i	Mass fraction of component i in feed
L	Liquid fraction of the feed flow
x_i	Mass fraction of component i in liquid phase
V	Vapour fraction of feed flow
y_i	Mass fraction of component i in gas phase

Using equation 3.15 and 3.16 and K_i for CO_2 and H_2O, we get equation 3.17 which is also called the **Rachford-Rice Flash equation** [51]. This is solved numerically to get the VLE information.

$$\sum_i \frac{z_i * (K_i - 1)}{1 + \frac{V}{F} * (K_i - 1)} = 0 \tag{3.17}$$

Where:

F	Feed flow into flash tank
z_i	Mass fraction of component i in feed
L	Liquid fraction of the feed flow
V	Vapour fraction of feed flow
K_i:	Ratio of y_i and x_i

Pressure Calculation:

Pressure in the flash tank is calculated using the assumption that the gas mixture in the flash tank behaves as an ideal gas.

The net gas moles in the flash tank is given by equation 3.18 and also depicted in Figure3.10 below:

$$n_{flash} = n_{DesorberIn} + n_{FMIn} - n_{FMOut} \tag{3.18}$$

Where:

n_{flash}	Net gas moles in flash tank
$n_{DesorberIn}$	Gas moles added in flash tank by Desorber
n_{FMIn}	Gas moles added in flash tank by FM sub-system
n_{FMOut}	Gas moles removed from flash tank by FM sub-system

The net gas volume in the flash tank is given by equation 3.19 below:

$$V_{gas} = V_{flash} - V_{liquid} \tag{3.19}$$

Where:

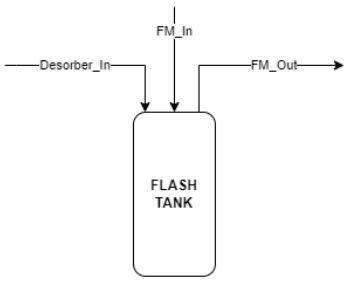

Figure 3.10: Flash Tank with Inlet and Outlet gas streams

V_{gas}:	Gas volume in flash tank
V_{flash}:	Flash tank volume
V_{liquid}:	Liquid volume in flash tank

Using equation 3.18 and 3.19 and ideal gas law, pressure in the flash tank is calculated as below 3.20:

$$P_{flash} = \frac{n_{flash} \cdot R \cdot T}{V_{gas}} \tag{3.20}$$

Where:

P_{flash}	Pressure in Flash tank
n_{flash}	Net gas moles in flash tank
V_{gas}	Gas volume in flash tank
R	Universal gas Constant
T	Temperature

3.2. FM Model

The working of the FM sub-system has been explained in section 1.3.2. FM sub-system has two main functions, to dehumidify the CO_2 captured by DAC to $\leq$ 2 % relative humidity levels and then compress the dried CO_2 to high pressure (55 bar) for use downstream in the MS sub-system. One of the major focus area for the thesis was to identify the operational scenarios arising out of integration of DAC and FM sub-system and to design control schemes to control the integrated system. For this, it was required to model the behaviour of the FM system and integrate this model with DAC system model (described in previous section 3.1). In the next section, the modelling of components of the FM sub-system has been described.

3.2.1. Compressor Model

The compressor in the FM sub-system compresses the captured CO_2 to higher pressures (55bar). The compressor model developed for this work uses the compressor parameters to describe the mass/mole flow in the FM sub-system. The vapor output from the DAC sub-system is drawn to the FM sub-system by the suction of the compressor. The flow compressed by the compressor is sent to the buffer tank for storage and further use downstream. From the buffer tank, a part of flow is diverted back to the DAC flash tank to control the pressure in the flash tank(described in Flash tank model in section 3.8).

The schematic of the Compressor model is shown in Figure3.11 below.

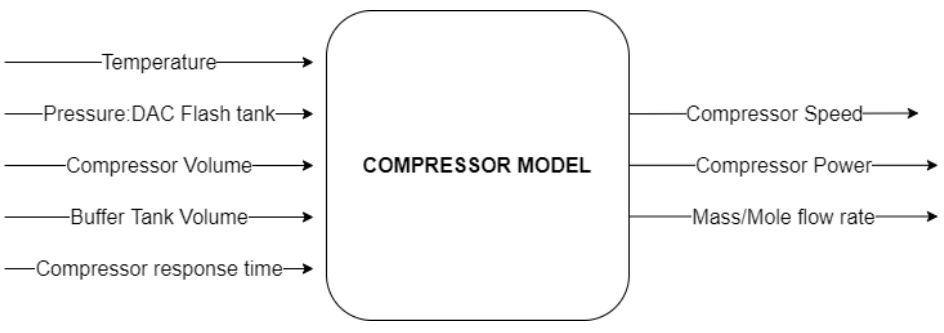

Model Assumptions

The assumptions used in the compressor model are mentioned below:

1. The compressor model was based on experimental investigation on a different compressor model (lower compressor capacity) than the one currently being used in the ZEF FM system (higher capacity compressor). It has been assumed that the results for the new compressor would scale directly with the compressor volume and all other factors will remain the same.

2. The leakage factor and volumetric efficiency are modelled to be a only function of compressor speed. In the actual system, with the efficiency will vary depending on production tolerance, operating temperature, pressure ratio etc.

3. The pressure drop due to flow through the FM system has been neglected.

4. The inlet of the compressor is assumed to be at thermal equilibrium with the flash tank and ambient temperature.

5. It has been assumed that the drying system behaves ideally and the input to the compressor is only pure CO_2.

6. For modelling the flow across the capillary tube, Darcy-Weisbach equation has been used and it has been assumed that the flow is incompressible. For low pressures ($\leq$10 bar), the assumption will not lead to major deviation, however for modelling high pressure system, the assumption will not hold.

7. The response time of solenoid valve operations have not been considered.

8. Compressor response time has been considered to be constant for the entire compressor speed range.

Model Inputs

The inputs used for the compressor model are mentioned below:

- **Temperature:** The vapour outlet from the DAC Flash tank, which is assumed to be in thermal equilibrium with the ambient temperature. The same temperature is taken as input temperature for the compressor model and is used to calculate the density at suction, compressor power requirement and mass/mole flow rate.

- **Pressure DAC Flash Tank:** DAC Flash tank pressure is used as an input to the PID controller which determines the compressor operating speed so as regulate the mass/mole flow and maintain the flash tank pressure at atmospheric pressure level.

- **Compressor Volume:** Compressor volume or cubic capacity is the volume of compressor chamber that is swept per rotation of the compressor. This is a user defined input to the model to determine the mass/molar flow rate.

- **Buffer Tank volume:** Buffer tank volume is also user defined input. It determines the buffer tank pressure based on compressor mass flow rate into the buffer tank. Further, the pressure of the buffer tank determines the bypass flow rate going back to the flash tank for pressure control.

- **Compressor response time:** Compressor response time can be described as the time taken by the compressor to reach the defined set-point speed. This is the physical lag which will be present in the system due to its inertia. The same was be determined experimentally on the test setup and was used as input to the system.

Symbol	Input Parameter	Unit
T_{amb}	Ambient Temperature	[^{o}C]
P_{flash}	Flash tank pressure	[Pa]
V_{cmpr}	Cubic capacity of compressor	[m^3 s^{-1}]
V_{buffer}	Flash tank volume	[m^3]
T_{res}	Compressor response time	[rpm s^{-1}]

The outputs from the compressor model are mentioned below:

- **Compressor Speed:** In order to control the pressure in the flash tank, a PID controller is used to determine the compressor speed which in turn determines the compressor mass/mole flow rate.
- **Mass/mole flow rate**; The compressor speed determined by the PID controller along with compressor capacity, inlet temperature and net efficiency is used to calculate the compressor mass/mole flow rate as per equation 3.21 and 3.22 described in section 3.2.1.
- **Compressor Power:** The model also determines the compressor power consumption using equation 3.27 described in section 3.2.1.

Symbol	Input Parameter	Unit
N_{rpm}	Compressor speed	[rpm]
$\acute{m}_{cmpr}$	Compressor mass flow rate	[kg s^{-1}]
P_{cmpr}	Compressor Power	[W]

Model Description

Mass Flow through Compressor For modelling the mass flow through the compressor, following are the main equations which were considered [52].

$$\dot{V}_{cmpr} = V_{cc} * \frac{N_{rpm}}{60} * \eta_{vol} * (1 - f_{leak}) \tag{3.21}$$

$$\dot{M}_{cmpr} = \dot{V}_{cmpr} * \rho_{\text{suction}} \tag{3.22}$$

$$\dot{n}_{\text{cmpr}} = \dot{M}_{\text{cmpr}} / mw_{\text{suction}} \tag{3.23}$$

Where:

$\acute{V}_{cmpr}$	Compressor volumetric flow rate
V_{cc}	Cubic capacity of compressor
N_{rpm}	Compressor Speed (in rpm)
η_{vol}	Volumetric efficiency of compressor
f_{leak}	Leakage factor
$\acute{M}_{cmpr}$	Compressor mass flow rate
$\rho_{suction}$	Density of gas at compressor inlet
$\acute{n}_{cmpr}$	Compressor molar flow rate
$mw_{suction}$	Molar mass of gas at compressor inlet

Volumetric Efficiency For estimation of volumetric efficiency, actual mass flow measurement data from ZEF's compressor test setup, as seen in Figure[3.12] below, was used.

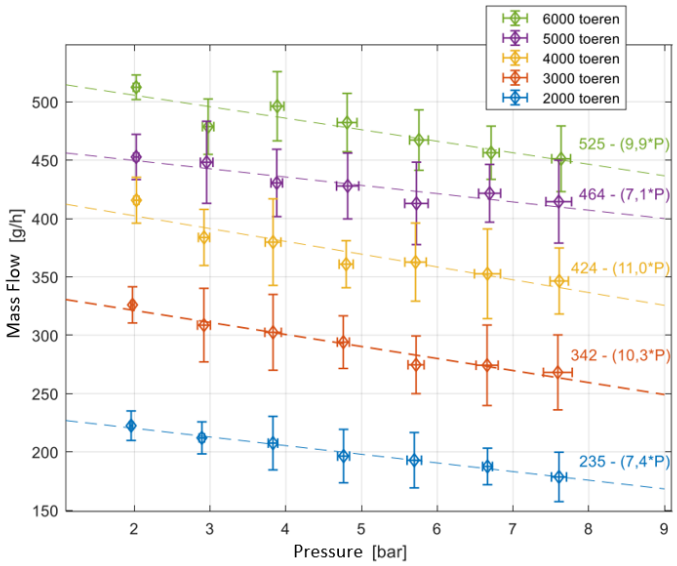

Figure 3.12: Actual Mass flow vs Discharge pressure of compressor for different compressor speed [53]

Since in the actual measurements, the effect of leakage factor and volumetric efficiency get combined, so using the above data a net efficiency factor (η_{net}) which is defined as given in equation 3.24 below was defined.

$$\eta_{net} = \eta_{vol} \cdot (1 - f_{leak}) \tag{3.24}$$

Using the experimental results shown in Figure[3.12], the net efficiency is then estimated a function of compressor speed.

$$\eta_{\text{net}} = f\left(N_{rpm}\right) \tag{3.25}$$

With these values, equation 3.21, 3.22 and 3.23 can be calculated for different compressor speeds and the mass/mole flow at compressor suction can be calculated.

Compressor Temperature and Energy requirement

The compressor discharge temperature will be calculated using the polytropic compression equation 3.26 given below [54]:

$$T_2 = T_1 \left(\frac{P_2}{P_1}\right)^{\frac{\gamma_c - 1}{\gamma_c}} \tag{3.26}$$

For calculation of compressor work, following equation is used:

$$W_{\text{comp}} = \frac{\dot{m}_{cmpr}}{\eta_{\text{cmpr}}} \left[\frac{\gamma_c}{\gamma_c - 1}\right] \frac{P_1}{\rho_1} \left[\left(\frac{P_2}{P_1}\right)^{\gamma_c - 1/\gamma_c} - 1\right] \tag{3.27}$$

Where:

T_1	Compressor inlet temperature
T_2	Compressor outlet temperature
P_1	Compressor inlet pressure
P_2	Compressor outlet pressure

γ_c	Polytropic coefficient
$\acute{M}_{cmpr}$	Compressor mass flow rate
$\eta_{\ cmpr}$	Compressor efficiency
ρ_1	Density at compressor inlet

γ_c the polytropic coefficient used for the model is taken from the work of Bergstein et al. [48] on the ZEF compressor setup. The value of polytropic coefficient (γ_c) obtained was $\sim$ 1.05-1.1. For this model, γ_c=1.1 will be used.

3.2.2. Buffer Tank model

CO_2 buffer tank was modelled as a simple vessel with 1 inlet, the compressor outlet stream and 2 solenoid valve connected outlets, 1 bypass valve to the flash tank and 1 outlet valve to the downstream line via capillary tubes. The flow through the capillary tube is modelled using Darcy–Weisbach (shown in equation 3.28) [20] relation.

$$\frac{\Delta p}{L} = \frac{128}{\pi} \cdot \frac{\mu Q}{D_c^4} \tag{3.28}$$

Model Assumptions

The main assumptions used for the Buffer tank model are as below:

- The gas in the buffer tank is assumed to behave as an ideal gas.
- It is assumed that the compressor outlet stream is pure CO_2.
- The buffer tank is assumed to be at thermal equilibrium with the atmosphere.
- For the flow through capillary tube modelled using Darcy–Weisbach relation, it is assumed that the CO_2 gas in buffer tank behaves as incompressible gas and the flow is assumed laminar to simplify calculations. The assumption remains valid for low pressure difference between buffer tank and flash tank ($\leq \approx$ 8bar).

Model Inputs and Outputs

The model inputs for the Buffer tank model are below:

- **Mass/mole flow rate:** The mass/mole flow rate from compressor model is the inlet flow rate to the system.
- **Temperature:** As stated in the assumptions, the buffer tank temperature is considered to be same as ambient temperature.
- **Volume:** Buffer tank volume is user defined input.
- **Capillary Dimensions:** The dimensions of capillary tube is also user defined input.
- **Pressure gradient:** The pressure gradient between Buffer tank- flash tank and buffer tank-downstream line is an input to calculate flow across capillary tube.

The outputs of the Buffer tank model are as below:

- **Pressure:** Buffer tank pressure calculated assuming ideal gas behaviour is an output from the model.

- **Mass/Mole flow:** The mass/mole flow rate through the capillary tube is an output of the buffer tank model. The same is also used as input for the flash tank model to calculate net mole flow in the flash tank as described earlier 3.8.

3.3. Integrated DAC+FM Model

The micro-models described in section 3.1 and 3.2 were then integrated to get the final integrated DAC+FM sub-system. The control schemes were also incorporated in the integrated model and the same was then validated using the representative experimental setup. The experimental setup and validation results are explained in chapter 4.

3.3.1. Control Schemes

In order to ensure that the system behaves as per requirement, it is essential to include control schemes to deal with the disturbances. In a control system, the parameter that is required to be controlled is termed as control variable, the parameters which can be varied to control the system are called manipulated variables and variables which cannot be controlled are termed as external disturbances [55].

For the integrated system, process parameters are depicted in Figure[3.13 and 3.14] below. The same is discussed in detail in Chapter 5

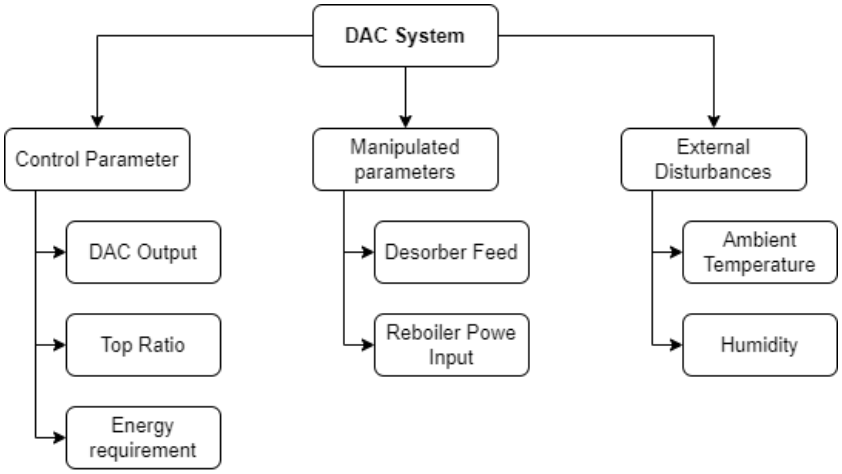

Figure 3.13: DAC system process parameters

The control schemes developed for DAC and FM system to ensure optimum output from the DAC and FM system are described below:

Production Control:
For the DAC system, production and energy targets have been described in Table[1.1]. This is the average target for the day and the actual production may be lower or higher than this value. For this purpose, a control strategy was designed which can be used to ramp-up or ramp-down the DAC production by varying the ratio of desorber feed flow (M_{feed}) to reboiler power input ($Q_{reboiler}$), ($\frac{M}{Q}$).

M_{feed} and $Q_{reboiler}$ are varied such that the ratio,($\frac{M}{Q}$) remains same. In this way, the production from DAC can be ramped up/down as per requirement. Figure[3.15] below represents this control scheme.

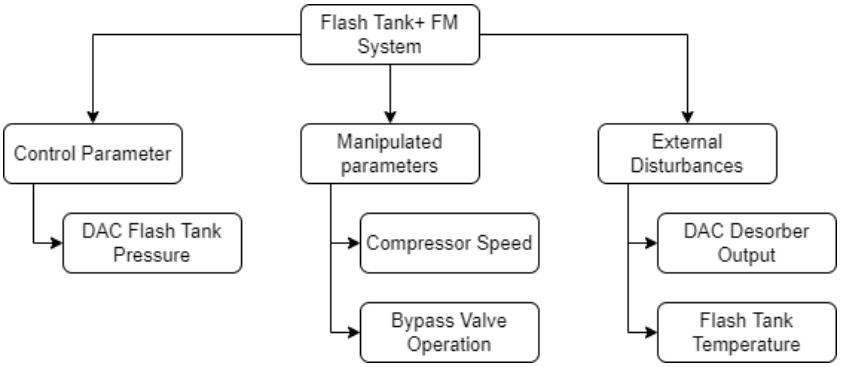

Figure 3.14: Flash tank+FM system process parameters

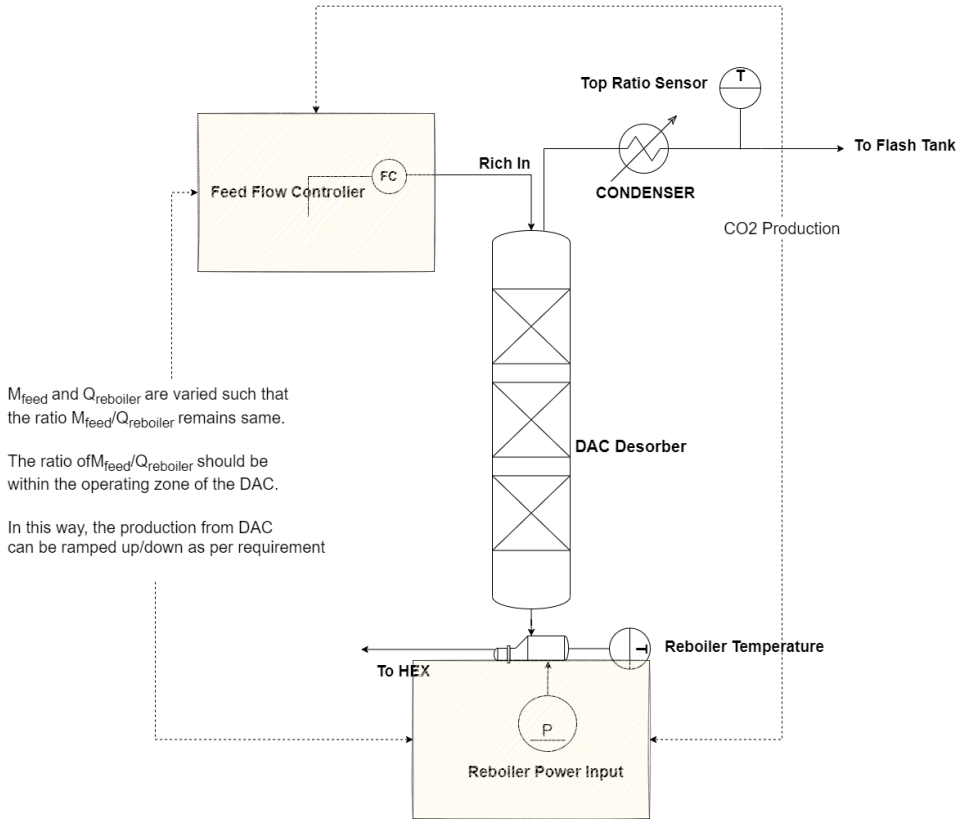

Figure 3.15: DAC production control loop

Assumptions

The main assumptions used for DAC production control scheme are as below:

-
- It is assumed that the system is under steady state operation and the changes made to ($\frac{M}{Q}$) ratio is after desorber is under steady state.
- The temperature limitation of 120^{o}C is applied on the system; this implies $Q_{reboiler}$ is only increased till desorber temperature is $\leq$ 120^{o}C.

- The mass transfer limitation in the desorber which can restrict desorption of CO_2 and H_2O at high M_{feed} is neglected while calculating the production from the desorber.

The working of the control scheme has been discussed in section 5.3.1.

Flash tank pressure control scheme:
The flash tank pressure control loop works to control the pressure in the flash tank by simultaneous operation of the Compressor and Bypass solenoid valve.
The compressor is operated using PID control and draws vapour from the flash tank and compresses and stores it in the buffer tank. From the buffer tank, a solenoid bypass valve is connected back to flash tank and operates based on flash tank pressure to control the pressure. In this way, the pressure is maintained in flash tank and continuous operation of the compressor is ensured.

The H_2O collected in the flash tank is periodically drained out via a solenoid valve which is operated based on the level sensor in the flash tank. This ensures that a minimum gas volume is always present in the flash tank which is necessary for the pressure control.

Schematic of the control developed for the flash tank pressure control is depicted in Figure[3.16] below.

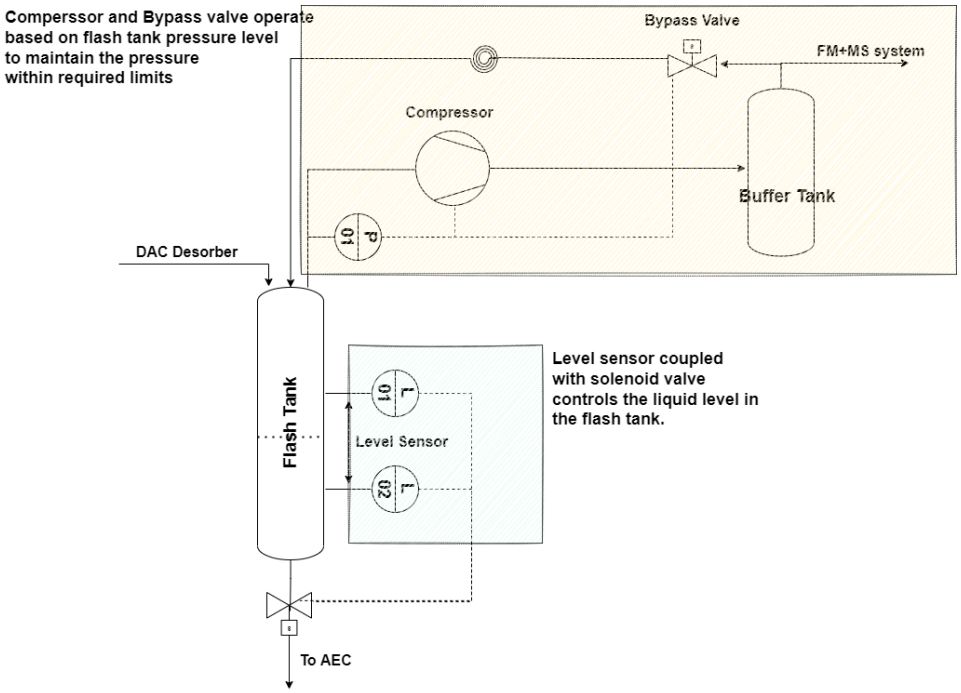

Figure 3.16: Flash tank pressure control loop

The working of the control scheme has been described in section (5.3.2).

4

Experiment setup and Methodology

In this chapter, the experimental setup for validation of system model and the pressure control scheme for the integrated DAC+FM system is described. The chapter covers the description of the setup, experiments performed and the assumptions considered for the experiments.

4.1. Experimental Setup

4.1.1. MiniDAC Setup:

In this section the experimental setup used for validation of the integrated DAC+FM model and operational scenarios is described in detail. The setup used (referred to as MiniDAC), is a prototype setup which was designed and built during previous teams at ZEF. The setup and the measurement points used for the experiments are shown in the P&I diagram in Figure 4.1 and the setup is shown in Figure 4.2 below.

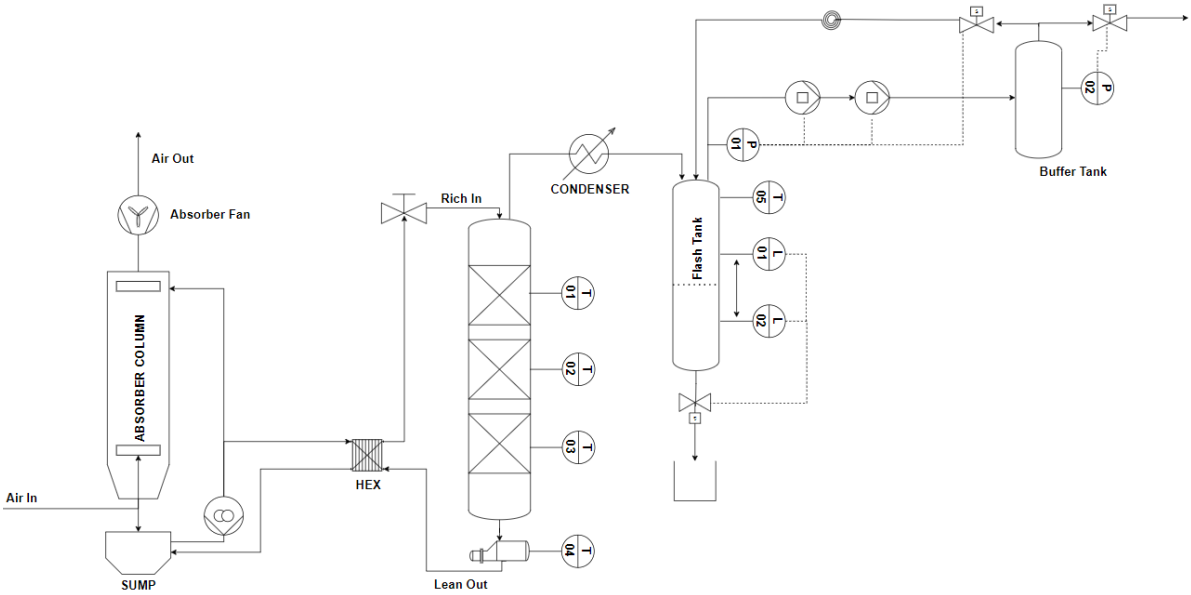

Figure 4.1: P&I diagram of MiniDAC test setup

The measurement points in the P&I diagram 4.1 represent the following:

Symbol	Measurement Parameter	Unit
T01	Desorber Temperature Point 1	$[^oC]$
T02	Desorber Temperature Point 2	$[^oC]$
T03	Desorber Temperature Point 3	$[^oC]$
T04	Re-boiler Temperature	$[^oC]$

Symbol	Measurement Parameter	Unit
T05	Flash Tank Temperature	$[^oC]$
P01	Flash Tank pressure	[Pa]
P02	Buffer Tank pressure	[Pa]
L01	Liquid level sensor flash tank 1	[-]
L02	Liquid level sensor flash tank 2	[-]

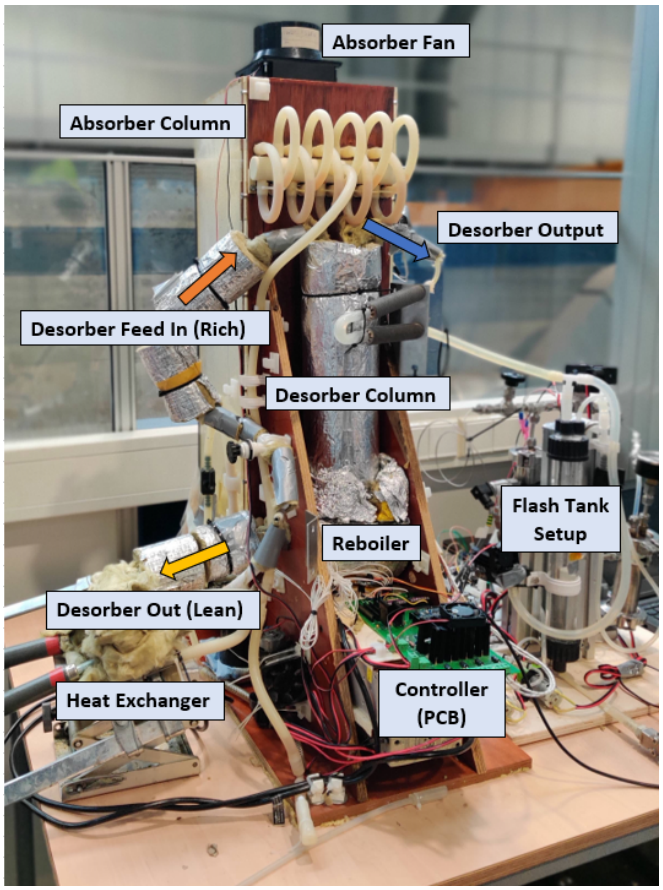

Figure 4.2: MiniDAC test setup

The process flow of the setup is described below:

- The recycle pump (RP) draws sorbent from the Sump, one part of which goes to the Absorber while the other part goes to the desorber. The mass flow to the desorber is controlled via a needle valve (NV), while the overall flow rate from the recycle pump is PWM controlled using Arduino, the interface and control for which developed by ZEF.

- The sorbent flowing to the desorber, goes through a heat exchanger where it is heated up using the hot sorbent exiting the reboiler.

- The Fan (F) which control the air flow in the absorber section is also PWM controlled using Arduino (same as recycle pump) using ZEF GUI.

- The temperature of the Reboiler (R) is PID controlled using Arduino using the ZEF GUI.

- As sorbent flows into the Desorber, it fills up till the level of sorbent reaches the overflow level, which is governed by the height at which the outlet sorbent outlet pipe is placed relative to bottom

of the desorber. The sorbent exiting the desorber goes through the heat exchanger, where it heats up the incoming rich sorbent and finally ends up in the absorber sump.

- The temperature of the reboiler governs the sorbent temperature in the desorber and as it reaches the boiling temperature of the sorbent, CO_2 and H_2O start to desorb from it. The vapor exits the desorber from the top.

- The vapour exiting the Desorber is passively cooled using the finned tube heat exchangers. This condenses the H_2O in the vapour, while CO_2 remains in gaseous form.

- This cooled H_2O and CO_2 mixture then go to the flash tank, where liquid settles at the bottom and vapour phase gets collected at the top part of the flash tank.

4.1.2. Flash Tank Setup

The Flash tank setup went through multiple iterations which is explained in detail in Appendix A. The P&I diagram of the final setup and the setup itself is shown in Figure 4.1 and 4.3 respectively.

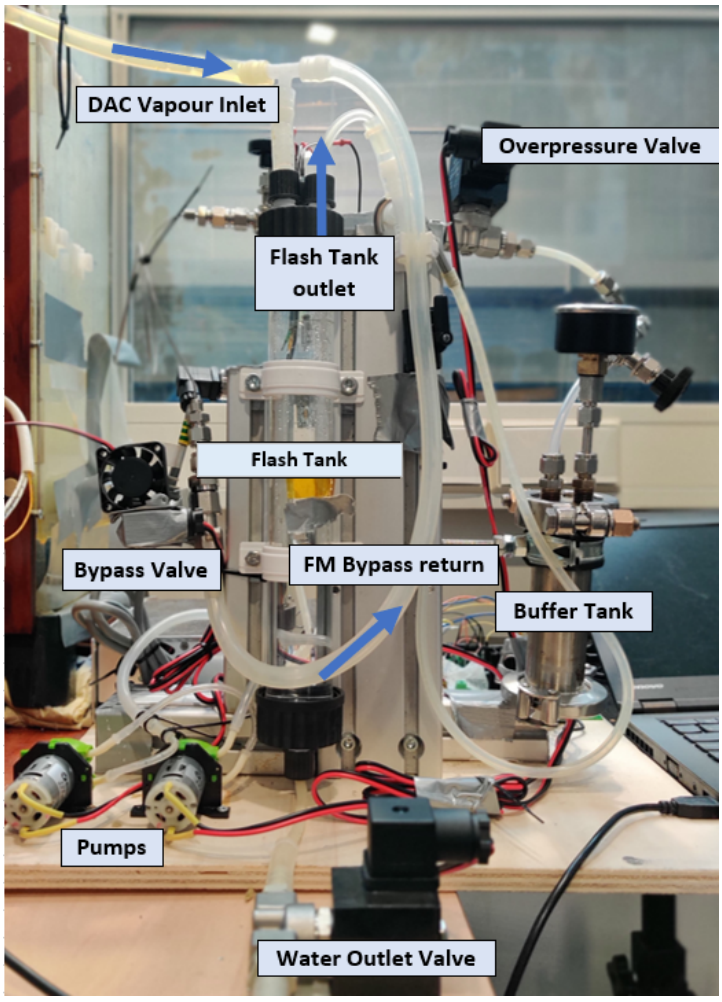

Figure 4.3: Flash tank test setup

The process flow of the setup is described below:

- The passively cooled CO_2 and H_2O mixture from DAC desorber, enters the flash tank. The liquid fraction settles at the bottom, while the vapour fraction is collected at the top part of the flash tank.

- The outlet of the flash tank is connected to two peristaltic pumps (P1 & P2) in series. These pumps are used to compress the vapour fraction of the flash tank outlet, and is then stored in the Buffer tank. The pumps are PID controlled based on the pressure in the flash tank using the ZEF Arduino GUI.

- The buffer tank has two outlets which are both connected to solenoid valves. One of the valves (V1) is operated based on the flash tank pressure to bypass fraction of compressed CO_2 through a capillary tube, back to the flash tank to maintain the pressure in the flash tank. The other valve (V2) operates to maintain the pressure in the buffer tank to the target pressure level.

- The pumps (P1 and P2) and the two valves (V1 and V2) operate together to control the pressure in the flash tank at the target level.

4.2. Experiments

4.2.1. MiniDAC Experiments

At first, experiments were performed in order to determine the performance of the MiniDAC system. The same is explained in detail below:

1. **Desorber Experiments:**
   In order to determine the desorber performance and use the data for model validation following experiments were performed. The results were also used to determine the control strategies to be used for integrated DAC+FM system.

   The results of the experiment are presented in the Appendix A

   (a) **Startup and Steady state**: In these experiments, the MiniDAC setup was run a fixed reboiler temperature set point, which was decided on the basis of previous experiments on MiniDAC at ZEF. The startup and steady state temperatures at different locations of the desorber column was measured. This data was further used to validate the dynamic behaviour of the system model developed for this work.

   (b) **Desorber Cool-down**: After running the desorber at target temperature till steady state, the feed to the desorber and the heater power input was turned off and the cooling down of the desorber was monitored. Using this data, the heat loss through the system was estimated and the same was used in the heat loss model for each stage the desorber model.

   (c) **Cyclic Capacity and Energy requirement:** For measurement of cyclic capacity, sorbent samples were collected from sump and desorber outlet to measure the sorbent rich and lean composition respectively using FTIR analysis (A) of the collected sample. Further, using the cyclic capacity, mass flow rate and reboiler power input, energy requirement for CO_2 capture using MiniDAC setup was measured. The same was also used to validate the desorber model.

   (d) **CO_2 purity measurement:** The purity of CO_2 in the vapour stream desorbed from the MiniDAC setup was measured using Haffmans CO_2 purity tester setup [56]. The results obtained were used to validate the flash tank model. (A)

   Assumptions for the experiment:

   - It is assumed that the vapour stream from Desorber is the binary mixture of CO_2 and H_2O and behaves as an ideal gas.

   - The setup is assumed to be leak tight and same was tested before starting experiments. Hence the pressure fluctuations observed are only due to desorption/absorption of CO_2 and H_2O into the sorbent.

- The pressure drop within the desorber column is neglected.
- The feed flow rate of sorbent in the desorber is assumed to be constant. The same is regulated using a needle valve and the setting of the needle valve was kept constant during all the experiments.

2. **Absorber Experiments:**
   In order to determine the absorber performance and use the obtained results to develop and validate the absorber model, following experiments were performed.

   (a) **Loading vs Humidity:** In order to quantify the effect of absolute humidity on rich loading of water in the sorbent, experiments were performed with only the absorber running (i.e. desorber was kept off) and sorbent samples were collected at specific intervals. The humidity and temperature during the test was logged and the samples were analysed using FTIR to measure the effect of humidity on water loading in the sorbent.

   Assumptions:

   - The rate of air flow, counter current to flow of sorbent assumed to be constant and is controlled using PID controlled Fan. The Fan setting was kept constant for the tests.
   - The sorbent flow rate to the absorber is assumed to be constant. The same is controlled using PID recycle pump. The pump settings are kept constant throughout the tests.
   - The composition of the sump is assumed to be uniform. The time between sorbent sample collection was kept much higher ($\approx$ 10 times) than residence time of sorbent in the absorber column.

The results of the experiment are presented in the Appendix A.

4.2.2. Flash tank experiments:

Before starting the experiments to identify control schemes for the integrated DAC+FM system, it was necessary to identify the operating scenarios the integrated system will encounter. The identified operating scenarios (for system with no leaks) are described below:

1. The outlet of the DAC flash tank is connected to the compressor in the FM system. So, when CO_2 starts filling in the flash tank. If the flow out of flash tank to the FM system is lower than inflow (due to compressor malfunction or low mass flow from compressor), then pressure in the flash tank and thus the desorber will start rising. This will start pushing the liquid sorbent out of the desorber and at the extreme all the sorbent will be pushed out and DAC operation will stop. The same is depicted in Figure[4.4] below. Since the density of sorbent is $\approx$ 1000 kg m^{-3}, so 1cm of liquid corresponds to $\approx$ 1 mbar of hydro-static pressure given by equation 4.1.

$$P = \rho g h \tag{4.1}$$

   Where:

P:	Fluid Pressure
ρ:	Fluid density
g:	Acceleration due to gravity
h:	Height of fluid

   For MiniDAC setup, height of sorbent in the desorber column, (shown as $h_{sorbent}$ in Figure[4.4]

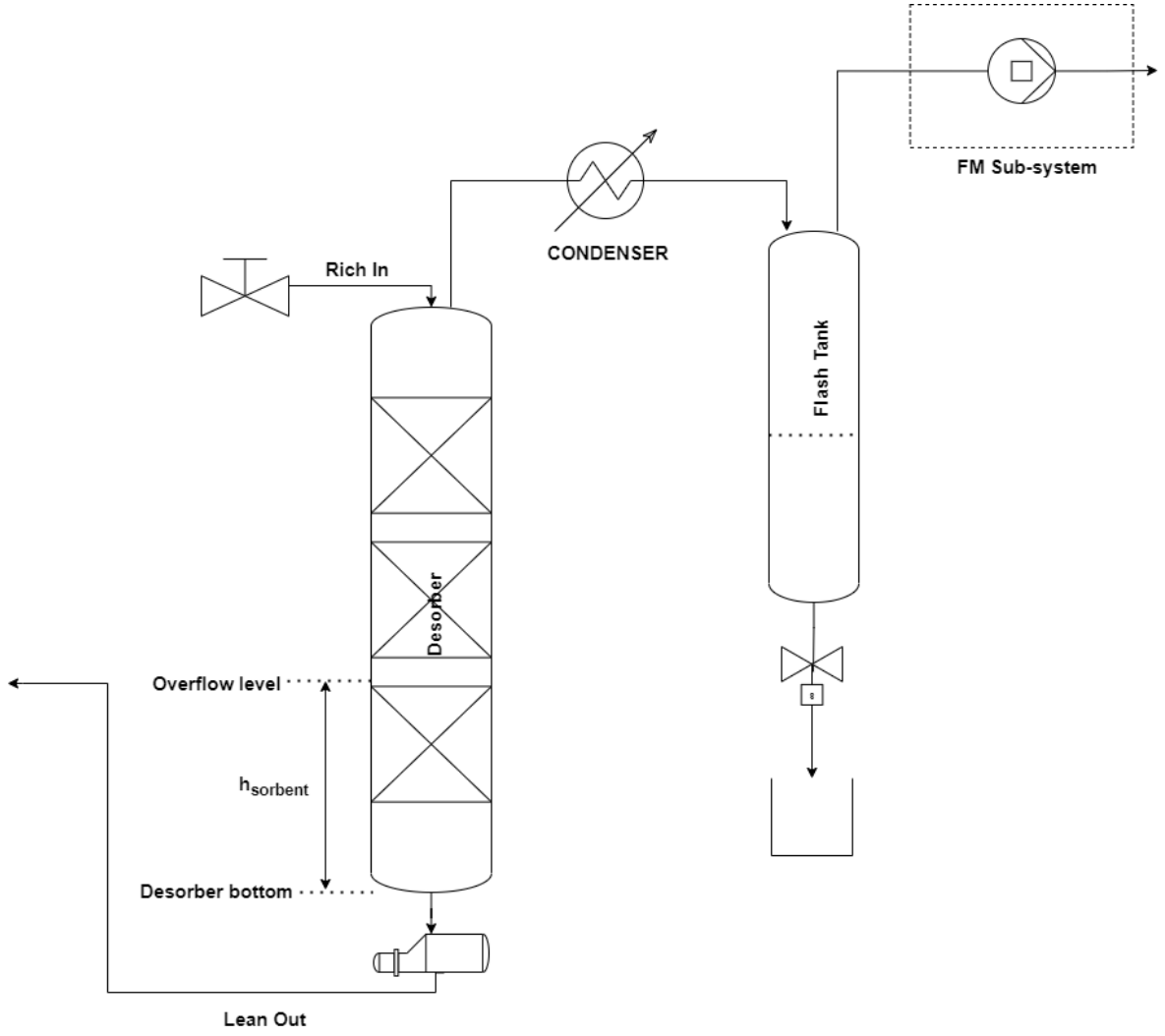

Figure 4.4: In case of high pressure in the system, sorbent will start overflowing out of desorber, and at extreme limit all sorbent will be purged out of desorber

is 10cm, so the safety limit for higher pressure in the system will be 10mbar above atmospheric pressure. As operation limit for this work, the higher pressure limit was defined at 5mbar above atmospheric pressure.

2. For 2^{nd} scenario, the compressor operating to draw vapour from the flash tank can operate at higher mass flow than inlet flow from DAC to the flash tank. This will result in suction pressure in the flash tank and at the extreme if the suction pressure becomes too high, it can result in sorbent being drawn out from the desorber to the flash tank, or can results in drawing in air from the desorber overflow line as shown in Figure[4.5].

   For the MiniDAC, h_{vapour} (which is total desorber height minus the height of sorbent in desorber), is 20cm while h_{sump} is 35cm. So, using equation 4.1, the safety limit for low pressure is 20mbar below atmospheric. For operation limit for this work, the low/suction pressure limit was defined at 5mbar below atmospheric pressure.

3. The last scenario identified for the integrated system, was after shutdown of the system which can be due to end of the production period, power unavailability, issue in systems downstream etc. In this condition, as the sorbent in the desorber cools down, the H_2O vapour will start to re-condense and the desorbed CO_2 still in the desorber will be reabsorbed by the sorbent. This will

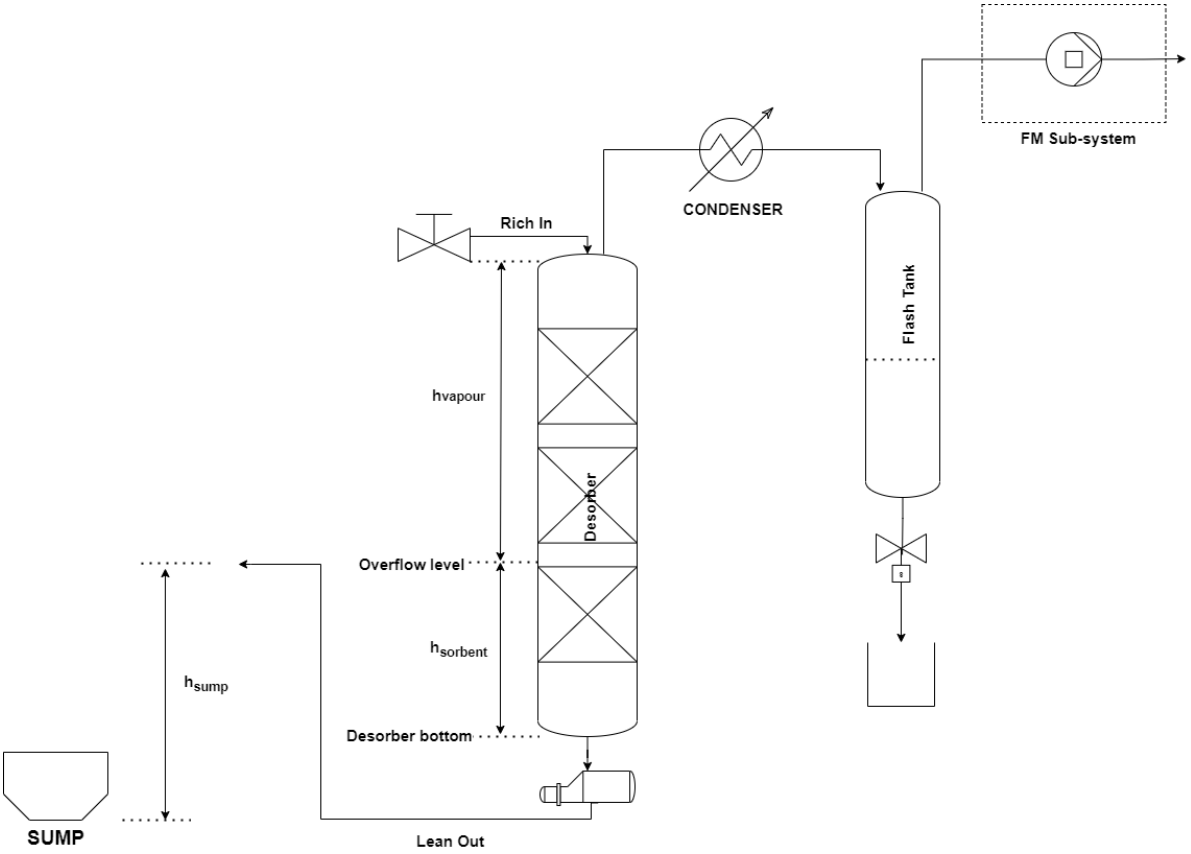

Figure 4.5: In case of suction pressure in the system, sorbent will be drawn into the desorber from overflow line and in extreme case either the sorbent can flow into the flash tank or it may start drawing air from the overflow line.

create suction pressure in the system and can lead to a situation similar to what was described in the previous scenario.

With these scenarios, the target for the flash tank pressure control experiments was identified as below:

Table 4.3: Pressure limit for the MiniDAC system

Parameter	Description	Safety Limit	Operation Limit	Unit
P_{max}	Max pressure in flash tank (above P_{atm})	10	5	[mbar]
P_{min}	Min pressure in flash tank (below P_{atm})	20	5	[mbar]

- **Integrated MiniDAC+Flash Tank experiments:**
  The main objective of the flash tank experiments have been described in section 4.3. To achieve the same, multiple configurations of the experimental setup as described in Appendix A, were designed and implemented. The P&I diagram of the final setup is shown in Figure 4.1. The experiments performed included the following:

  1. The pump PID control and control of solenoid valve, V1 and V2 was calibrated to ensure the pressure in the system was maintained within $\pm$5 mbar relative to atmospheric pressure as per the requirement mentioned in 4.3.

2. The effect of gas volume in flash tank (Flash tank volume-Liquid volume in flash tank), on pressure fluctuations were evaluated.

3. The maximum pressure level in the buffer tank to ensure the pressure level target for flash tank control is met was determined experimentally.

The assumptions used for these experiments are mentioned below:

- The vapour mixture in the flash tank was assumed to behave as an ideal gas. The assumption holds as the maximum pressure in the system, which was in the buffer tank system was limited to 2.2bar.

- The system was assumed to be leak proof. The leak tightness of the system was checked before the experiment and thus the pressure fluctuation in the system are only on account of vapor from desorber, mass flow due to pump and valves in the system.

The results of the experiment are presented in section 5.3.2.

5

Results and Discussions

In this chapter the research questions and objectives identified in Chapter1 are discussed in detail and answers to the same are provided.

5.1. System performance parameters:

What parameters influence the performance of DAC+FM system and their effect on each sub-system?

In order to understand the effect of external disturbances on the performance of DAC+FM system, the impact on individual sub-system of DAC+FM system was evaluated.

5.1.1. DAC System:

In previous works at ZEF [26],[19], the parameters which affect the DAC performance were evaluated in detail. The main parameters are listed below:

- **Absorber Parameters:**
  - **Ambient Temperature:** The absorption of CO_2 in the sorbent is an exothermic reaction and is more favourable at lower temperatures [22]. Figure[5.1] shows the VLE loadings of CO_2 in TEPA-H_2O mixture for different temperature and CO_2 partial pressure.

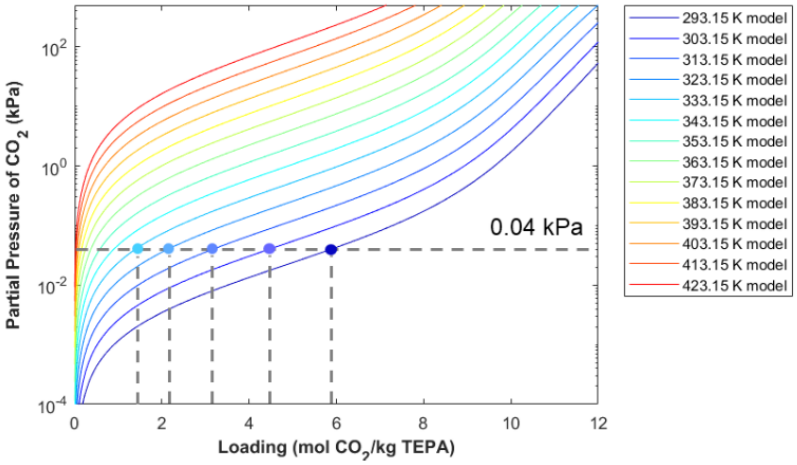

Figure 5.1: CO_2 loading in 80%TEPA-20%H_2O mixture for different temperatures. The dotted line at P=0.04 kPa is the partial pressure of CO_2 in atmosphere. CO_2 loading in TEPA goes down with increase in temperature[19]

As can be seen from the graph, CO_2 VLE loadings decrease with increase in temperature, and thus the rich CO_2 loading in the sorbent will be impacted by ambient temperature.

  - **Humidity:** H_2O loading in the sorbent is majorly affected by the absolute humidity of the ambient air. The rate of absorption of H_2O as compared to rate of CO_2 absorption, is also

an order of magnitude higher for the sorbent which has been selected by ZEF [26]. Figure [5.2] depicts the impact of humidity on VLE loading of H_2O in the sorbent.

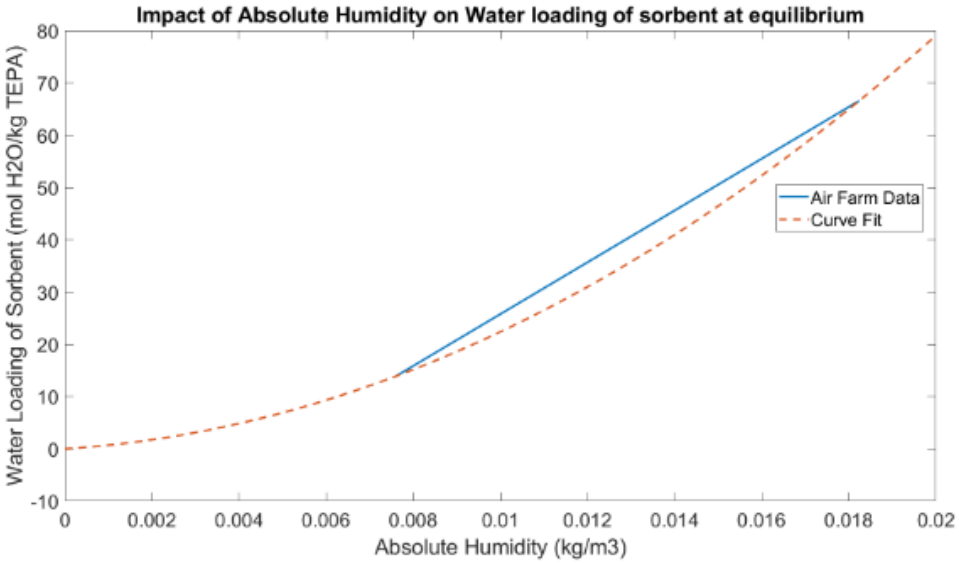

Figure 5.2: Effect of absolute humidity on equilibrium water loading in the sorbent [26]

Moreover, the H_2O loading in the sorbent affects the viscosity; viscosity of sorbent decreases with increase in H_2O loading and vice-versa. This has an impact on the power required to pump the sorbent.

- **Absorber area/length:** This is a design parameter and does not change during the operation of the DAC system. The area/length of the absorber and the STY of CO_2 and H_2O, determine the amount of each species that is absorbed as the sorbent moves through the absorber.

- **Sump Holdup:** Sump holdup, or mass of sorbent acts as dampener for change in concentrations in the sump due to mixing of rich and lean sorbent streams. Higher the sump holdup, more the dampening effect on sump concentrations [27].

- **Desorber Parameters:**

  - **Desorber feed flow rate:** The feed flow rate to the desorber directly affects the production from the DAC. At the same time, the energy required to heat up the feed also increases with increase in feed flow rate, hence in order to control production, desorber flow rate and reboiler power input should be varied in conjunction. The same in explained in section 5.3.1.

  - **Feed inlet temperature:** Feed inlet temperature directly affects the reboiler power required to heat up the feed to desorption temperature. The desorber feed passes through the heat exchanger where it is heated up with hot lean sorbent exiting the desorber. Higher the feed temperature, better the efficiency of the CO_2 production.

  - **Desorber Temperature:** Desorption of CO_2 and H_2O from the sorbent is favourable at higher temperatures. Previous work by Dubhashi et.al, [27] has showed that higher desorber temperatures, lower lean loadings are possible at lower holdup time.
    However, at higher temperature ($\approx$ 120^{o}C) sorbent degradation also becomes prominent. For ZEF's DAC system, maximum temperature of 120^{o}C has been selected as the target to ensure degradation remains within limits.

  - **Sorbent Holdup:** Sorbent holdup in the desorber constitutes a major portion of system thermal mass which needs to be heated up to desorption temperature. This also determines the hold up time of sorbent in desorber.

  - **System pressure:** System pressure determines the VLE conditions in the desorber. Previous work at ZEF [57],[27], showed that by increasing the system pressure the top ratio and energy requirement of the DAC system can be improved at fixed desorber temperature. However, for as per ZEF's requirement the target is to operate the desorber at atmospheric pressure in-order to simplify the overall system and reduce the failure points in the system.

    However, for ZEF DAC system, target is to operate at atmospheric pressure. Operating at atmospheric pressure simplifies the entire system as it eliminates the requirement of pumps and valves to maintain high pressure in the system; thereby reducing the failure points in the DAC system.

    Appendix C contains more detailed information on the same

- **DAC Flash Tank Parameters:**

  - **DAC Desorber outlet:** DAC desorber outlet is the input and the external disturbance for flash tank system.

  - **Flash tank volume:** Volume of flash tank is inversely related to the pressure fluctuation in flash tank, i.e., higher the volume lower the pressure fluctuation.

  - **Flash tank temperature:** Flash tank temperature influences the vapour-liquid fraction of CO_2 and H_2O in the flash tank. At higher temperature, the fraction of H_2O in the vapour phase is higher and vice-versa.

    Appendix C contains more detailed information on the same

5.1.2. FM System:

- **DAC Vapour fraction:** Vapour fraction in DAC flash tank is the input and an external disturbance for the compressor system.

- **Compressor capacity:** Mass flow rate of the compressor is directly related to compressor capacity, i.e., swept volume per stroke. Higher the capacity, higher the volumetric/mass flow rate of compressor.

- **Compressor Speed range:** The minimum and maximum operating speed of the compressor is determined by the manufacturer. This determines the operating range of the compressor.

- **Response time:** Compressor response time is the time taken by the compressor to reach steady state when compressor speed is changed from one speed to another. Higher the response time, longer the time taken by compressor to reach steady state.

5.1.3. Summary:

Figure[5.3] below depicts the parameters which affect the performance of the DAC+FM system.

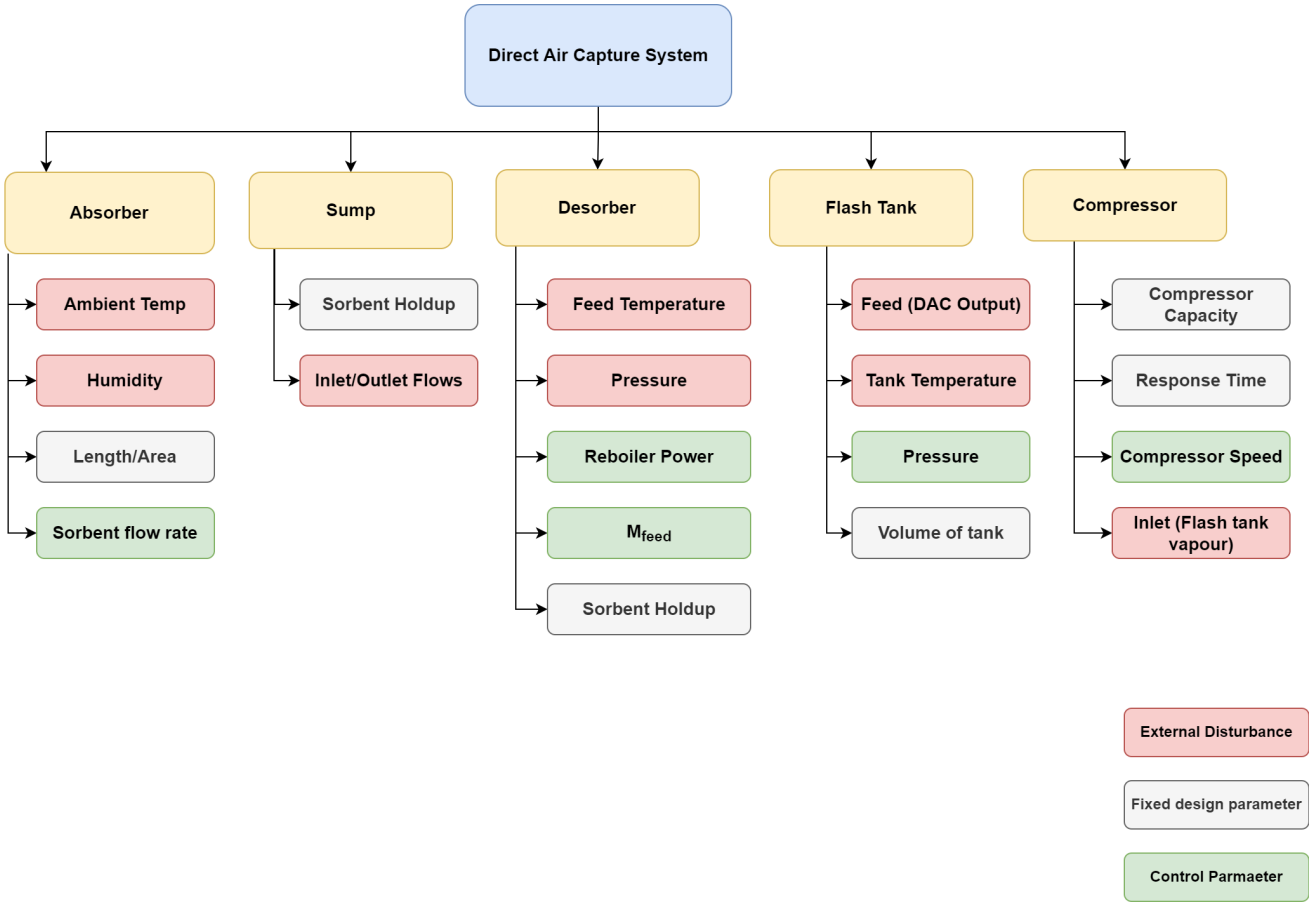

Figure 5.3: Parameters which affect the performance of the DAC+FM system

5.2. Operational scenarios for DAC+FM system:

What are the operating scenarios under which ZEF DAC+FM system will operate and what process constraints are associated with operation under these scenarios?

For determining the operating scenarios of the DAC+FM sub-system, the operation limit for each subsystem was first identified.

5.2.1. DAC System:

For the DAC system, the external disturbances and process parameters which affect the system performance and output have been mentioned in section 5.1.1. The combination of these external disturbances, i.e., Absolute humidity and ambient temperature and process parameters i.e., desorber feed flow rate and desorber temperature/heat input will result in the following operational scenario for the DAC system. Figure 5.4 summarises the operational scenario for the DAC system, which have been explained in detail in the next section.

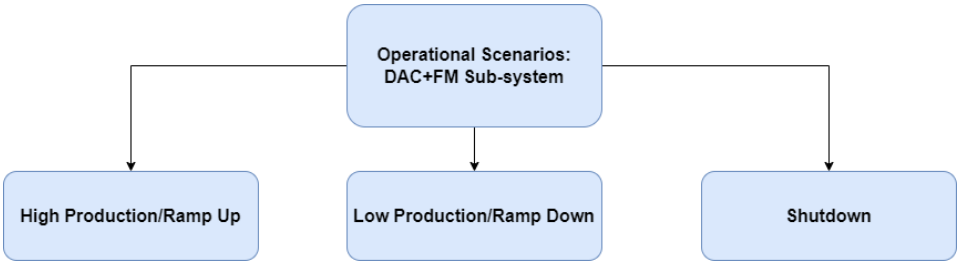

Figure 5.4: DAC Operational scenarios

High Production/Ramp-up:

One of the operational scenarios for the DAC system is high production/production ramp-up of DAC. The same is described in Table[5.1] below.

Table 5.1: External disturbance like High humidity, low ambient temperature will result in higher rich H_2O and CO_2 loading in the sorbent which will result in higher desorber output. Similarly, increase in sorbent feed to the desorber and/or heat input/desorber temperature will also increase the desorber output

Parameter	Condition	Effect
Humidity	High humidity: High H2O rich loading	High DAC output
Temperature	Low temperature: High CO2 rich loading	
Mass flow	Increase in desorber mass flow (*constant desorber temperature)	
Desorber Heat Input	Higher heat input (*constant mass flow)	

Low Production/Ramp-down:

Another operational scenario for the DAC system is lower production/production ramp-down of DAC. The same is described in Table[5.2] below.

Table 5.2: External disturbance like low humidity, high ambient temperature will result in low rich H_2O and CO_2 loading in the sorbent which will result in lower desorber output. Similarly, reducing sorbent feed to the desorber and/or heat input/desorber temperature will also decrease the desorber output

Parameter	Condition	Effect
Humidity	Low humidity: Low H2O rich loading	Low DAC output
Temperature	High temperature: Low CO2 rich loading	
Mass flow	Lower desorber mass flow (*constant desorber temperature)	
Desorber Heat Input	Lower heat input (*constant mass flow)	

System Shutdown:

Shutdown of the DAC system, which can be due to end of production period, power unavailability or downstream system issue is another operational scenario the DAC system will encounter. Figure 5.5 depicts the scenario of DAC system shutdown.

After system shutdown, as the desorber cools down the evaporated H_2O will start condensing, followed by re absorption of desorbed CO_2. If the system is leak tight, then this will result in suction pressure (below atmospheric) in the system, else if the system is not leak tight, then air will be drawn in the system to take place of the condensed/re-absorbed vapour. Figure 5.5 depicts the scenario of DAC system shutdown.

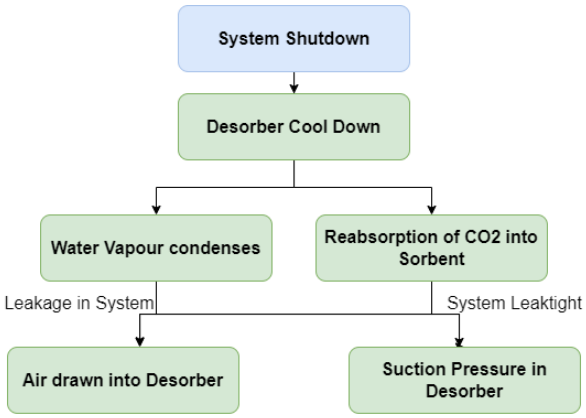

Figure 5.5: DAC shutdown will result in cooling down of the desorber which will result in condensation of H_2O vapour and re absorption of CO_2 in the sorbent. This will ultimately result in suction pressure in the system if it is leak tight, else it result in air being drawn into the system

DAC Operation limit: For the operational limits, maximum production rate for CO_2 was considered 1.5 times the average daily production target for CO_2 while the minimum rate was considered as the no production condition. This gives the operation range for CO_2 output from DAC, tabulated in Table 5.3 below.

Table 5.3: DAC Desorber Operation range

Parameter	Description	Value	Unit
CO_{2max}	Maximum CO_2 production rate from DAC	3.26E-3	[mol s^{-1}]
$CO_{2target}$	Target CO_2 production rate from DAC	2.17E-3	[mol s^{-1}]
CO_{2min}	Minimum CO_2 production rate from DAC	0	[mol s^{-1}]

5.2.2. FM System:

For the FM sub-system the operational limits is set as the compressor operation limit. The same was determined experimentally at ZEF. The compressor specification finalised by the FM team at ZEF are mentioned in Table[1.3]. For this compressor, the minimum and maximum flow rate was determined experimentally at ZEF, which will be used as the operational limit for the FM system, shown in Table 5.4 below.

Table 5.4: FM Compressor Operation range

Parameter	Description	Value	Unit
$\acute{n}_{cmpr-max}$	Max Compressor flow rate	7.92E-3	[mol s^{-1}]
$\acute{n}_{cmpr-min}$	Min Compressor flow rate	3.17E-3	[mol s^{-1}]

5.2.3. DAC+FM system

From Table 5.3 and 5.4 it can be seen that there is a range of DAC and Compressor operation, for which there is a mismatch between minimum compressor flow rate and DAC production rate. The same is shown in Figure5.6 below.

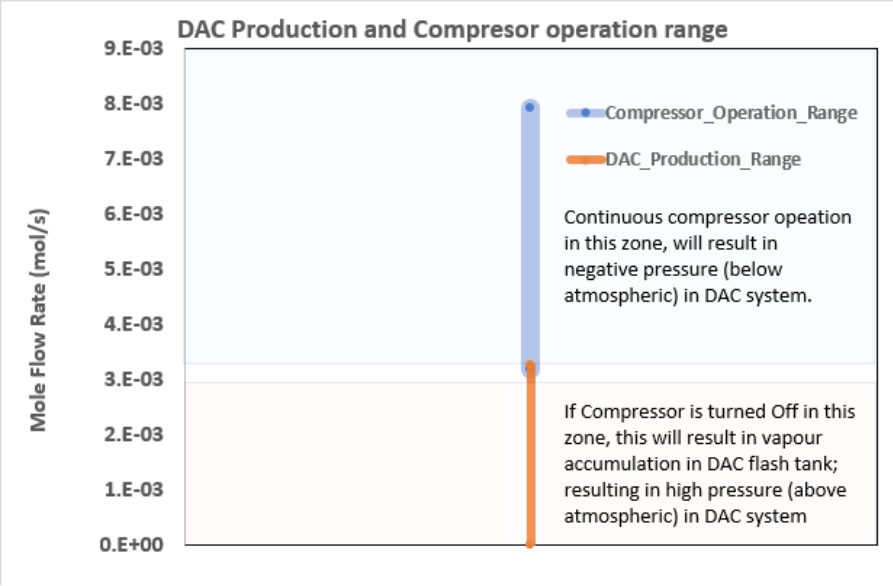

Figure 5.6: DAC Production and Compressor operation range. It can be seen that there is a very small zone of overlap between them. Thus, if DAC production is lower than the minimum compressor operation zone, then for this region there will be more flow drawn by FM sub-system from the DAC flash tank than flow entering flash tank from DAC desorber.

- If DAC production is lower than the minimum compressor operation limit, then for this region there will be more flow drawn by FM sub-system from the DAC flash tank than flow entering flash tank from DAC desorber; this will result in suction pressure in the DAC system.

- If the compressor remains off during the period where DAC production is below compressor minimum operation, then it will result in more flow into the flash tank, resulting in high pressure in the DAC system.

A possible solution for this is to run the compressor in intermittent manner, (ON-OFF control). However, the same is not desirable, as repeated On-Off compressor operation can result in excessive wear in compressor resulting in reduction in compressor lifetime.

The process constraints that integrated DAC+FM system will encounter is described below:

Sorbent overflow due to high pressure:

This operational scenario will arise when production from DAC is accompanied with *compressor operating at mass flow lower than DAC production* (or compressor malfunction).

This will result in higher pressure in the DAC system as accumulation will take place in DAC flash tank, and in worst case will lead to sorbent from desorber being purged out due to pressure on liquid column. The maximum pressure limit is determined by the sorbent level in the desorber (4.2.2).

Figure 5.7 depicts the scenario described above.

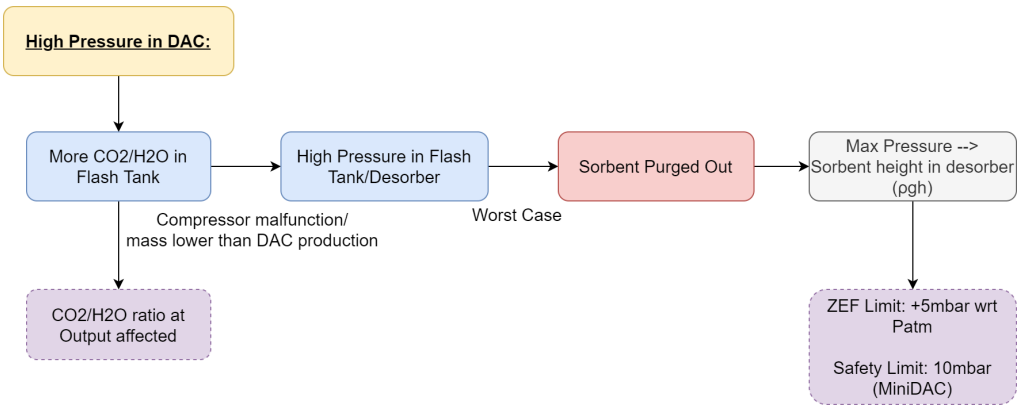

Figure 5.7: Operational scenario which will result in high pressure in the DAC system which in worst case will result in sorbent being purged out of desorber

Sorbent drawn in due to low pressure:

This operational scenario will arise when production from DAC is accompanied with *compressor operating at mass flow higher than DAC production*.

This will result in suction pressure in the DAC system as more moles will be removed from flash tank by compressor than being added by Desorber. In worst case, it will lead to sorbent overflowing from desorber to the flash tank or air being drawn in from overflow port depending on gas height in desorber column and height of overflow port from sump (4.2.2).

Figure 5.8 depicts the scenario described above.

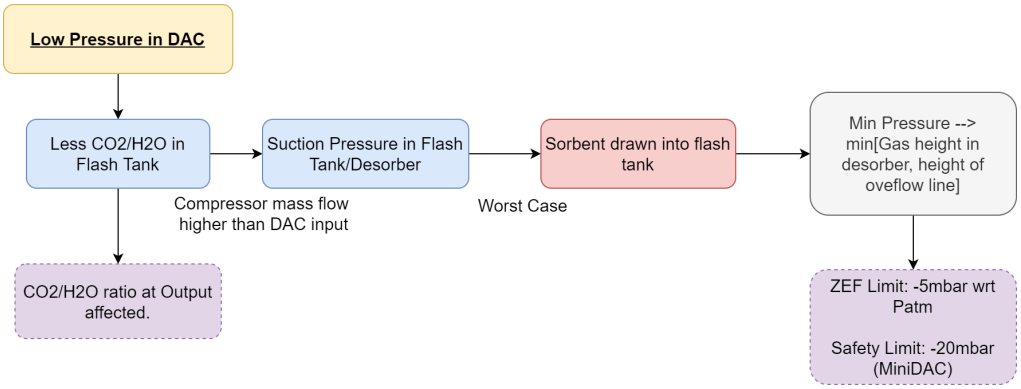

Figure 5.8: Operational scenario which will result in low pressure in the DAC system which in worst case will result in sorbent being drawn into DAC flash tank

System Shutdown:
As described previously 5.2.1, system shutdown will result in negative pressure in the system due condensation of evaporated H_2O vapour and re-absorption of desorbed CO_2.

The maximum drop in pressure for safety limits is same as for previous point, i.e., 20mbar below atmospheric pressure, while ZEF target for the same was set at 5mbar below atmospheric pressure.

Figure 5.9 depicts the scenario described above.

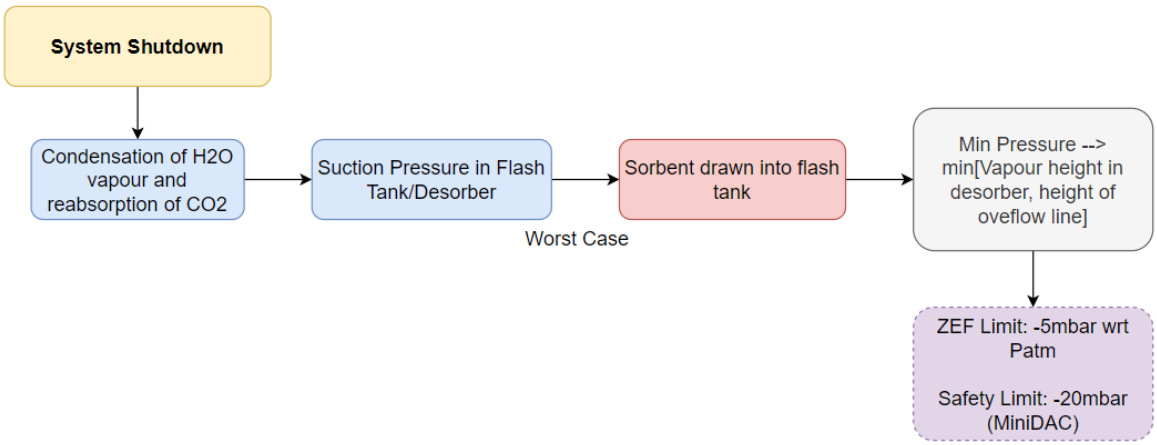

Figure 5.9: System shutdown will result in low pressure in (leak tight) DAC system which in worst case will result in sorbent being drawn into DAC flash tank

5.3. Control strategies for DAC+FM system operation:

What control strategies can be used to ensure ZEF target performance levels are met for the identified operating scenarios?

In order to control the DAC+FM system under required target limits, different control schemes were developed. The scheme developed for the Flash tank pressure control was validated using the experimental test setup (described in Chapter 4), while the other control schemes for DAC production control was developed using the system model described in Chapter3. The control schemes are described in detail in the next sections.

5.3.1. DAC Production Control:

An ideal control scheme for the DAC system would involve controlling the production at required target level and maintaining the energy requirement to low levels. In order check the feasibility of the same, a control scheme was designed through which the DAC production can be controlled by varying ratio of M_{feed} and $Q_{reboiler}$, ($\frac{M}{Q}$).

The same is explained in Figure[5.10] below; consider a DAC system operating at steady state generating 1X output. The net DAC output can be doubled, by having two such systems, which is analogous to doubling the mass flow and reboiler power to the single system, considering other parameters remain the same.

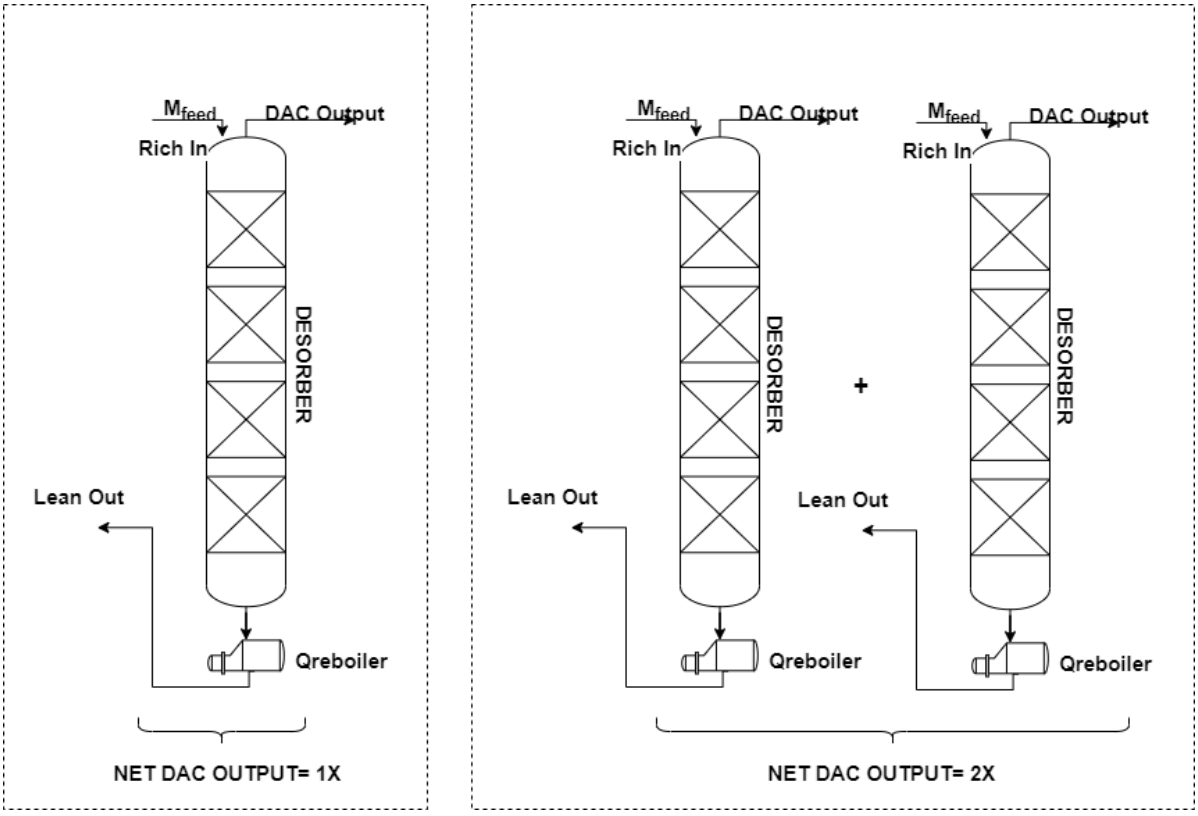

Figure 5.10: The production of a DAC system operating under steady state can be doubled by having two of the same system. This situation is analogous to doubling the mass flow and reboiler power to the single system considering other parameters of the desorber are not changed. Thus by varying M_{feed} and $Q_{reboiler}$, production can be ramped up/down provided ($\frac{M}{Q}$) ratio remains same

The same has been demonstrated for two different humidity conditions below. The humidity conditions chosen are low humidity of 0.005 kg m^{-3} and high humidity of 0.02 kgm^{-3}, based on the yearly variation

in humidity as observed in Sahara climate [27].

- **Low Humidity condition:**

  For this case, it has been assumed that humidity values are low (0.005 kgm^{-3}) and remain constant during the operation. The results obtained for scenario is shown in Figure[5.11] below.

  - The operating zone for DAC operation is limited to $\frac{M}{Q}$ ratio of 2.8E-5 to 1E-4 [(mol/J)]. This range is quite small compared to high humidity operation (5.12).
  - It is possible to achieve targetCO_2 production of 2.17E-3 and energy requirement of $\leq$ 400 kJ/mol CO_2 for $\frac{M}{Q}$ ratio of 2.8E-5 to 4E-5 [(mol/J)].However, for the same operating range H_2O production is much lower than target because of low humidity and low water loadings.
  - Thus it is possible to control the CO_2 output and energy output of DAC for low humidity condition, but the H_2O production and thus the top ratio target cannot be achieved.

- **High Humidity condition:**

  For this case, it has been assumed that humidity values are high (0.02 kgm^{-3}) and remain constant during the operation. The results obtained for scenario is shown in Figure[5.12] below

  - The operating zone DAC operation is limited to $\frac{M}{Q}$ ratio of 1E-5 to 3E-4 [(mol/J)]. This range is much higher compared to low humidity operation (5.11).
  - It is possible to achieve targetCO_2 production of 2.17E-3 mol/s for $\frac{M}{Q}$ ratio of 1.5E-5 to 4.7E-5 [(mol/J)]. While energy requirement target is achieved for $\frac{M}{Q}$ ratio of 4.7E-5 to 9E-5 [(mol/J)]. H_2O production target is achieved for $\frac{M}{Q}$ ratio of 7.2E-5 to 3E-4 [(mol/J)].
  - In summary there is a mismatch between the $\frac{M}{Q}$ ratio where production target can be achieved and when efficient operation can be ensured. Further, because of high humidity, H_2O production is high and thus top ratio at DAC outlet is always higher than target of 3:1.

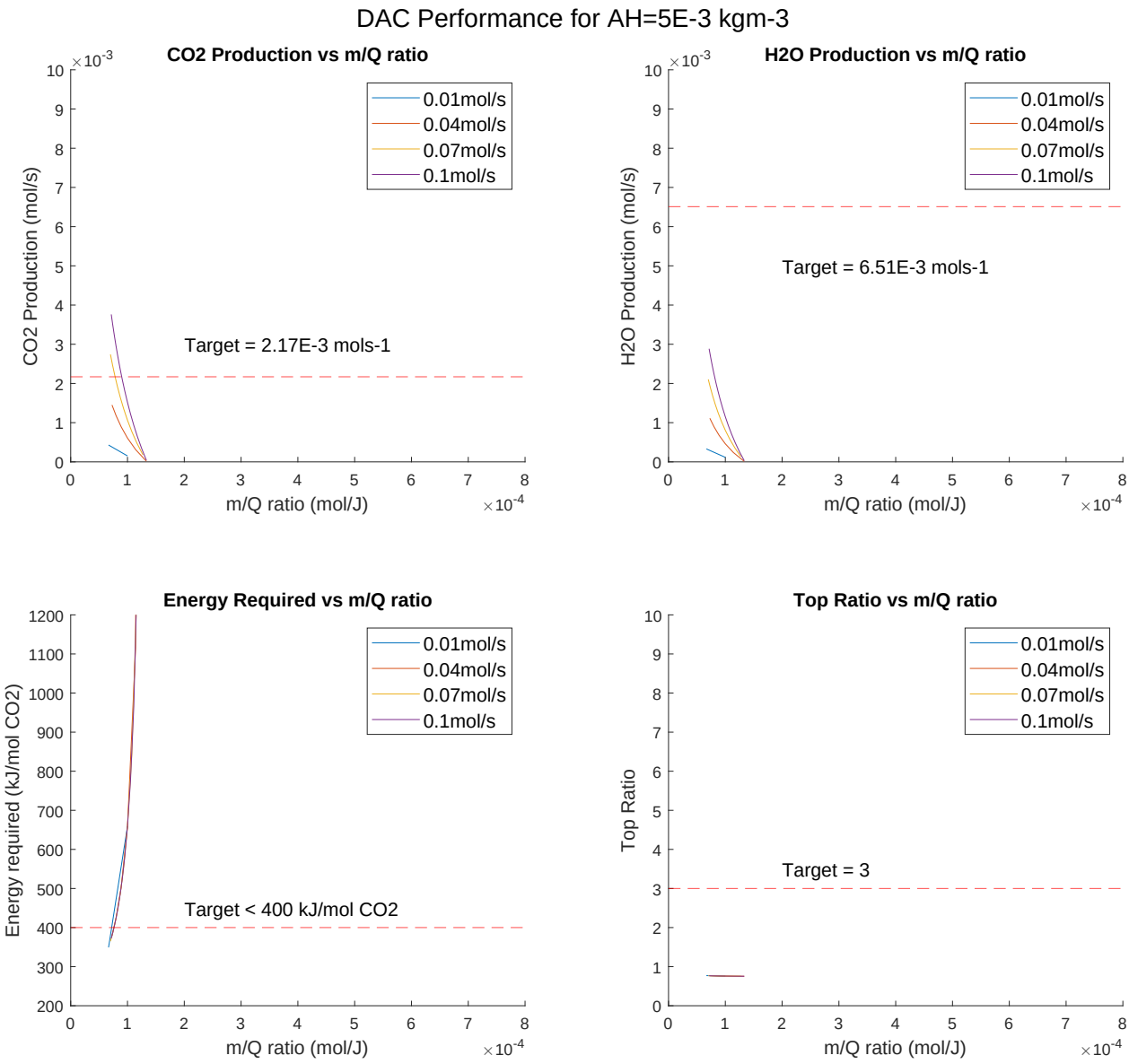

Figure 5.11: For low humidity condition (AH=5E-3 kg^{-3}), the operation window with DAC production is small. Within this operation zone, it is possible to achieve CO_2 production and energy requirement target, however H_2O production is too low and thus top ratio target cannot be achieved even at higher mass flows

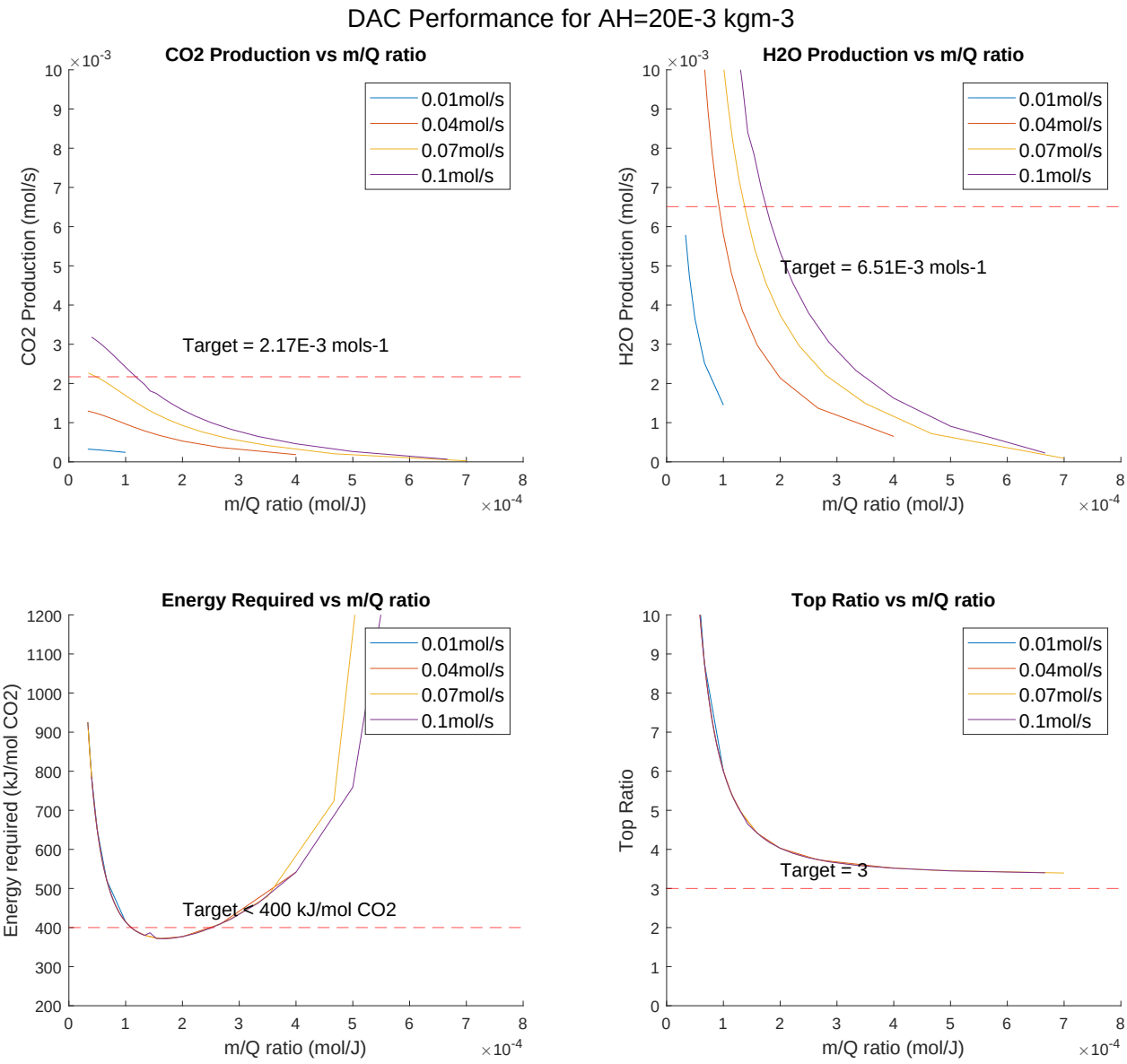

Figure 5.12: For high humidity condition (AH=20E-3 kg m^{-3}), the operation window with DAC production is relatively larger. Within this operation zone, it is possible to achieve CO_2 production and energy requirement target, however H_2O production is too high due to higher water loading and thus top ratio greater than target is achieved

5.3.2. Flash Tank Pressure control:

The flash tank pressure control loop works to control the pressure in the flash tank by simultaneous operation of the Compressor and Bypass solenoid valve.
The compressor is operated using PID control and draws vapour from the flash tank and compresses and stores it in the buffer tank. From the buffer tank, a solenoid bypass valve is connected back to flash tank and operates based on flash tank pressure to control the pressure. In this way, the pressure is maintained in flash tank and continuous operation of the compressor is ensured.

The H_2O collected in the flash tank is periodically drained out via a solenoid valve which is operated based on the level sensor in the flash tank. This ensures that a minimum gas volume is always present in the flash tank which is necessary for the pressure control.

Schematic of the control developed for the flash tank pressure control is depicted in Figure[5.13] below.

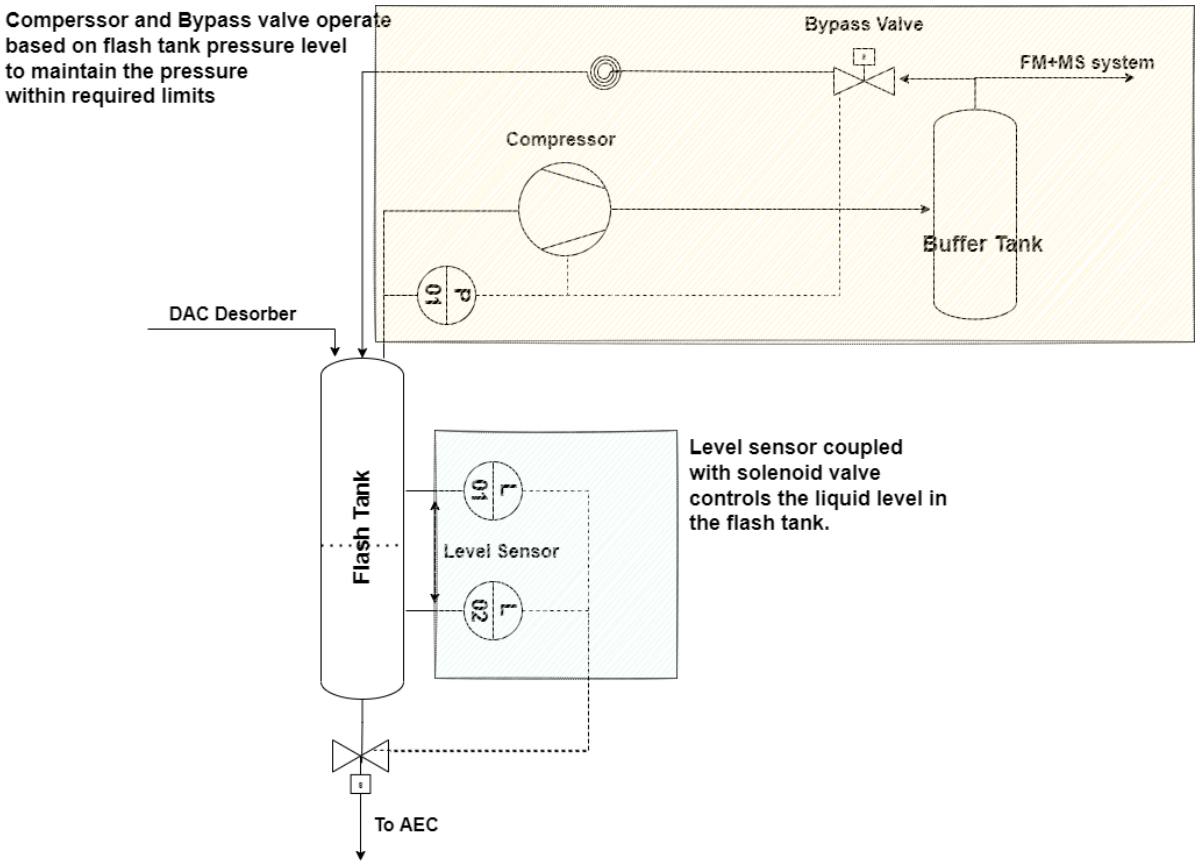

Figure 5.13: Flash tank pressure control loop

The main requirement for the flash tank pressure control model is to maintain the pressure in the flash tank to $\pm$5 mbar relative to atmospheric pressure (as described in section 4.2.2).

The control scheme developed for the same is as shown in Figure[5.14] below.

The working of the control scheme is explained below:

- The control is activated, when Pressure in the flash tank exceeds user defined threshold (P_{on}) and is deactivated if the pressure falls below a defined threshold (P_{off}).

- Once the control is active, then if the flash tank pressure is higher than control threshold ($P_{Control_{high}}$), then compressor (FM system) is operated using PID control to reduce the pressure in the flash

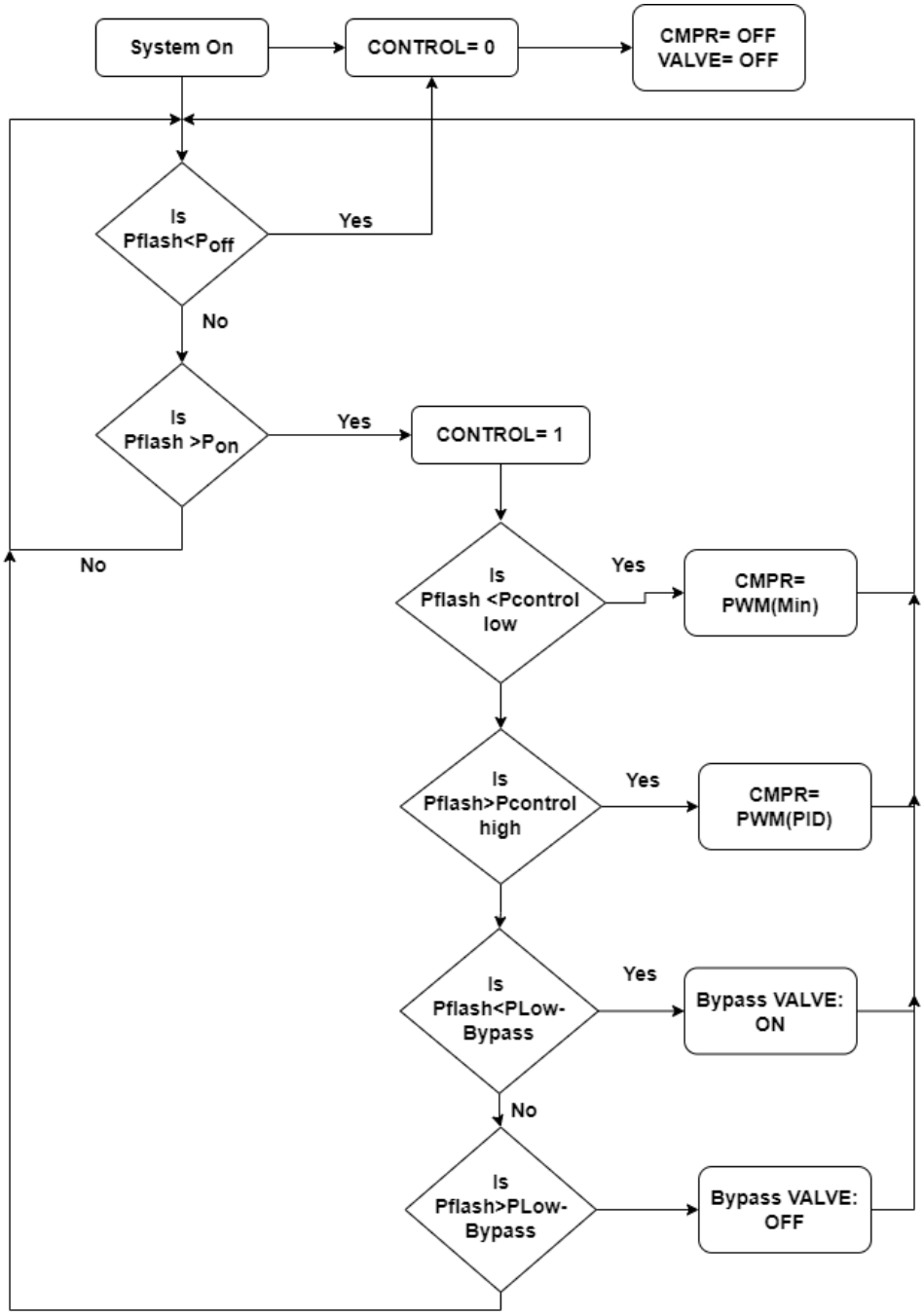

Figure 5.14: Flash tank pressure control scheme

tank. If the pressure is lower than control threshold ($P_{Control_{high}}$) but higher than switch-off threshold (P_{off}), then compressor will operate at its minimum operating condition.

- For the bypass valve control, if the pressure in the flash tank is lower than bypass low threshold ($P_{Low-bypass}$), then solenoid valve of the bypass control from buffer tank to flash tank is turned on. The solenoid valve turns off if the pressure in flash tank is higher than bypass high threshold ($P_{high-bypass}$).

Other control schemes evaluated during the work are described in Appendix A.

5.4. Optimum Control Strategy for DAC+FM system:

What is the optimum control strategy for the operation of DAC+FM system which meets the ZEF's requirements?

The control strategy, described in the the previous section for DAC production control (5.3.1) and flash tank pressure control (5.3.2) can be used together to operate DAC+FM system as per ZEF's requirement. The same is described in the next section.

5.4.1. DAC production control for varying humidity condition:

In order to check the feasibility of the control for varying humidity conditions, the control scheme was validated on a day's humidity data captured during experiments on MiniDAC setup. The humidity data for the day and corresponding H_2O rich loadings as predicted by the absorber model is shown in Figure[5.15] below:

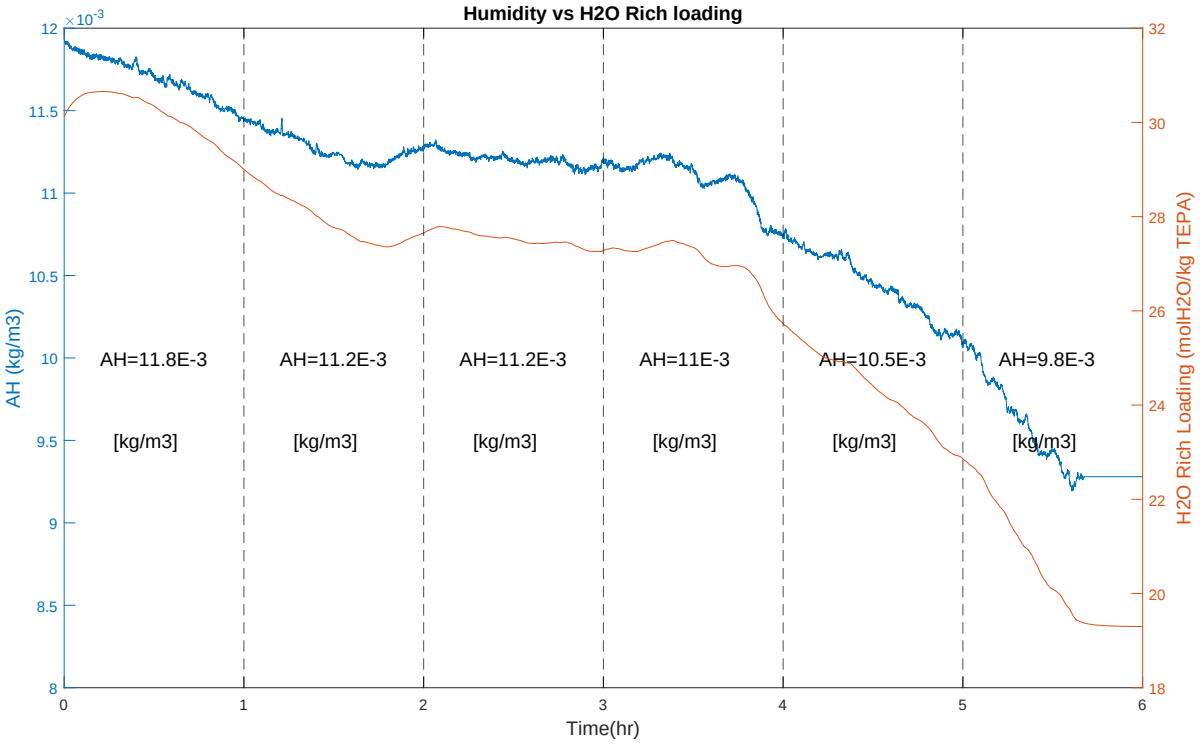

Figure 5.15: Variation in rich H_2O loading in the sump with absolute humidity as predicted by integrated system model. The humidity value ranges from 12E-3 to 9E-3 kgm^{-3} during the day and to simplify the control scheme, average humidity value for every hour is considered as input. The same is mentioned for each hour in the figure

Control scheme for the same to get achieve target production, efficiency and top ratio is described as below:

- **DAC Operation 0-1hours:**
  Average humidity level for this time is taken as 11.8E-3 kg/m3. The performance for the chosen $\frac{M}{Q}$ ratio is shown in Figure[5.16] and Table[5.5]below.

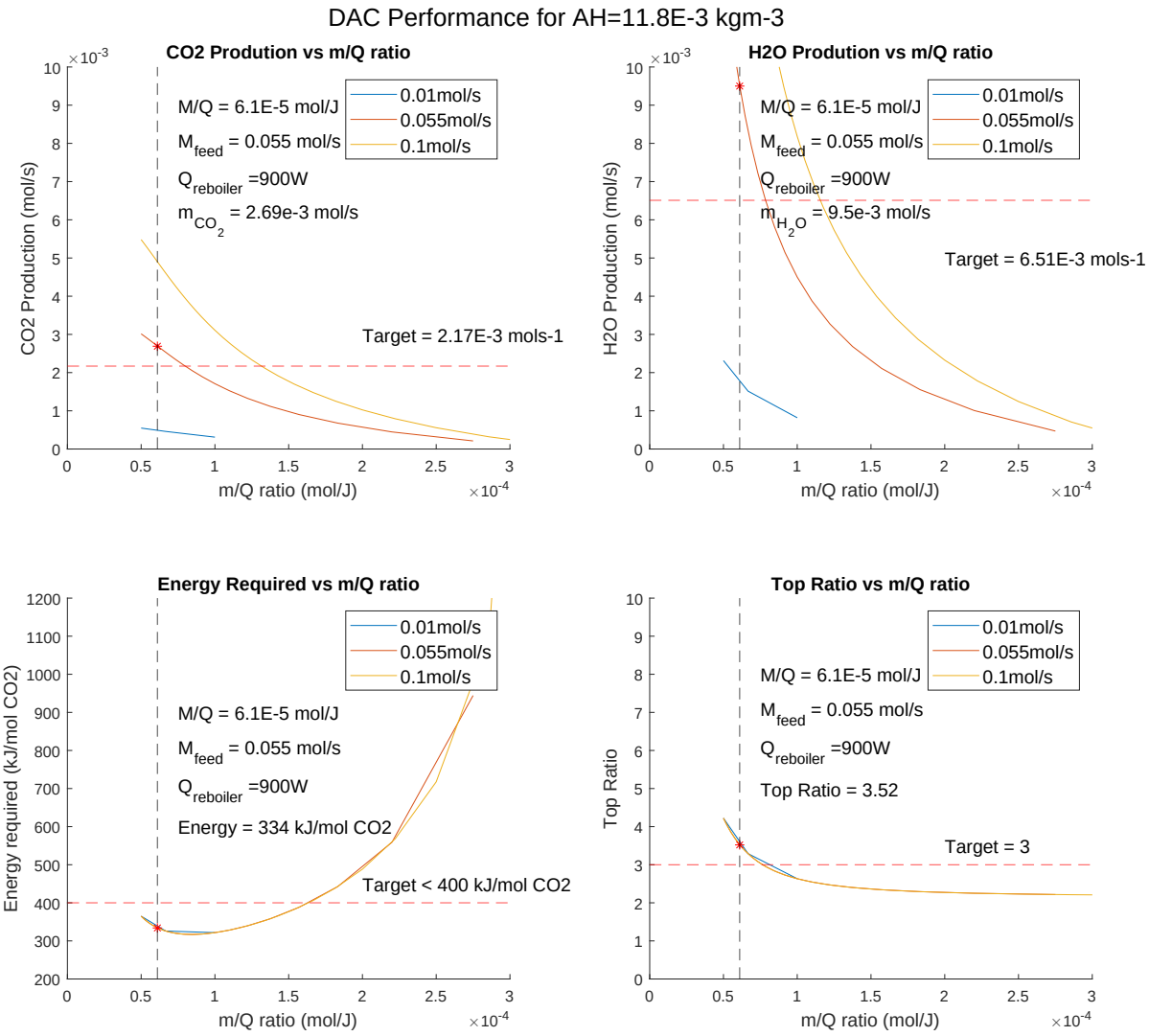

Figure 5.16: DAC production and energy requirement for **humidity level of 11.8E-3 kg/m3**. At chosen $\frac{M}{Q}$ ratio (shown in red * on the graph), CO_2 production, H_2O production and energy requirement targets are being met; however because of the humidity condition, the top ratio is higher than 3.

Table 5.5: DAC production summary for 0-1hour of operation

Parameter	Description	Value	Unit
$\acute{M}_{feed}$	Desorber feed flow rate	5.5E-2	[$mols^{-1}$]
$\acute{Q}_{reboiler}$	Reboiler input	900	[W]
Top ratio	Top ratio (H_2O:CO_2)	3.5:1	[-]
E_{req}	Energy required	334.1	[kJ/mol CO_2]
n_{CO2}	Moles CO_2 produced	9.7	[mol CO_2]
n_{H2O}	Moles H_2O produced	34.2	[mol H_2O]

- **DAC Operation 1-4hours:**
  Average humidity level for this time is taken as 11.2E-3 kg/m3. The performance for the chosen $\frac{M}{Q}$ ratio is shown in Figure[5.17] and able[5.6]below.

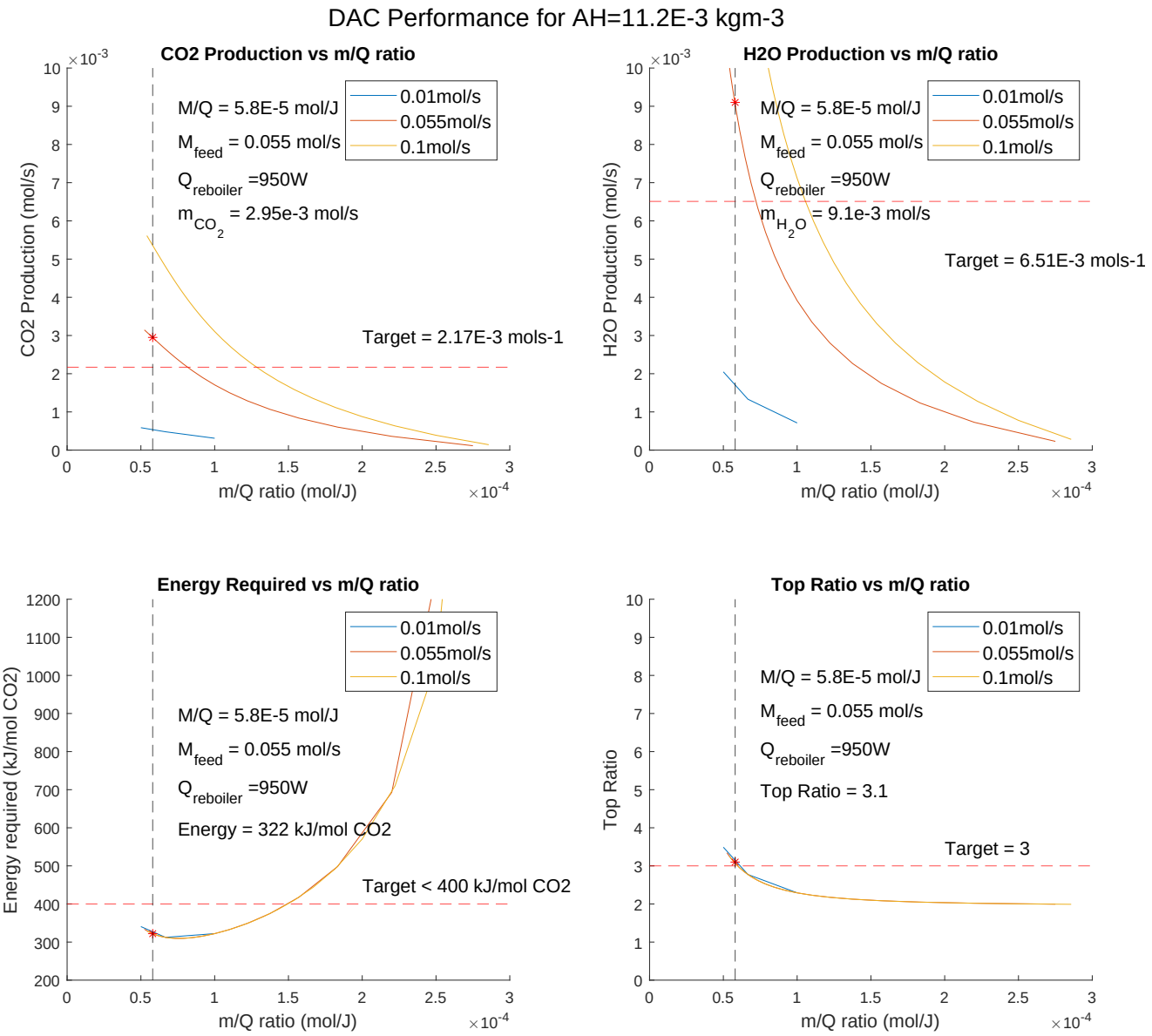

Figure 5.17: DAC production and energy requirement for **humidity level of 11.2E-3 kg/m3**. At chosen $\frac{M}{Q}$ ratio (shown in red * on the graph), CO_2 production, H_2O production and energy requirement targets are being met; however similar to 5.16, because of the humidity condition, the top ratio is higher than 3

Table 5.6: DAC production summary for 1-4hour of operation

Parameter	Description	Value	Unit
$\acute{M}_{feed}$	Desorber feed flow rate	5.5E-2	[$mols^{-1}$]
$\acute{Q}_{reboiler}$	Reboiler input	950	[W]
Top ratio	Top ratio (H_2O:CO_2)	3.1:1	[-]
E_{req}	Energy required	322	[kJ/mol CO_2]
n_{CO2}	Moles CO_2 produced	31.2	[mol CO_2]
n_{H2O}	Moles H_2O produced	98.3	[mol H_2O]

- **DAC Operation 4-5hours:**
  Average humidity level for this time is taken as 10.5E-3 kg/m3. The performance for the chosen

$\frac{M}{Q}$ ratio is shown in Figure[5.18] and Table[5.7]below.

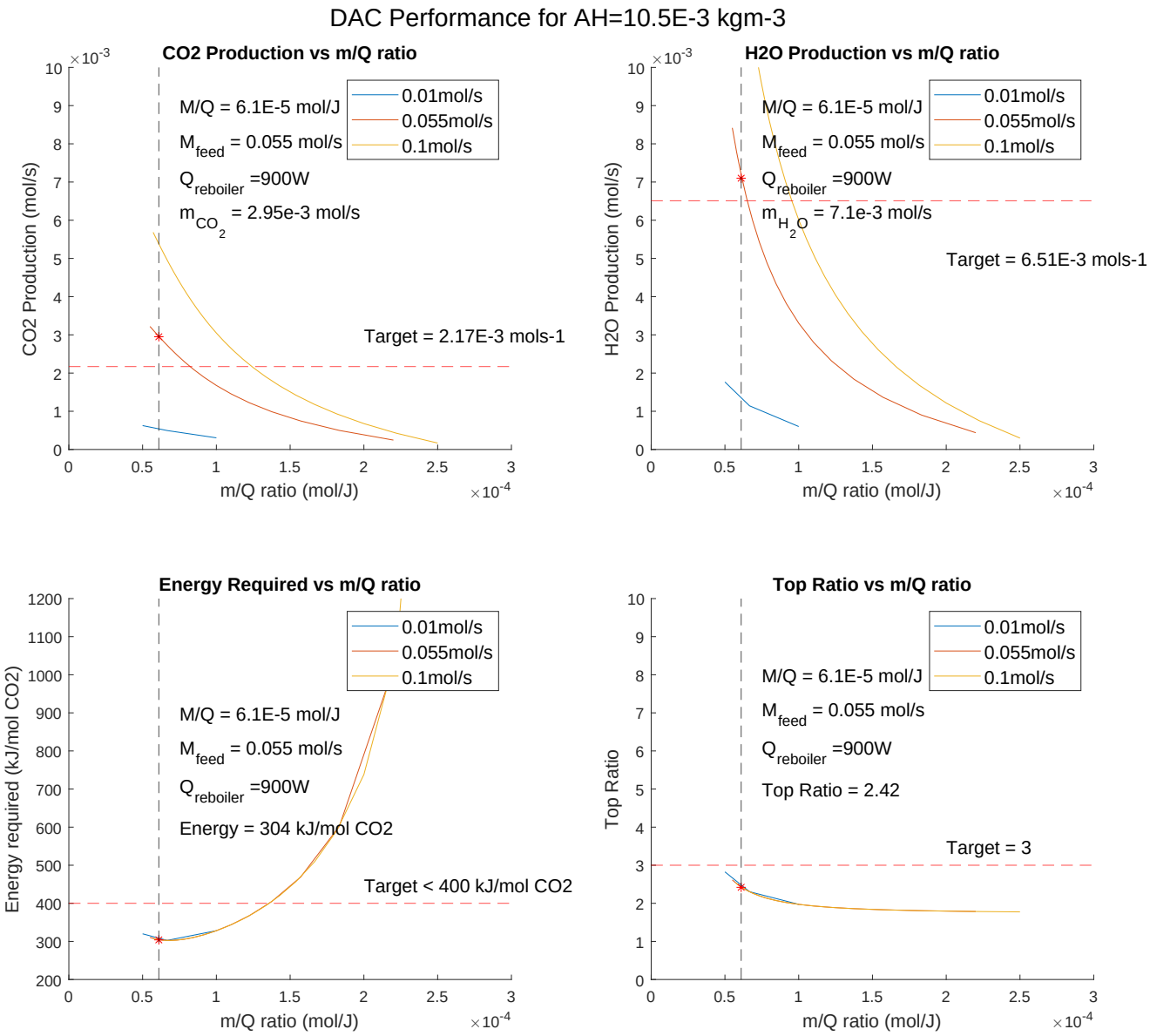

Figure 5.18: DAC production and energy requirement for **humidity level of 10.2E-3 kg/m3**. At chosen $\frac{M}{Q}$ ratio (shown in red * on the graph), CO_2 production and H_2O production and energy requirement targets are being met; however because of the humidity condition, the top ratio is lower than 3

Table 5.7: DAC production summary for 4-5hour of operation

Parameter	Description	Value	Unit
$\acute{M}_{feed}$	Desorber feed flow rate	5.5E-2	[$mols^{-1}$]
$\acute{Q}_{reboiler}$	Reboiler input	900	[W]
Top ratio	Top ratio (H_2O:CO_2)	2.41:1	[-]
E_{req}	Energy required	304	[kJ/mol CO_2]
n_{CO2}	Moles CO_2 produced	10.6	[mol CO_2]
n_{H2O}	Moles H_2O produced	25.6	[mol H_2O]

- **DAC Operation 5-6hours:**
  Average humidity level for this time is taken as 9.5E-3 kg/m3. The performance for the chosen $\frac{M}{Q}$ ratio is shown in Figure[5.19] and Table[5.8]below:

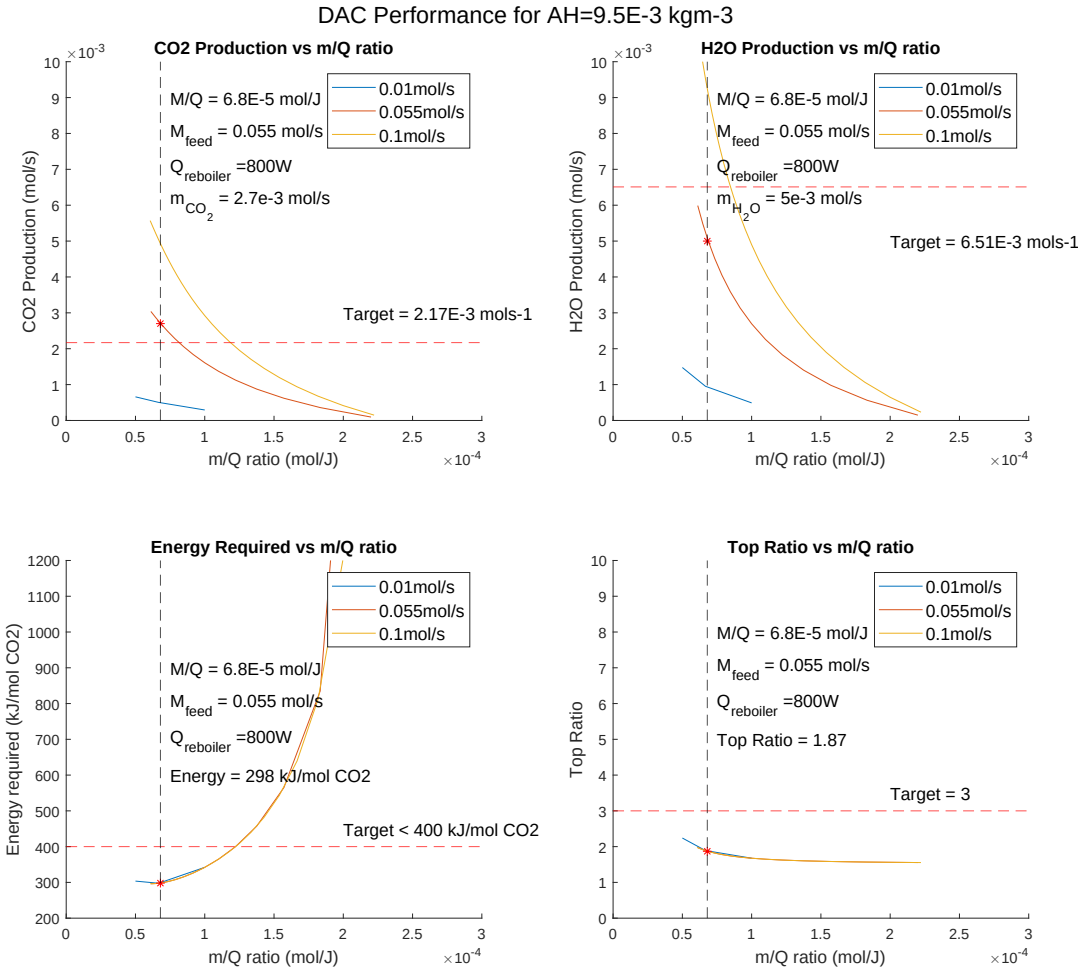

Figure 5.19: DAC production and energy requirement for **humidity level of 10.2E-3 kg/m3**. At chosen $\frac{M}{Q}$ ratio (shown in red * on the graph), CO_2 production and H_2O production and energy requirement targets are being met; however because of the humidity condition, the top ratio is lower than 3

Table 5.8: DAC production summary for 5-6hour of operation

Parameter	Description	Value	Unit
$\acute{M}_{feed}$	Desorber feed flow rate	5.5E-2	[mols^{-1}]
$\acute{Q}_{reboiler}$	Reboiler input	800	[W]
Top ratio	Top ratio (H_2O:CO_2)	1.85:1	[-]
E_{req}	Energy required	298	[kJ/mol CO_2]
n_{CO2}	Moles CO_2 produced	9.7	[mol CO_2]
n_{H2O}	Moles H_2O produced	18	[mol H_2O]

- **Total DAC production:**
  Summary of 6 hour DAC operation is tabulated in Table[5.9] below:

Table 5.9: DAC production summary 6 hour operation

Parameter	Description	Value	Unit
n_{CO2net}	Net moles CO_2 produced	61.9	[mol CO_2/day(6h)]
n_{H2Onet}	Net moles H_2O produced	176.1	[mol H_2O/day(6h)]
E_{input}	Net energy input	5.45	kWh/day(6h)]

5.4.2. Flash tank pressure control scheme:

The control scheme was validated on the MiniDAC test setup (described in Chapter4). The results are shown below:

- **Startup and Steady-state operation:** In the MiniDAC setup, flash tank pressure control was implemented (4.2.2) and the setup was in startup- steady state operation for ≈ 2 hours.

  System behaviour of MiniDAC setup with Flash tank control is shown in Figure[5.20] and [5.21]below:

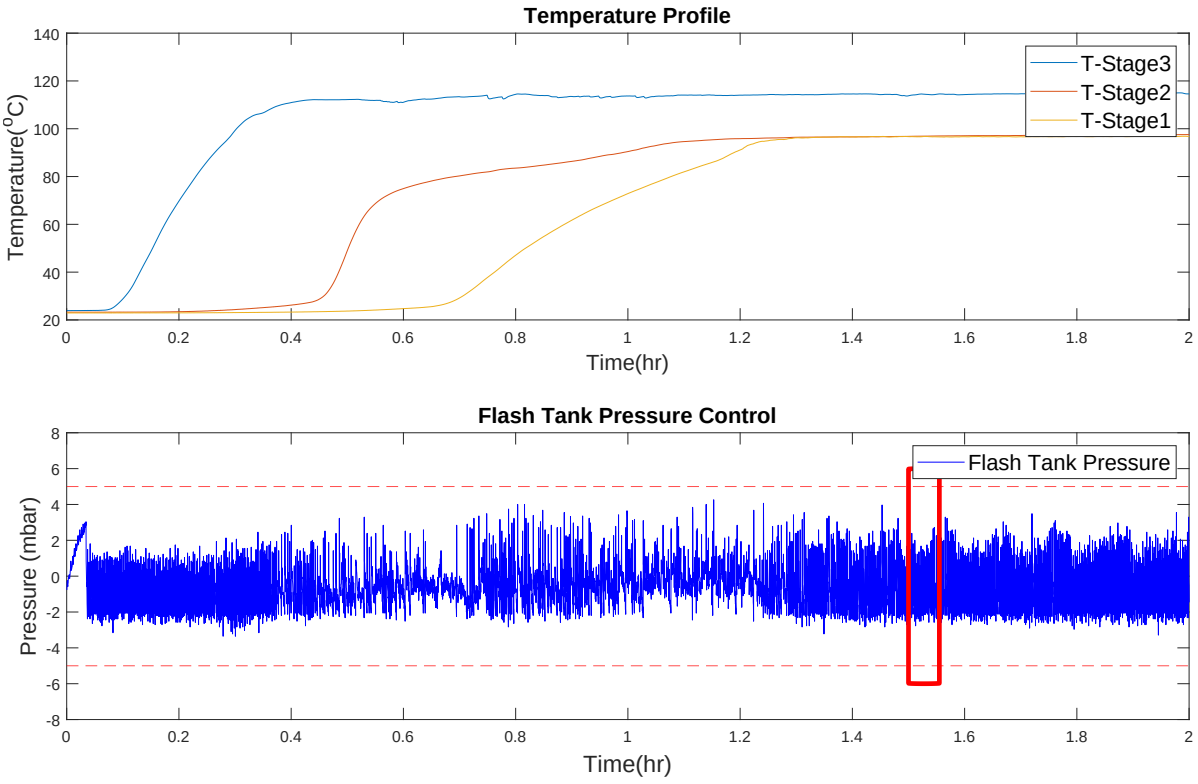

Figure 5.20: The figure on top shows the temperature variation in desorber of MiniDAC test setup during startup and steady state operation

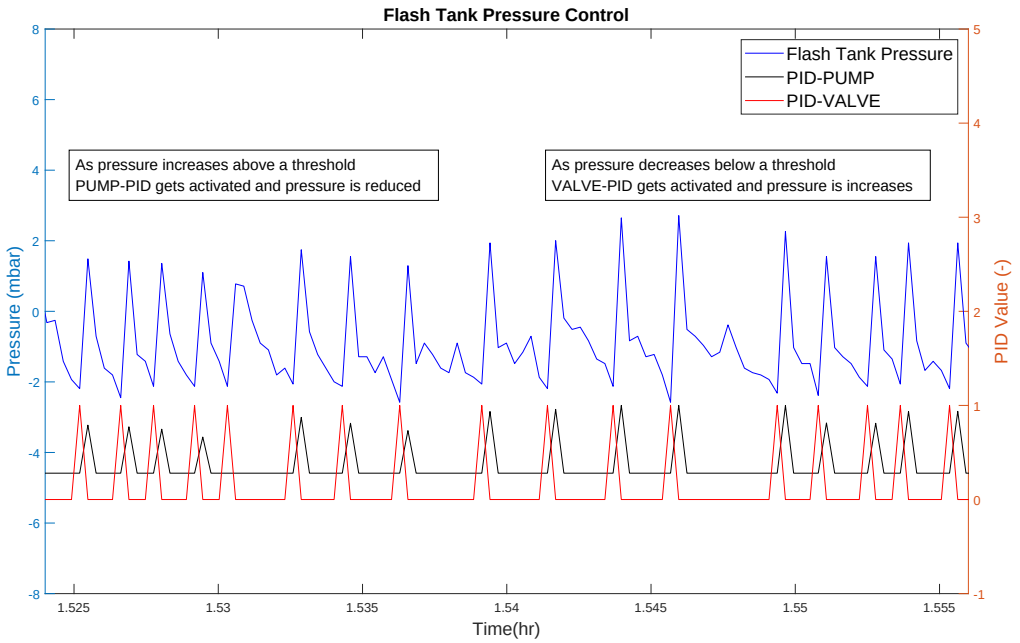

Figure 5.21: Pressure Control in flash tank in the highlighted region from 5.20.As can be seen, when pressure increase above a threshold, PUMP-PID gets activated and pressure is reduced; and as pressure drops below a threshold, Bypass valve gets activated and pressure is increased

The results of the test to validate the control scheme are tabulated in Table [5.10] below:

Table 5.10: Results for Startup and Steady-state operation of MiniDAC setup with Flash tank pressure control

Parameter	Description	Value	Unit
$P_{flashMax}$	Max flash tank pressure (above P_{atm})	4.26	[mbar]
$P_{flashMin}$	Min flash tank pressure (below to P_{atm})	4.12	[mbar]
$n_{CO2Cmpr}$	Net moles CO_2 compressed	4.96E-2	[mol CO_2]
n_{CO2Byp}	Net moles CO_2 purged back via bypass	1.49E-2	[mol CO_2]
n_{CO2net}	Net moles CO_2 captured	3.47E-2	[mol CO_2]

Extrapolating this data for final ZEF setup:

- In the final system, being developed at ZEF, the difference between target DAC production rate and minimum compressor flow rate (5.2.3) is 1E-3 mol $CO_2 s^{-1}$.
- This implies that 1E-3 mol $CO_2 s^{-1}$ will have to be bypassed from buffer tank to flash tank to control the pressure.
- This bypass rate corresponds to $\approx$ 43% of captured CO_2 being purged back to flash tank.

- **Shutdown operation:** During shutdown operation the system behaviour is shown in Figure[5.22] and [5.23] below:

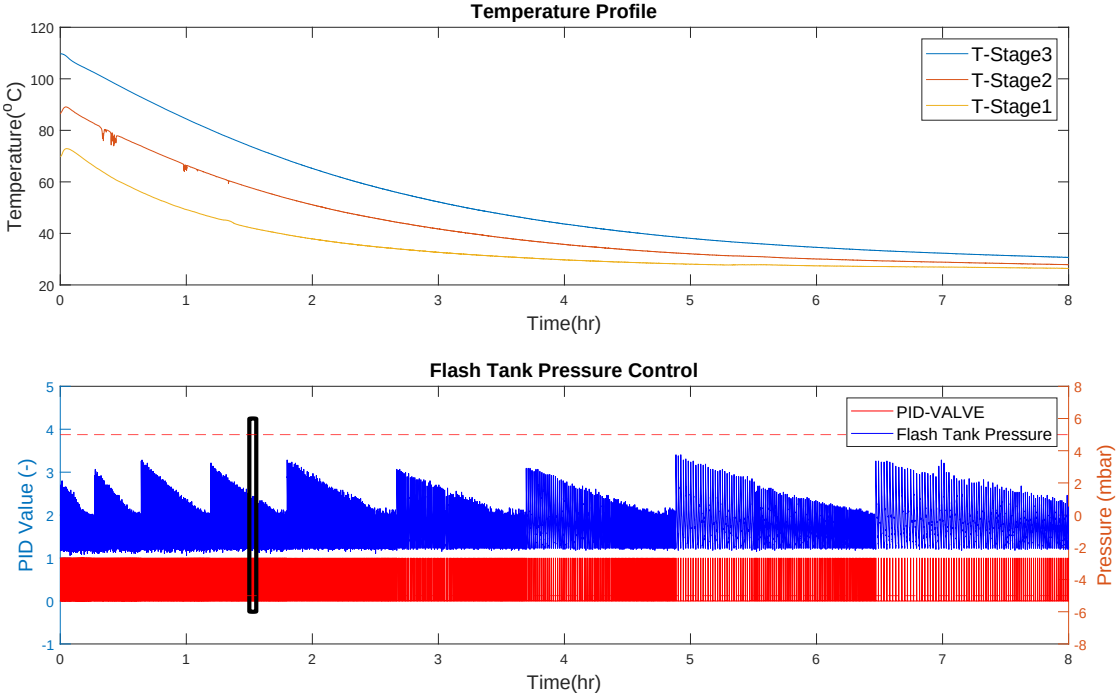

Figure 5.22: The figure on top shows the temperature of the MiniDAC desorber at different points of column during shutdown of MiniDAC setup. As the desorber cools down, pressure in the system drops (due to H_2O condensation) and this pressure is controlled by purging captured CO_2 from buffer tank to flash tank. The same is shown in figure at the bottom. Pressure fluctuation in the flash tank, remains within the target of $\pm$ 5mbar with flash tank pressure control. The highlighted region is shown in Figure[5.23] in more detail

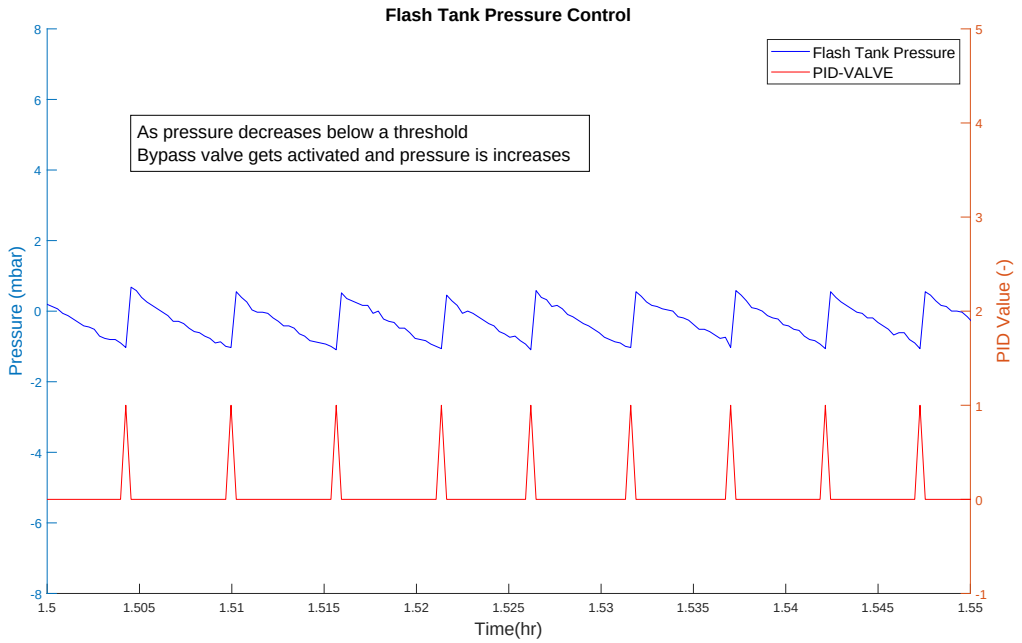

Figure 5.23: Pressure Control in flash tank in the highlighted region from 5.22.As can be seen, when pressure drops below a threshold, bypass valve gets activated and pressure is increased

The results of the test to validate the control scheme during shutdown operation are tabulated in Table [5.11] below:

Table 5.11: Results for shutdown operation of MiniDAC setup with Flash tank pressure control

Parameter	Description	Value	Unit
$P_{flashMax}$	Max flash tank pressure (above P_{atm})	2.03	[mbar]
$P_{flashMin}$	Min flash tank pressure (below to P_{atm})	1.25	[mbar]
n_{CO2net}	Net moles CO_2 captured (during startup and steady state)	3.47E-2	[mol CO_2]
n_{CO2Byp}	Net moles CO_2 purged back via bypass (shutdown)	1.48E-2	[mol CO_2]
n_{CO2net}	Net moles CO_2 captured	1.98E-2	[mol CO_2]

Extrapolating this data for final ZEF setup:

- In the final system, being developed at ZEF, desorber and flash tank volume is ≈7 times higher than in MiniDAC. This implies that net CO_2 required to maintain target pressure in DAC system will be ≈ 7 times higher than CO_2 required for MiniDAC setup, i.e. 1.05E-1 mol CO_2.
- Net CO_2 produced in MiniDAC is 4.96E-2 in the total operation time for the experiment (≈2.8 hours). In the same time, the final setup average production will be 21.7 mol CO_2.
- This implies in the final setup ≈ 0.5% of CO_2 produced will have to be purged back to maintain system pressure at the same target level as MiniDAC.

6

Conclusions

6.1. System performance:

The main parameters which affect the performance of different sub-system of DAC and FM system are mentioned below:

- **DAC absorber** performance is affected by variation in ambient conditions (temperature and humidity). H_2O absorption in the sorbent is mainly governed by humidity and while change in temperature affects the loading of CO_2 in the sorbent.

- **Sump** acts as dampener for the variation in sorbent loading due to mixing of rich and lean sorbents. Higher the sump initial loading, slower will be change in sorbent composition over the course of DAC operation.

- **DAC Desorber** performance is dynamically affected by the composition and amount of rich feed entering the desorber and heat input from the reboiler. System pressure also affects the performance as VLE is impacted by change in pressure.

  The temperature of feed and sorbent holdup in the desorber impact the power requirement as they constitute the major thermal mass of the system which is to be heated up for desorption.

- **Flash tank** performance is affected by the temperature of the tank and the volume of the tank. The fraction of H_2O in vapour form increases with temperature and thus will impact the dehumidification requirement of the FM system.

  Pressure in flash tank is a function of the tank volume; higher the volume, lower the pressure fluctuations in the system. During dynamic operation, the pressure is regulated by FM system flow rate.

- **Compressor** performance is directly governed by the compressor capacity, speed and corresponding mass flow rates. The compressor can only operate in a fixed range of compressor speed which limits the minimum and maximum flow rate of the system.

6.2. Operational Scenarios:

The operational scenarios for the DAC+FM system operation is governed by the operating range of the respective sub-systems. In current ZEF system, there is a large mismatch between operating range of DAC and FM system because of which there are three main operating scenarios which the integrated system will encounter.

- **High DAC production/High Pressure:** If the DAC output is higher than compressor mass flow rate, then because of accumulation of vapour in DAC flash tank will result in higher system pressure.

This will result in sorbent being pushed out from desorber due to static pressure on liquid column and in worst case will result in all sorbent being purged out of desorber.

- **Low DAC production/Low pressure:** If DAC output is lower than compressor flow rate, this will result in more vapour being drawn out of flash tank than entering from DAC output and will cause negative pressure (lower than atmospheric pressure) in the system.

  The negative pressure will result in more sorbent being drawn into desorber from overflow port and in worst case can result in overflow of sorbent from desorber to flash tank or air drawn in to desorber from overflow port.

- **DAC Shutdown:** Cooling down of desorber after shutdown will result in re-condensation of H_2O vapours and re-absorption of desorbed CO_2 (still in desorber) back into sorbent. This will result in negative vapour pressure in the desorber system and can result in situation like 'low production/low pressure' condition described above.

6.3. Control Schemes:

- **DAC Production control:**
  - **Operation range controlled by water loading in sorbent:** One of the major takeawaya from this control scheme is that operation DAC system is mainly governed by water loading in the sorbent, which in turn is affected majorly by absolute humidity in the atmosphere.
  - **Water production vs Humidity:** At very low humidity conditions, (5E-3 kgm^{-3}), it is not possible to meet H_2O production targets at any $\frac{M}{Q}$ ratio with desorber maximum temperature limitation of 120^o C.

    On the other hand, for high humidity conditions, the H_2O production is much higher and for all $\frac{M}{Q}$ values, the ratio of $\frac{H_2O}{CO_2}$ is always higher than target of 3:1.
  - **Vary top ratio target:** As described in above point, H_2O production is largely dependent on humidity conditions, which varies throughout the day. Hence it is more preferable to have a variable top ratio target depending on humidity condition so as to have average daily production in the ratio 3:1 (as shown in 5.4.1).

- **Flash Tank pressure control:**
  - **Bypass Control:** The control system with compressor/pump operating at its minimum speed or above, coupled with bypass valve from buffer tank to flash tank, is able to control the pressure in the flash tank to target of $\pm$5mbar relative to atmospheric pressure.
  - **CO_2 bypass:**
    - **Startup-Steady state operation:** With current ZEF configuration, the mismatch in DAC production and compressor operation range the amount of CO_2 needed to be bypassed from buffer tank to flash tank will be $\approx$ 43% of total CO_2 production from DAC.
    - **DAC Shutdown:** Extrapolating the experiment data on MiniDAC for final ZEF setup, we get that $\approx$0.5% of CO_2 captured by DAC system will have to be purged back to maintain system pressure in the system after shutdown.

7

Recommendations

7.1. Design Recommendations:

- **Sorbent-Diluent ratio:** For the current sorbent diluent ratio, the sensitivity of variations in water loading with humidity and corresponding vapour pressure change in high 7.1. This makes controlling both top ratio and total production at target limit extremely difficult. More research should be done to identify sorbent diluent mixtures with less sensitivity in change in vapour pressure with loading.

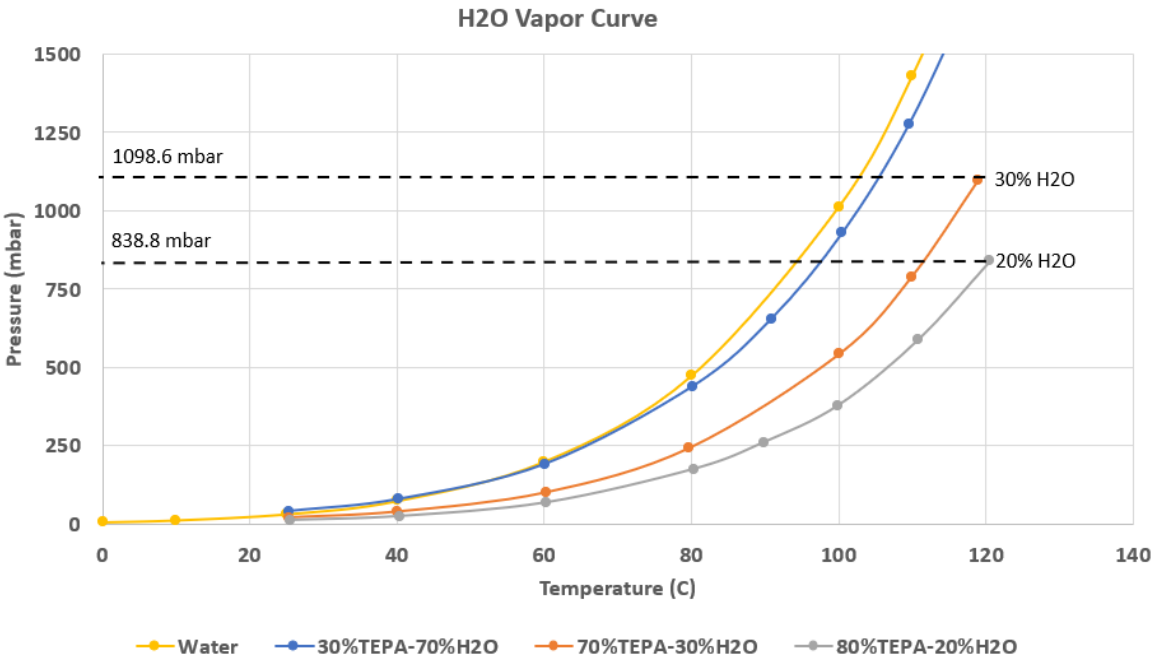

Figure 7.1: Vapour curve for TEPA-H_2O VLE mixture. It can be seen that ≈10% increase in H_2O loading in the sorbent, results in ≈30% increase in H_2O vapour pressure [19]

- **Impact of CO_2 purge back to control negative pressure:** The control scheme developed for control of negative pressure in the system due to mis match between DAC production and compressor flow rate (5.2.3). This will require ≈43% of captured CO_2 to be purged back to maintain the pressure based on current DAC production and compressor mass flow rate. Hence to avoid this loss in net production and efficiency, it is important to match DAC output and compressor flow rates.

  This can be done by either using a compressor with smaller minimum mass flow rate or by increasing DAC production rate.

- **Production control scheme:** The production control scheme gives an indication of how the $\frac{M}{Q}$ ratio can be used to ramp up/down DAC production. However, in order to implement the control in actual plant control it is required to include heat losses, heat/mass transfer limitation effects and dynamic effect of change in sorbent loading to get a more realistic picture of the control.

7.2. Model Recommendations:

7.2.1. Absorber Model:

- **More accurate CO_2 STY curve:** The space time yield (STY) curve used for CO_2 is based on assumption that the rate of change of CO_2 partial pressure with VLE loading remains constant which is not valid for the entire range of operation. To accurately determine the dependence of CO_2 STY on ambient temperature, more experimental data at controlled temperature and humidity condition should be performed.

- **Effect of viscosity:** The effect of viscosity on absorption of CO_2 and H_2O has been neglected in the model. However, viscosity affects the residence time of sorbent in the absorber and will also impact the diffusion of CO_2 and H_2O into the sorbent. Further, change in ambient temperature and water loading in the sorbent also affects the viscosity of the sorbent. Hence it is necessary to include the effect of viscosity in the absorber model to improve the dynamic response of the model.

- **Degradation model:** Oxidative degradation takes place can take place in the absorber as the sorbent is exposed to air. Since the sorbent residence time in the absorber is much higher compared to residence time in desorber, hence oxidative degradation will be prominent in the absorber. Consequently, it is desirable to include the degradation effect due to oxygen in the absorber model which can then be used to predict sorbent lifetime.

7.2.2. Desorber Model:

- **VLE data for low temperature:** The desorber model uses extrapolation of experimental VLE data which is valid for temperatures higher than $\approx$100 ^{o}C which is then extended to predict desorber VLE conditions for lower temperatures as well. Hence in order to improve accuracy desorber model at lower temperatures, experimental data for lower temperatures is also required which should then be incorporated into the model.

- **Estimation of desorber pressure:** Currently the desorber model, requires pressure as input to determine VLE composition at each time step. The limitation of this is that during system shutdown, the model cannot predict the negative pressure developed due to re-condensation of H_2O as desorber temperature goes down. The model can be improved instead to use the temperature data to predict the vapour pressure of the system and then can be used to model the negative pressure observed during system shutdown.

- **Heat Exchanger for Desorber feed:** In the current model, heat exchanger which heats up the incoming rich feed to the desorber using the heat from outgoing lean sorbent has not been modelled. Including the heat exchanger will make the desorber model more complete.

- **Volatility of TEPA-PEG:** Desorber model assumes that TEPA and PEG are non-volatile mixtures and vapour phase is a binary mixture of CO_2 and H_2O. In reality, some TEPA and PEG will also evaporate and the same should also be incorporated in the model by first experimentally determining the extent of TEPA PEG evaporation.

- **Effect of pressure fluctuation on sorbent level in desorber:** The pressure fluctuation in the system due to DAC and FM interaction has been included only to calculate the VLE composition in the desorber stages. However, in reality the pressure fluctuation will alter the liquid level in the desorber, which in turn will change the thermal mass in the system. Hence the effect on liquid level in the desorber due to pressure fluctuation should be included in the model.

7.2.3. FM Model:

- **Integration of drying system model:** The vapour from DAC flash tank is assumed to be pure CO_2; however in reality depending on flash tank temperature, it can contain significant amount of H_2O. Depending on the drying system technology finalised for ZEF system, the drying system model should be integrated in the system to include the dynamics of the same.

- **Compressor data with limit sample parts:** The compressor model uses experimental curve for mass flow rate and efficiency. However, the same is based on experimental results on a single compressor. In order to have more accurate model, experiments should be performed with minimum and maximum tolerance sample in terms of leakages to get more robust model.

- **Compressor response time:** The compressor response time used in the model is based on experimental results on different make of compressor than the one finally being used in the FM system. Hence the experiments to check the response time for different compressor speeds should be performed and the same should be included in the model.

- **Joule-Thomson cooling due to expansion using capillary:** The capillary tubes used in the system will result in cooling down of CO_2 stream when it is purged from high pressure to low pressure due to Joule-Thomson cooling. The effect of same should be included in the model.

References

[1] *Milankovitch (Orbital) Cycles and Their Role in Earth's Climate – Climate Change: Vital Signs of the Planet*. URL: https://climate.nasa.gov/news/2948/milankovitch-orbital-cycles-and-their-role-in-earths-climate/ (visited on 02/27/2022).

[2] NASA. *GISS Surface Temperature Analysis (v4) Analysis Graphs and Plots*. URL: https://data.giss.nasa.gov/gistemp/graphs_v4/.

[3] Bert Metz et al. *CARBON DIOXIDE CAPTURE AND STORAGE*. Tech. rep. Cambridge: Cambridge University Press, 2005.

[4] *The Paris Agreement | United Nations*. URL: https://www.un.org/en/climatechange/paris-agreement (visited on 02/27/2022).

[5] Angela Dibenedetto, Antonella Angelini, and Paolo Stufano. "Use of carbon dioxide as feedstock for chemicals and fuels: homogeneous and heterogeneous catalysis". In: *Journal of Chemical Technology & Biotechnology* 89.3 (Mar. 2014), pp. 334–353. ISSN: 1097-4660. DOI: 10.1002/JCTB.4229. URL: https://onlinelibrary-wiley-com.tudelft.idm.oclc.org/doi/full/10.1002/jctb.4229.

[6] Kiane de Kleijne et al. "Limits to Paris compatibility of CO2 capture and utilization". In: *One Earth* 5.2 (Feb. 2022), pp. 168–185. ISSN: 25903322. DOI: 10.1016/J.ONEEAR.2022.01.006. URL: https://doi.org/10.1016/j.oneear.2022.01.006.

[7] Mahdi Fasihi, Olga Efimova, and Christian Breyer. "Techno-economic assessment of CO2 direct air capture plants". In: *Journal of Cleaner Production* 224 (July 2019), pp. 957–980. ISSN: 09596526. DOI: 10.1016/j.jclepro.2019.03.086. URL: https://linkinghub.elsevier.com/retrieve/pii/S0959652619307772.

[8] Noah McQueen et al. "A review of direct air capture (DAC): scaling up commercial technologies and innovating for the future". In: *Progress in Energy* 3.3 (July 2021), p. 032001. ISSN: 2516-1083. DOI: 10.1088/2516-1083/abf1ce. URL: https://iopscience.iop.org/article/10.1088/2516-1083/abf1ce.

[9] David W. Keith et al. "A Process for Capturing CO2 from the Atmosphere". In: *Joule* 2.8 (Aug. 2018), pp. 1573–1594. ISSN: 25424351. DOI: 10.1016/J.JOULE.2018.05.006. URL: https://doi.org/10.1016/j.joule.2018.05.006.

[10] *Pre-Processing of a CO₂ feedstream in a CCUS methanol microplant | TU Delft Repositories*. URL: https://repository.tudelft.nl/islandora/object/uuid%3A1d1dbf9f-8bef-4f66-aefe-71d9a70e4be9?collection=education (visited on 02/27/2022).

[11] Jennifer Wilcox et al. "Advancing adsorption and membrane separation processes for the gigaton carbon capture challenge". In: *Annual Review of Chemical and Biomolecular Engineering* 5 (2014), pp. 479–505. ISSN: 19475438. DOI: 10.1146/annurev-chembioeng-060713-040100.

[12] Alain Goeppert et al. "Carbon Dioxide Capture from the Air Using a Polyamine Based Regenerable Solid Adsorbent". In: (2011). DOI: 10.1021/ja2100005. URL: https://pubs.acs.org/sharingguidelines.

[13] *amine | chemical compound | Britannica*. URL: https://www.britannica.com/science/amine (visited on 02/28/2022).

[14] G. Puxty and M. Maeder. "The fundamentals of post-combustion capture". In: *Absorption-Based Post-Combustion Capture of Carbon Dioxide* (June 2016), pp. 13–33. DOI: 10.1016/B978-0-08-100514-9.00002-0. URL: http://dx.doi.org/10.1016/B978-0-08-100514-9.00002-0.

[15] Prakash D. Vaidya and Eugeny Y. Kenig. "CO2-Alkanolamine Reaction Kinetics: A Review of Recent Studies". In: *Chemical Engineering & Technology* 30.11 (Nov. 2007), pp. 1467–1474. ISSN: 1521-4125. DOI: 10.1002/CEAT.200700268.

[16] Lorenzo Costigliola et al. “Revisiting the Stokes-Einstein relation without a hydrodynamic diameter”. In: *The Journal of Chemical Physics* 150.2 (Jan. 2019), p. 021101. ISSN: 0021-9606. DOI: 10.1063/1.5080662. URL: https://aip.scitation.org/doi/abs/10.1063/1.5080662.

[17] *Direct Air Capture | TU Delft Repositories*. URL: https://repository.tudelft.nl/islandora/object/uuid%3A06760340-3f5b-4fb8-9342-12c708f30c2e?collection=education (visited on 02/28/2022).

[18] *Direct Air Capture: Desorption of CO2 and H2O from amines | TU Delft Repositories*. URL: https://repository.tudelft.nl/islandora/object/uuid%3Ac5052a20-6aa7-4f25-a76e-7cb3c363f46f?collection=education (visited on 03/02/2022).

[19] *An experimental and computational study of CO2 absorption in aqueous solutions of tetraethylenepentamine | TU Delft Repositories*. URL: https://repository.tudelft.nl/islandora/object/uuid%3A18e9f0d0-a732-4ce9-b06e-a7f5dbccac26?collection=education (visited on 02/27/2022).

[20] J D Seader, Ernest J Henley, and D Keith. Roper. *Separation process principles : chemical and biochemical operations*. English. 3rd ed. Hoboken, NJ SE - xxvi, 821 pages : illustrations ; 29 cm: Wiley, 2011. ISBN: 9780470481837 0470481838. URL: https://tudelft.on.worldcat.org/oclc/648148046.

[21] Graeme Puxty and Marcel Maeder. “A simple chemical model to represent CO2-amine-H2O vapour-liquid-equilibria”. In: *International Journal of Greenhouse Gas Control* 17 (Sept. 2013), pp. 215–224. ISSN: 17505836. DOI: 10.1016/J.IJGGC.2013.05.016. URL: http://dx.doi.org/10.1016/j.ijggc.2013.05.016.

[22] Wai Lip Theo et al. “Review of pre-combustion capture and ionic liquid in carbon capture and storage”. In: *Applied Energy* 183 (Dec. 2016), pp. 1633–1663. ISSN: 03062619. DOI: 10.1016/J.APENERGY.2016.09.103. URL: http://dx.doi.org/10.1016/j.apenergy.2016.09.103.

[23] Sahag Voskian et al. “Amine-Based Ionic Liquid for CO 2 Capture and Electrochemical or Thermal Regeneration”. In: (2020). DOI: 10.1021/acssuschemeng.0c02172. URL: https://dx.doi.org/10.1021/acssuschemeng.0c02172.

[24] Nithin B. Kummamuru et al. “Viscosity Measurement and Correlation of Unloaded and CO2-Loaded Aqueous Solutions of N-Methyldiethanolamine + 2-Amino-2-methyl-1-propanol”. In: *Journal of Chemical and Engineering Data* 65.6 (2020), pp. 3072–3078. ISSN: 15205134. DOI: 10.1021/acs.jced.0c00088.

[25] Ye Yuan, Brent Sherman, and Gary T. Rochelle. “Effects of Viscosity on CO2 Absorption in Aqueous Piperazine/2-methylpiperazine”. In: *Energy Procedia* 114 (2017), pp. 2103–2120. ISSN: 18766102. DOI: 10.1016/J.EGYPRO.2017.03.1345. URL: www.sciencedirect.com.

[26] Gijs Mulder. *Characterization, Optimization and Design of the Sorbent System for a Continuous Direct Air Capture System*. Tech. rep. 2020. URL: http://repository.tudelft.nl/..

[27] *Dynamic analysis and characterization of a desorption column for a continuous air capture process | TU Delft Repositories*. URL: https://repository.tudelft.nl/islandora/object/uuid%3Aa2931657-274d-4e2f-baab-f31d317974ce?collection=education (visited on 02/27/2022).

[28] Grégoire Léonard, Dominique Toye, and Georges Heyen. “Experimental study and kinetic model of monoethanolamine oxidative and thermal degradation for post-combustion CO2 capture”. In: *International Journal of Greenhouse Gas Control* 30 (2014), pp. 171–178. ISSN: 17505836. DOI: 10.1016/j.ijggc.2014.09.014. URL: http://dx.doi.org/10.1016/j.ijggc.2014.09.014.

[29] Stephen A Bedell. “Energy Procedia Oxidative degradation mechanisms for amines in flue gas capture”. In: *Energy Procedia* 00 (2008), pp. 0–000. DOI: 10.1016/j.egypro.2009.01.102. URL: www.elsevier.com/locate/XXXGHGT-9.

[30] Helene Lepaumier, Dominique Picq, and Pierre Louis Carrette. “New amines for CO2 Capture. I. mechanisms of amine degradation in the presence of CO2”. In: *Industrial and Engineering Chemistry Research* 48.20 (2009), pp. 9061–9067. ISSN: 08885885. DOI: 10.1021/ie900472x.

[31] Alexander K Voice, Fred Closmann, and Gary T Rochelle. “Oxidative degradation of amines with high-temperature cycling Selection and/or peer-review under responsibility of GHGT”. In: *Energy Procedia* 37 (2013), pp. 2118–2132. DOI: 10.1016/j.egypro.2013.06.091. URL: www.sciencedirect.com.

[32] Gouri Nayanar. “Internship Report Study of thermal degradation of Tetraethylenepentamine (TEPA)”. In: 5041627 (2021).

[33] Benedikt Paschke and Alfons Kather. “Corrosion of Pipeline and Compressor Materials due to Impurities in separated CO 2 from fossil-fuelled Power Plants”. In: 23 (2012), pp. 207–215. ISSN: 1876-6102. DOI: 10.1016/j.egypro.2012.06.030.

[34] ALIGN CCUS. “Variation in CO2 composition – defining safe operation windows. Recommendations on CO2 specification for ALIGN partners. Report D2.3.3”. In: 271501 (2020).

[35] Suoton P. Peletiri, Nejat Rahmanian, and Iqbal M. Mujtaba. “CO2 Pipeline design: A review”. In: *Energies* 11.9 (2018). ISSN: 19961073. DOI: 10.3390/en11092184.

[36] Mohammad Ahmad and Sander Gersen. “Water solubility in CO2 mixtures: Experimental and modelling investigation”. In: *Energy Procedia* 63 (2014), pp. 2402–2411. ISSN: 18766102. DOI: 10.1016/j.egypro.2014.11.263.

[37] Bjørn H. Morland, Arne Dugstad, and Gaute Svenningsen. “Corrosion of Carbon Steel in Dense Phase CO2 with Water above and below the Solubility Limit”. In: *Energy Procedia* 114.November 2016 (2017), pp. 6752–6765. ISSN: 18766102. DOI: 10.1016/j.egypro.2017.03.1807.

[38] E Dendy. Sloan and Carolyn Koh. *Clathrate hydrates of natural gases*. English. Boca Raton, 2008. URL: https://tudelft.on.worldcat.org/oclc/839656326.

[39] *Humidity Saturation Limits of Hydraulic and Lubrication Fluids*. URL: https://www.machinerylubrication.com/Read/28697/humidity-saturation-limits (visited on 02/26/2022).

[40] Vaisala. “HUMIDITY CONVERSION FORMULAS - Calculation formulas for humidity”. In: *Humidity Conversion Formulas* (2013), p. 16. URL: https://www.vaisala.com/sites/default/files/documents/Humidity_Conversion_Formulas_B210973EN-F.pdf.

[41] *Conceptual Design of a Novel Small-Scale CO2 Compressor | TU Delft Repositories*. URL: https://repository.tudelft.nl/islandora/object/uuid:8f4f1dcf-f3c1-4a6c-8607-32ccfc783f5e?collection=education (visited on 02/27/2022).

[42] Jianhua Wu and Ang Chen. “A new structure and theoretical analysis on leakage and performance of an oil-free R290 rolling piston compressor”. In: *International Journal of Refrigeration* 49 (2015), pp. 110–118. ISSN: 01407007. DOI: 10.1016/J.IJREFRIG.2014.10.007. URL: http://dx.doi.org/10.1016/j.ijrefrig.2014.10.007.

[43] Kuan Thai Aw and Kim Tiow Ooi. “A review on sliding vane and rolling piston compressors”. In: *Machines* 9.6 (2021). ISSN: 20751702. DOI: 10.3390/machines9060125.

[44] *Module 163: Rolling-piston rotary refrigerant compressors for air conditioning applications – CIBSE Journal*. URL: https://www.cibsejournal.com/cpd/modules/2020-06-toshiba/ (visited on 02/27/2022).

[45] Manfred Krueger. “Theoretical simulation and experimental evaluation of an hermetic rolling piston rotary compressor”. In: *Purdue University* (1988).

[46] *Simulation and comparison of leakage characteristics of R290 in rolling piston type rotary compressor | Elsevier Enhanced Reader*. URL: https://reader.elsevier.com/reader/sd/pii/S014070071500033X?token=FDDBC1B73349722BA090196C2BC2C6F5DF1E24536EC472D35754749384E394B515CEF902913FC03D9F82AC67D2C98ED6&originRegion=eu-west-1&originCreation=20220216141451 (visited on 02/16/2022).

[47] Luiz Gasche, Thiago Andreotti, and Macedo Maia. “Author ’ s personal copy A model to predict R134a refrigerant leakage through the radial clearance of rolling piston compressors ‘ le utilise ´ pour pre ´ voir les fuites du frigorige ‘ ne R134a a Mode ‘ piston roulant travers le jeu radial des compresseu”. In: ().

[48] *Conceptual Design of a Novel Small-Scale CO2 Compressor | TU Delft Repositories*. URL: https://repository.tudelft.nl/islandora/object/uuid:8f4f1dcf-f3c1-4a6c-8607-32ccfc783f5e?collection=education (visited on 02/27/2022).

[49] S Anbu, M Senthilkumar, and Assistant Professor. "Modelling and Analysis of Continuous Stirred Tank Reactor through Simulation". In: *Asian Journal of Engineering and Applied Technology* 7.1 (2018), pp. 78–83. URL: www.trp.org.in.

[50] Robert 1963- Holyst and Andrzej 1951- T A - T T - Poniewierski. *Thermodynamics for chemists, physicists and engineers LK - https://tudelft.on.worldcat.org/oclc/798917411*. English. Dordrecht ; 2012. URL: http://site.ebrary.com/id/10652722%20https://search.ebscohost.com/login.aspx?direct=true&scope=site&db=nlebk&db=nlabk&AN=2545944%20http://books.scholarsportal.info/viewdoc.html?id=/ebooks/ebooks2/springer/2012-08-27/1/9789400729995%20https://doi.org/10.1007/978-94-007-2999-5%20https://link.springer.com/book/10.1007%2F978-94-007-2998-8%20https://link.springer.com/book/10.1007%2F978-94-007-2999-5%20http://dx.doi.org.ezproxy.aub.edu.lb/10.1007/978-94-007-2999-5(off-campusaccess)%20http://www.vlebooks.com/vleweb/product/openreader?id=none&isbn=9789400729995.

[51] Sigurd Skogestad. *Chemical and energy process engineering*. Boca Raton: CRC Press Taylor & Francis Group, 2009. Chap. 11, pp. 284–325. ISBN: 9781420087550. URL: https://www.routledge.com/Chemical-and-Energy-Process-Engineering/Skogestad/p/book/9781420087550.

[52] N. Park, J. Shin, and B. Chung. "A new dynamic heat pump simulation model with variable speed compressors under frosting conditions". In: *Institution of Mechanical Engineers - 8th International Conference on Compressors and Their Systems* (2013), pp. 681–696. DOI: 10.1533/9781782421702.12.681.

[53] C S P Bootsman. "Characterisation of the CO2 drying system". In: February (2022), pp. 1–49.

[54] Michael J thermodynamica Moran 1939-. *Principles of engineering thermodynamics*. English. 7th ed. Hoboken, N.J SE - xiii, 928 p. : illustrations (some color) ; 28 cm: Wiley, 2012. ISBN: 0470918012 9780470918012. URL: https://tudelft.on.worldcat.org/oclc/821021557.

[55] Thomas E Marlin. *Process control : designing processes and control systems for dynamic performance*. English. 2nd ed. McGraw-Hill, 2000. ISBN: 0070393621 9780070393622 0071163573 9780071163576. URL: http://catdir.loc.gov/catdir/toc/mh023/99026739.html%20http://catdir.loc.gov/catdir/description/mh023/99026739.html.

[56] General Product and Customer Benefits. "HAFFMANS CPT CO 2 PURITY TESTER HAFFMANS CPT CO 2 PURITY TESTER". In: ().

[57] *Characterization and Design of a Stripper for a Continuous Direct Air Capture System | TU Delft Repositories*. URL: https://repository.tudelft.nl/islandora/object/uuid%3A2dfe2d61-c707-45e5-9a35-8a15101853ee?collection=education (visited on 02/28/2022).

[58] John Coates. "Interpretation of Infrared Spectra, A Practical Approach". In: *Encyclopedia of Analytical Chemistry*. Chichester, UK: John Wiley & Sons, Ltd, Sept. 2006. DOI: 10.1002/9780470027318.a5606. URL: http://doi.wiley.com/10.1002/9780470027318.a5606.

[59] *TQ Analyst™ Pro Edition Software*. URL: https://www.thermofisher.com/order/catalog/product/IQLAADGABZFAIXMAVF (visited on 08/17/2022).

[60] Nichtkompensierte Druckmeßumformer and Figures Abbildung Figura. "Uncompensated Pressure Transducers". In: (1998), pp. 1–4.

[61] "Datasheet SHT3x-DIS". In: (2015). URL: www.sensirion.com.

[62] Jasmin Kemper et al. "Evaluation and analysis of the performance of dehydration units for CO2 capture". In: *Energy Procedia* 63.April (2014), pp. 7568–7584. ISSN: 18766102. DOI: 10.1016/j.egypro.2014.11.792.

A

Experimental setup and results

A.1. Flash tank setup:

The flash tank setup to control the MiniDAC system pressure to target level as described in 4.3, went through multiple iterations before the final configuration (4.1.2) was fixed. The same have been described below.

A.1.1. Compressor/Pump 'On-Off' control:

The P&ID of the control scheme is shown in Figure [A.1]. For this control, the pump was operated in 'On/Off' control mode.

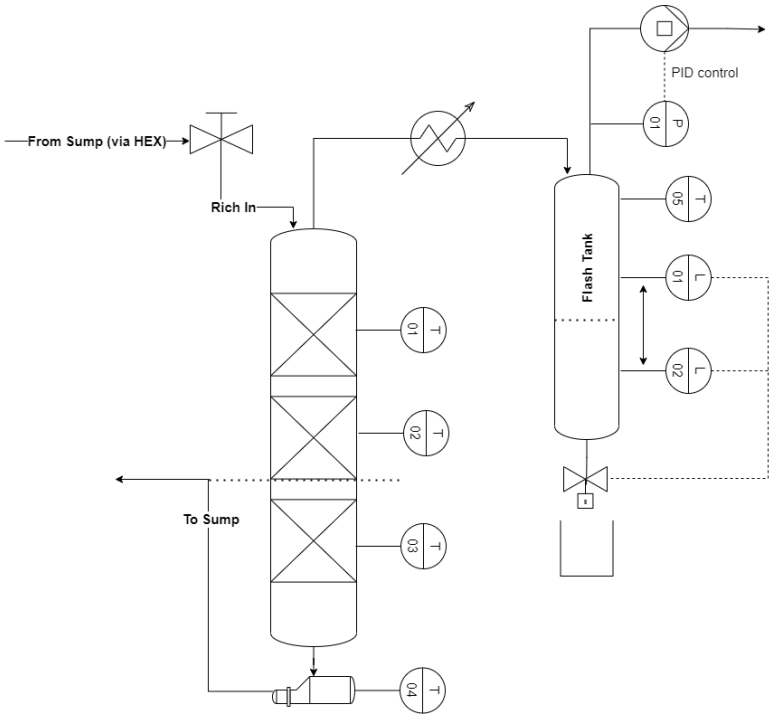

Figure A.1: P&ID of the 'On-Off' control for flash tank pressure control. The pump operation was controlled using PID controller for which system pressure was the input. If system pressure was higher than threshold then pump would operate based on PID controller to bring the pressure down to target level and if pressure was below a threshold, the pump would turn off.

Using this control, the pressure fluctuation in the flash tank was maintained within the target level of $\pm$ 5mbar relative to atmospheric pressure as shown in Figure[A.2] and [A.3].

Drawback:
Th 'On-Off' control configuration was not used as the final one based on below mentioned reasons:

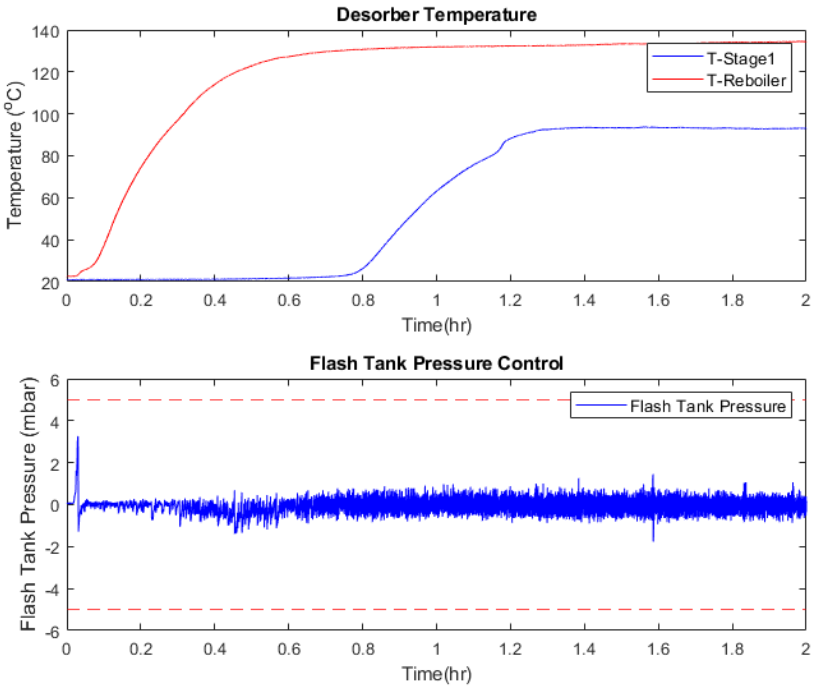

Figure A.2: The pressure is maintained between target of ±5mbar relative to atmospheric pressure with pump operated in On-Off mode using PID controller

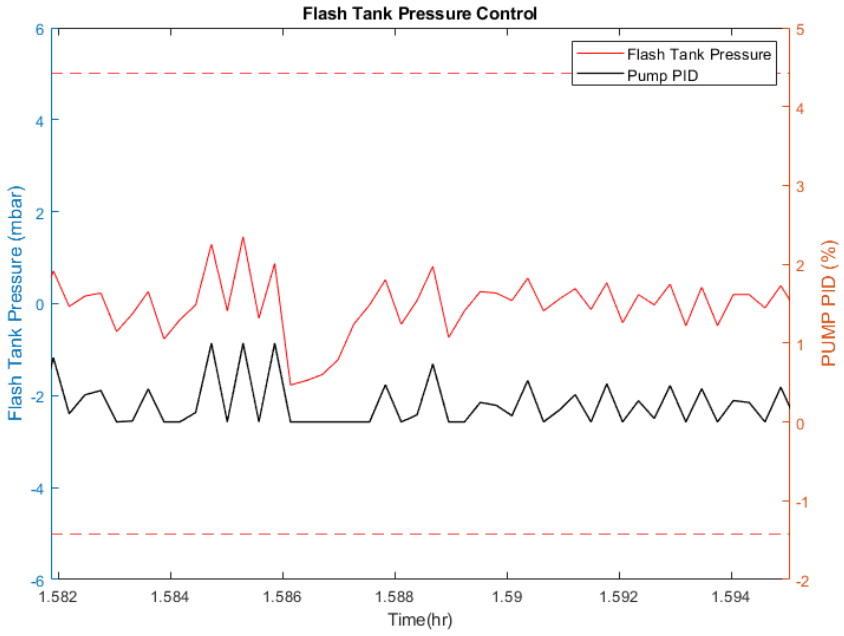

Figure A.3: The PID controller operates the pump between 0-1 (Off-On) mode and is able to control pressure to required target level

- Although the control worked as per requirement, the configuration was unsuitable as this involved operating the pump in repeated on-off operation mode. Using this control with a compressor would lead to deterioration of compressor lifetime as repeated on-off operation leads to wear in compressor.

- Further, the compressor can only operate above a minimum compressor speed as specified by the manufacturer. Hence the on-off control was deemed unsuitable for final implementation on the integrated DAC+FM system.

- During shutdown, as the desorber cooled down, the water vapour in the system re-condenses, resulting in negative pressure in the system. The same is shown in Figure[A.4] below.

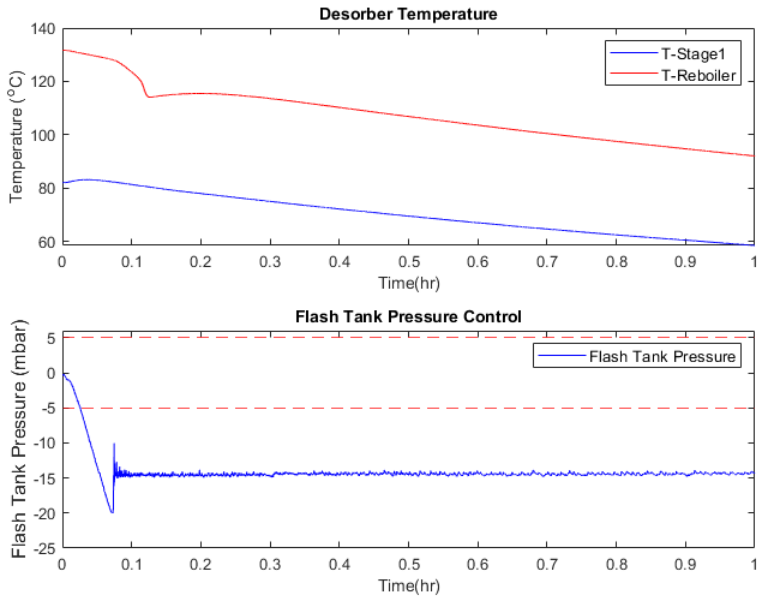

Figure A.4: As desorber cools down the water vapour re-condenses resulting in negative pressure in the system

This cannot be controlled using the on-off control strategy.

A.1.2. Bypass Control:

The next configuration was designed to tackle the issue of having to repeatedly turn the pump/compressor On and Off and operating the compressor above a minimum operating speed.

For this the pump operation was limited between 1 (maximum power) and a minimum power (0) threshold to simulate compressor operation between rated minimum and maximum operating speed. In order to ensure that pressure in the flash tank doesn't drop below the 5mbar threshold (below atmospheric pressure), a part of pump outlet was routed back to the flash tank via a solenoid valve. The operation of the valve was also controlled based on system pressure.

The P&ID of the configuration is shown below in Figure[A.5].

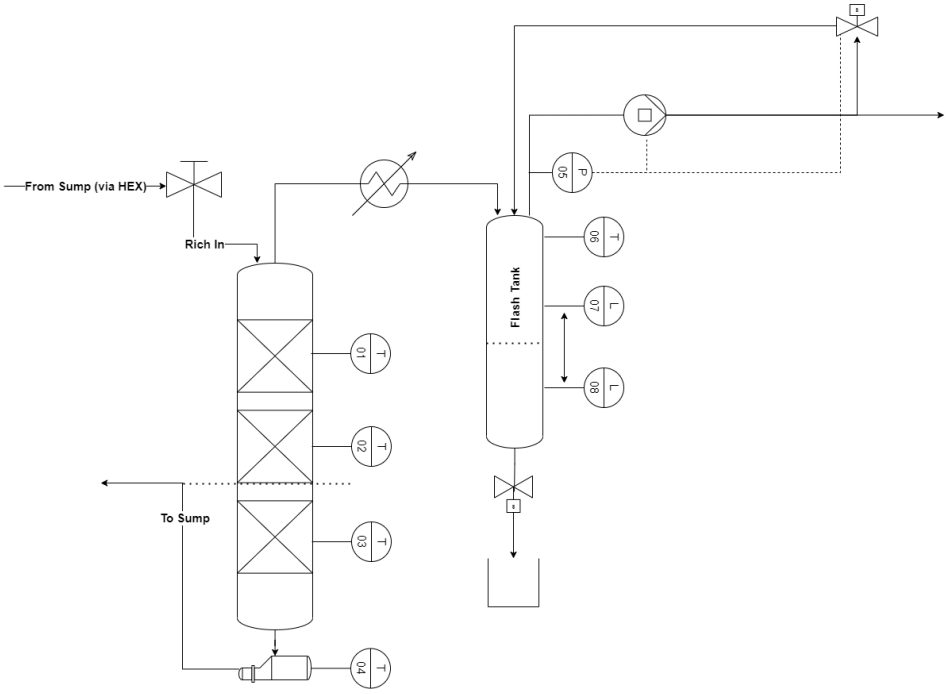

Figure A.5: P&ID of the bypass control for flash tank pressure control. The pump operation was controlled using PID controller between 1 and minimum power (0) to simulate compressor operation between minimum and maximum rated speed. Further a part of pump output was bypassed back to flash tank via solenoid valve to maintain flash tank pressure..

Using this control, the pressure fluctuation in the flash tank was maintained within the target level of ± 5mbar relative to atmospheric pressure as shown in Figure[A.6] and [A.7].

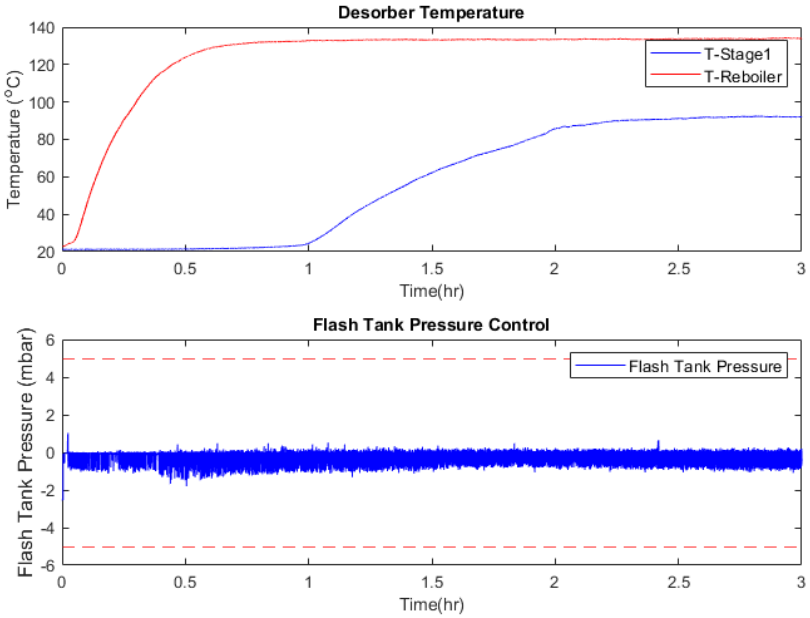

Figure A.6: The pressure is maintained between target of ±5mbar relative to atmospheric pressure with pump operated in On-Off mode using PID controller

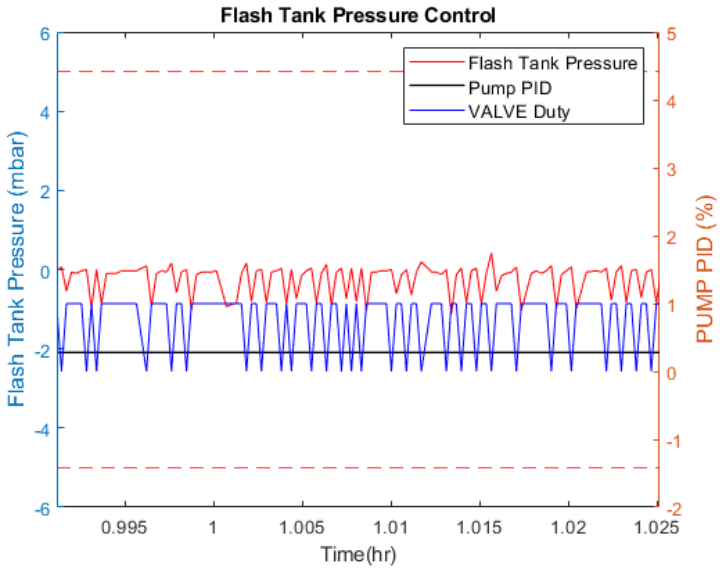

Figure A.7: The PID controller operates the pump between 0-1 (Off-On) mode and is able to control pressure to required target level

Drawback:

The bypass control worked to control the pressure during startup and steady-state operation. However, the issue of negative pressure after shutdown cannot be controlled using this control.

In order to control the negative pressure(A.4), the final control scheme (described in 4.3) was developed.

A.2. MiniDAC Test Results:

A.2.1. Desorber Test Results:

The test results obtained for desorber operation of MiniDAC under steady state is given below in Table [A.1]

Table A.1: MiniDAC desorber steady state operation results

Parameter	Description	Value	Unit
m_{feed}	Desorber feed flow rate	1.4	[g sorbet/min]
P_{pump}	Sorbent pump power input	21	[W]
P_{heater}	Heater power input (Steady state)	50	[W]
$Rich_{CO_2}$	Average Rich CO_2 loading	4.4	$[\frac{molCO_2}{kgTEPA}]$
$Lean_{CO_2}$	Average lean CO_2 loading	0.56	$[\frac{molCO_2}{kgTEPA}]$
Cyc Cap_{CO_2}	Average cyclic capacity CO_2 loading	3.84	$[\frac{molCO_2}{kgTEPA}]$
E_{req}	Average energy required for CO_2 capture	2865	$[\frac{kJ}{molCO_2}]$

A.2.2. CO_2 Purity test:

In order to measure the purity of CO_2 output from MiniDAC, Haffman's CO_2 purity tester was used. The specifications and accuracy of the equipment can be found at [56].

The results of CO_2 purity test are shown below in Table [A.2] and Figure [A.8]

Table A.2: Purity measurement of CO_2 output from MiniDAC

Parameter	Description	Value	Unit
CO_2 purity MiniDAC	Purity at MiniDAC outlet	99.5	[% (v/v)]
CO_2 purity MiniDAC (ZEF 8)	Purity at MiniDAC outlet (2021)	99.7	[% (v/v)]
CO_2 purity model	Purity from MiniDAC model	99	[% (v/v)]

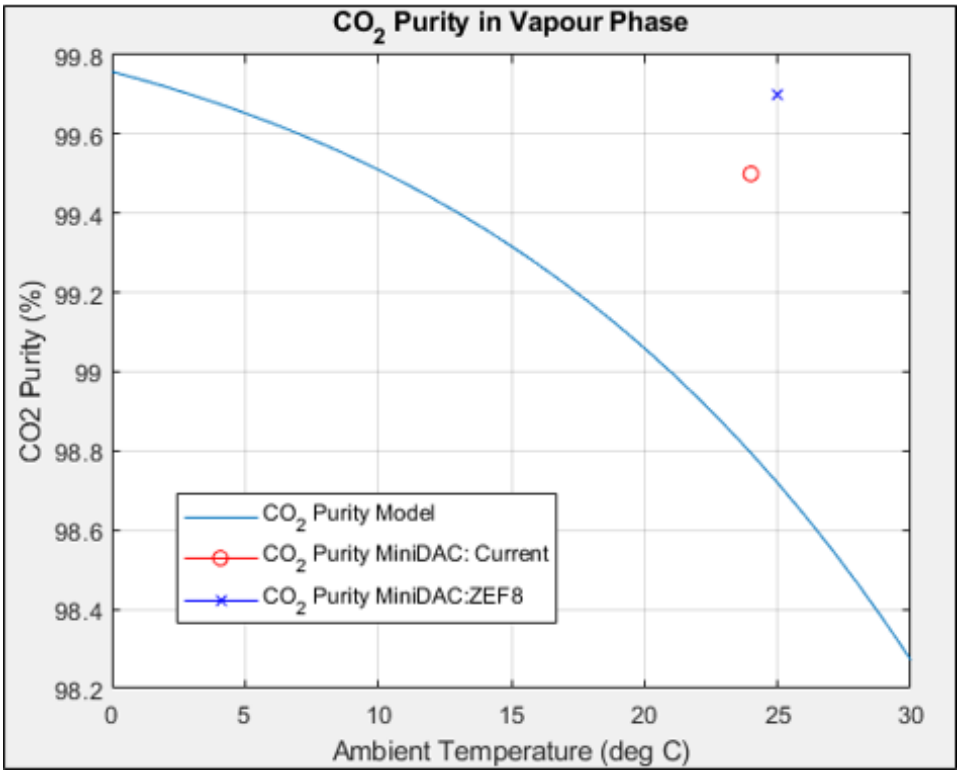

Figure A.8: Purity of CO_2 measured using Haffman's CO_2 purity tester

A.3. Measurement Equipment:

A.3.1. Fourier Transform Infrared Spectroscopy:

The analysis of rich and lean sorbent to quantify the composition of the sorbent was done using Fourier transform infrared spectroscopy (FTIR). Infrared spectroscopy is the study of interaction of light with matter; as a molecule absorbs infrared radiation, the chemical bonds present in the molecule begin to vibrate by either stretching, contracting, wagging or bending [58].

Through FTIR analysis, plot of the intensity of the radiation against the wave number of the light is generated. By analysing the position of the peaks, the intensities and the width of the spectrum the nature or type of chemical bonds present inside the molecule can be identified.

For the MiniDAC experiments, the rich and lean sorbent samples were analysed using Agilent Cary 630 FTIR A.9. The FTIR spectrum was analysed using TQ Analyst software [59] which was calibrated using reference samples of known concentration calibration curve for TEPA-PEG200-H_2O-CO_2 mixture.

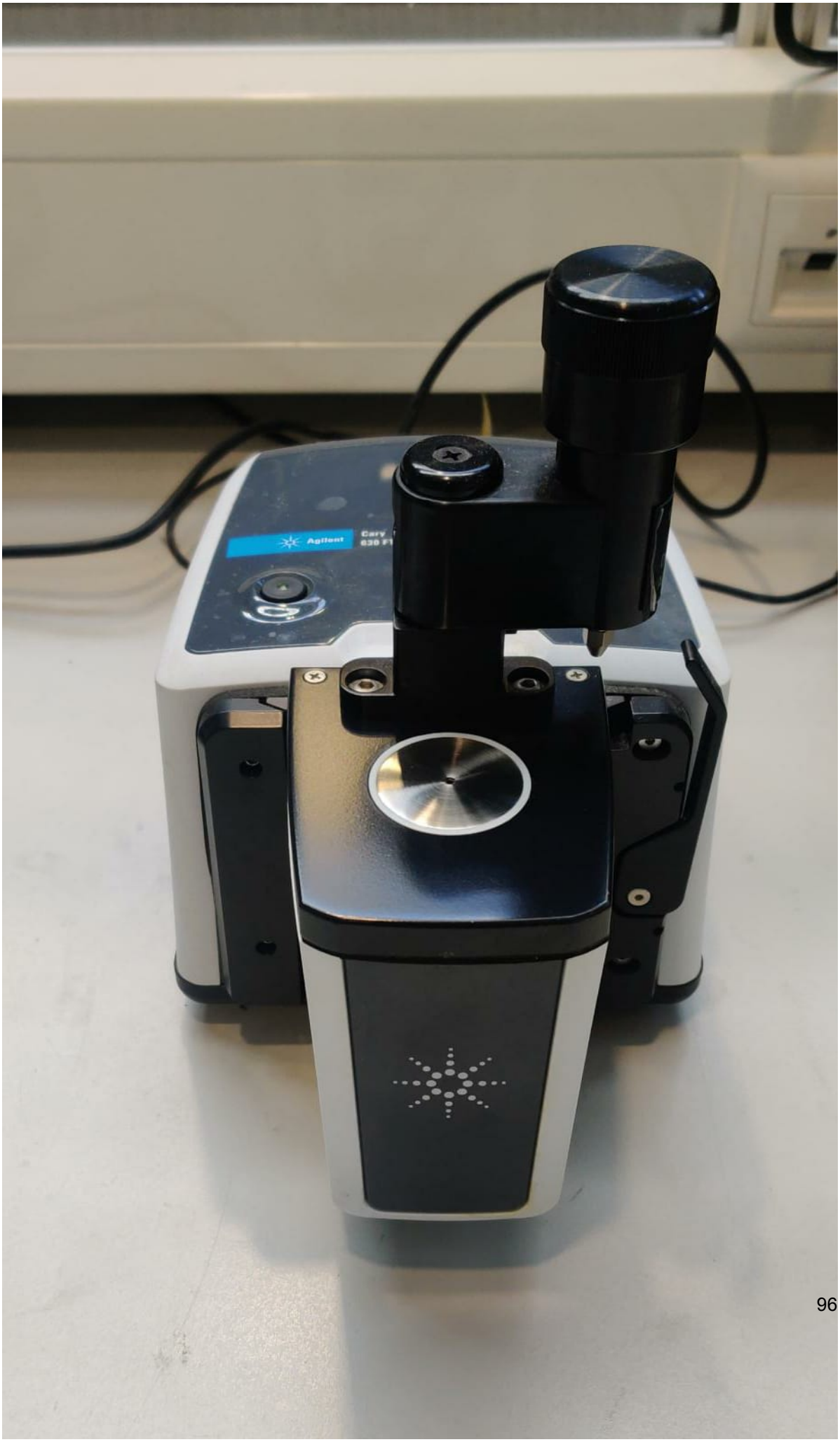
Agilent

A.3.2. Flash Tank Pressure:

Flash tank pressure was measured using Honeywell Differential pressure sensor (24PCEFA6D) [60]. One side of the pressure sensor was kept open to atmosphere and the other end was connected to flash tank to get the pressure of the flash tank relative to atmosphere. The accuracy of the same was 0.15%.

A.3.3. Humidity measurement:

For measurement of absolute humidity, Adafruit SHT31-D Temperature & Humidity Sensor was used. The accuracy of the same was $\pm$2% RH and $\pm 0.3^{o}$C. [61]

B

Appendix: Modelling Approach and Results

B.1. Absorber Model:

B.1.1. STY CO_2:

The STY curve for CO_2 is determined by extrapolation of experimentally obtained VLE data for CO_2 in TEPA-H_2O mixture at ZEF.

The procedure for determining STY of CO_2 at different temperature and CO_2 loading in the sorbent is shown in Figure[B.1] below.

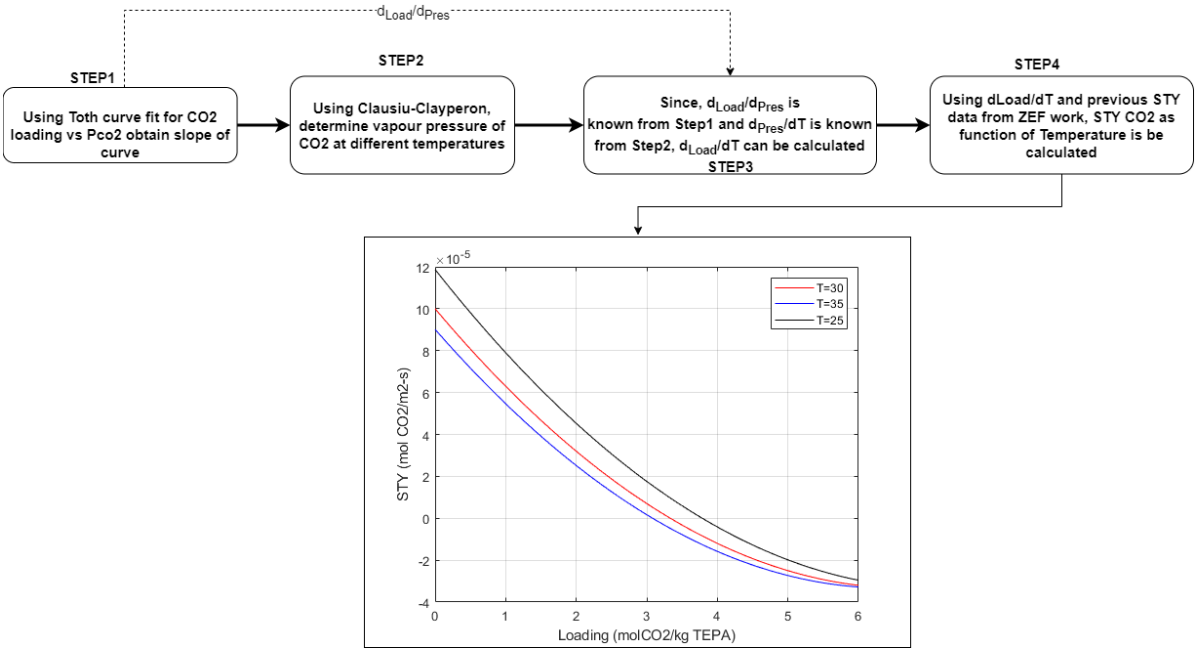

Figure B.1: Calculation procedure for determining STY CO_2 as function of temperature and an example STY curve for CO_2 based on the described algorithm

The same procedure is implemented in the Absorber model and calculates the STY at every time step based on input ambient temperature. Using this STY value, flow rate and composition of absorber inlet and area of absorber, CO_2 concentration in the outlet stream of absorber is determined.

B.1.2. STY H_2O:

The STY curve used for H_2O has been carried over from the previous work at ZEF by Dubhashi et. al. [27].

The STY curve used for H_2O is dependent on Humidity and current H_2O loading in the sorbent. The same is shown in Figure[B.2] below.

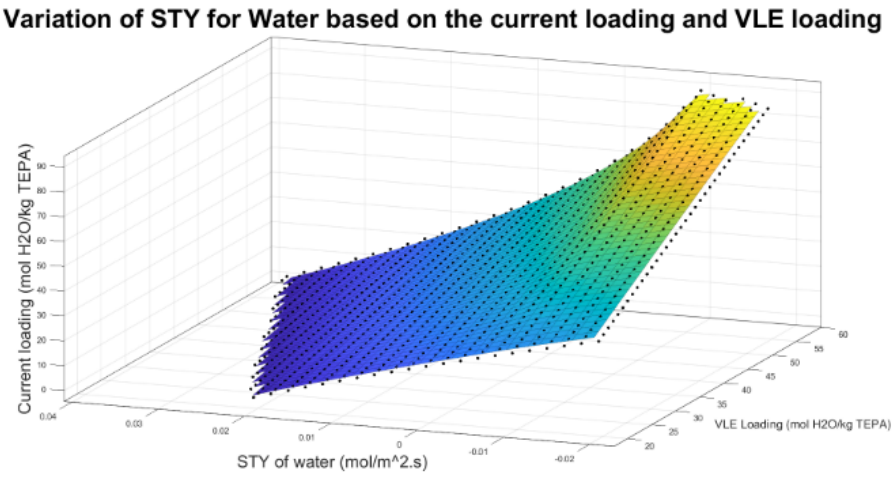

Figure B.2: STY of H_2O as a function of VLE H_2O loading and current H_2O loading in the sorbent

B.1.3. Absorber and sump model results:

Figure [B.3] shows the variation in rich loading of H_2O as calculated using the absorber and sump model with variation in humidity, simulated for typical weather condition observed during testing on MiniDAC test setup at ZEF.

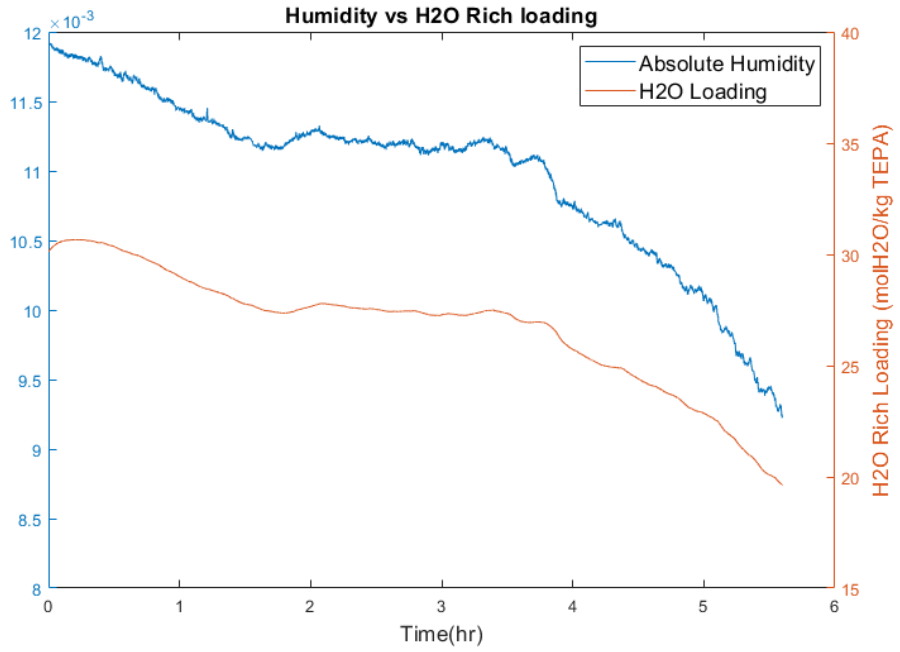

Figure B.3: Variation of rich H_2O loading with humidity calculated using the absorber and sump model

B.2. Desorber Model:

The desorber model results are shown in Figure [B.4] below.

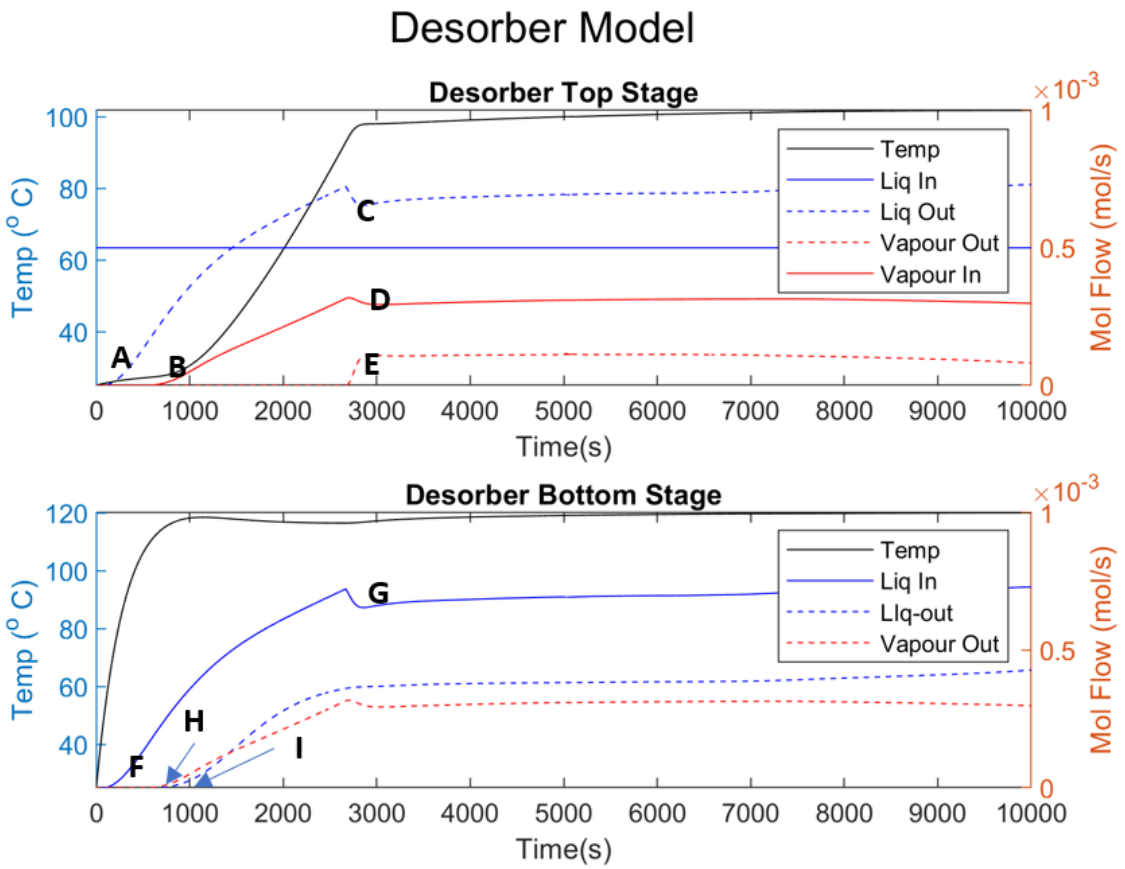

Figure B.4: Figure shows how the temperature, liquid and vapour level vary in the two stages of the desorber model. The main dynamic point shown in the figure are explained below

- **A:**As liquid holdup in top stage reaches its maximum, liquid starts to overflow to bottom stage.
- **B:**As vapour holdup in bottom stage reaches its maximum, vapour from bottom stage starts flowing to top stage.
- **C:** As temperature increases and liquid in top stage starts changing to vapour, liquid flowing to bottom stage decreases.
- **D:** As liquid to bottom stage decreases, the vapour flowing from bottom stage to top stage also decreases.
- **E:** As vapour in top stage reaches its maximum holdup, it starts to overflow and exits the top stage.
- **F:** Liquid overflow from top stage to bottom stage.
- **G:** This is same as point C. Liquid from stage top stage decreases as it starts changing to vapour in top stage.

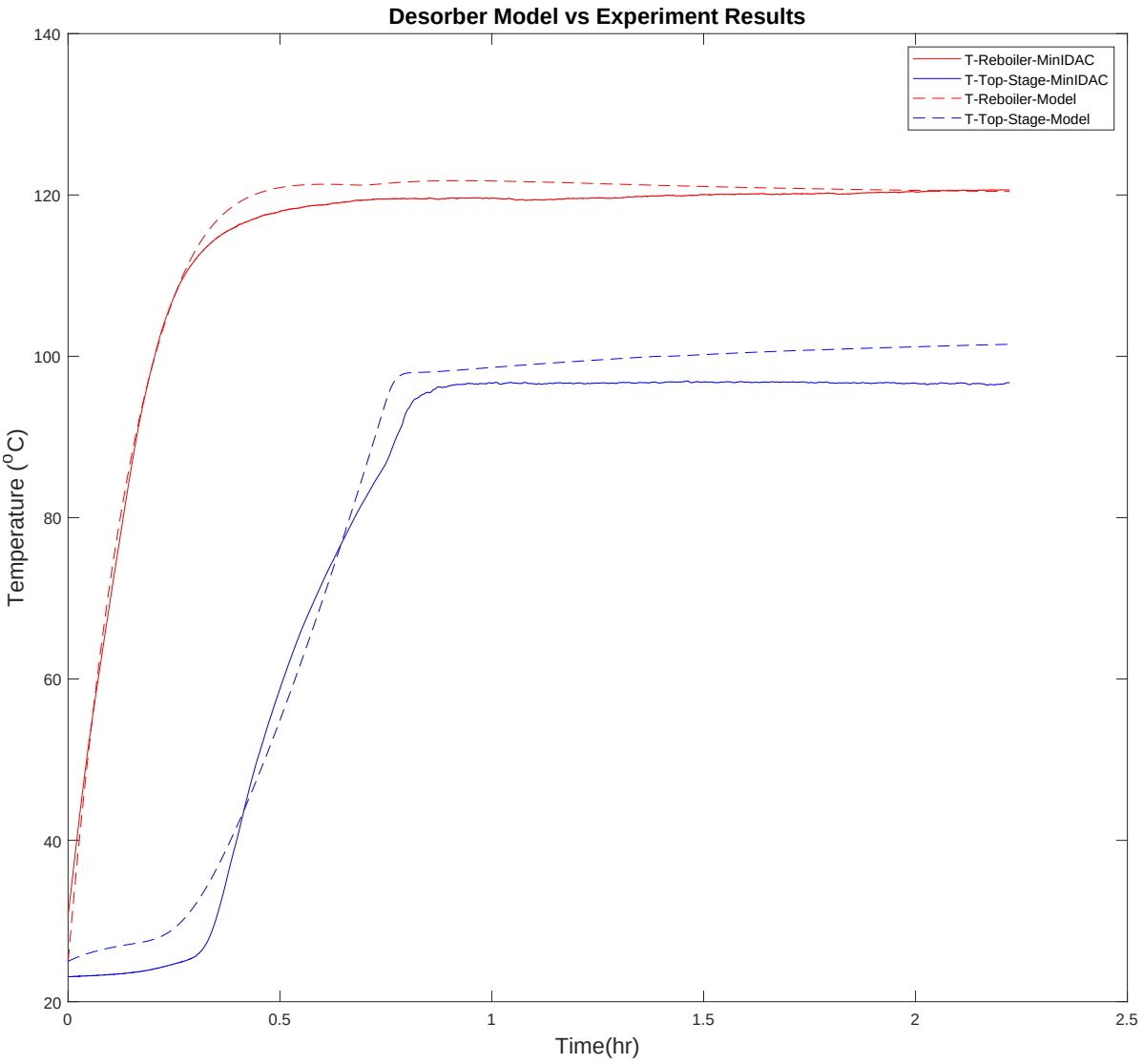

Figure B.5: Temperature profile in the Desorber during startup and steady state operation as predicted by the model matches well with the MiniDAC experimental results

- **H:** As vapour in bottom stage reaches its maximum holdup in bottom stage it starts to overflow to top stage (same as point B).

- **I:** As liquid in bottom stage reaches its maximum holdup it starts overflowing out back to sump.

The model predicts the temperature rise in the desorber as a function of parameters explained in 3.1.3. The modelled temperature profile in the desorber matches well the experimental results on the MiniDAC test setup as shown in Figure[B.5] below:

B.3. Flash tank model:

The working of the flash tank model has been described in 3.8. The output the flash tank generates is the flash tank pressure which is calculated by assuming ideal gas behaviour in the flash tank. For this calculation, flash tank gas volume which is calculated as the difference of total flash tank volume to total volume of liquid which enters the flash tank. Further, the flash tank liquid volume is maintained between a certain threshold which can be controlled by activating flash tank liquid outlet using level

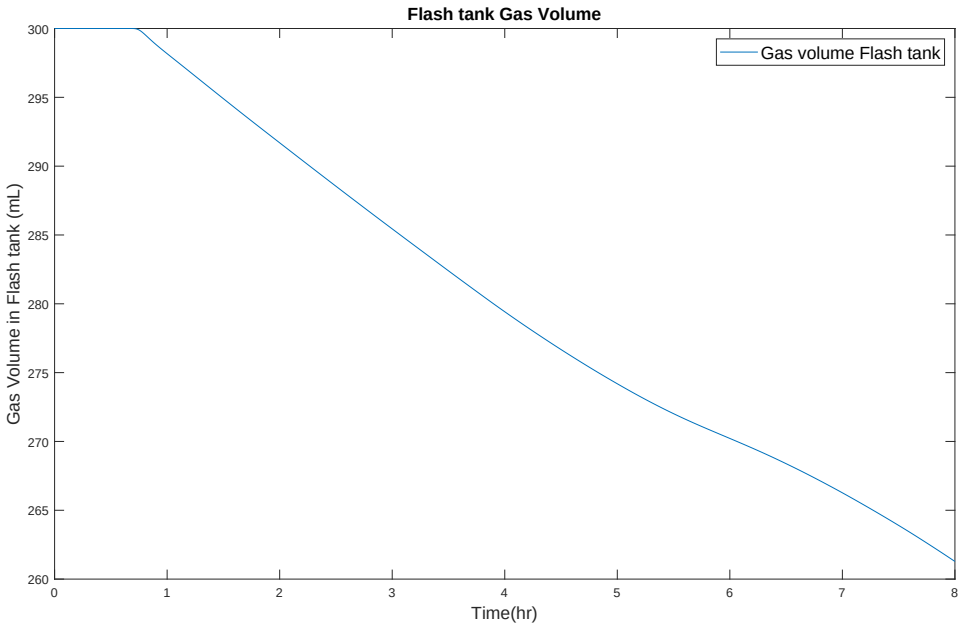

Figure B.6: As H_2O production from DAC increases the liquid level in flash tank starts to increase and consequently the gas volume decreases. This gas volume is used for calculating pressure in the flash tank

sensor in the flash tank.

Figure[B.6] shows how the flash tank gas volume varies with DAC production.

B.4. Integrated DAC+FM system model:

The results of pressure fluctuation in flash tank for the integrated DAC+FM system model is shown in Figure[B.7] and [B.8]below.

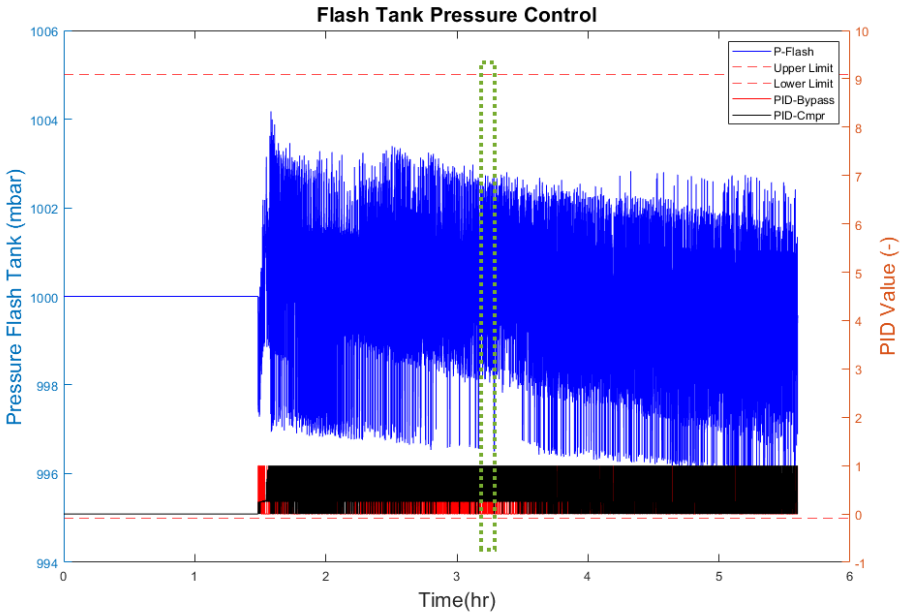

Figure B.7: Flash tank pressure fluctuation with flash tank pressure control 5.3.2 implemented in the mode. The pressure fluctuation is within target of $\pm$5mbar relative to atmospheric pressure. The highlighted region is zoomed in Figure[B.8] below

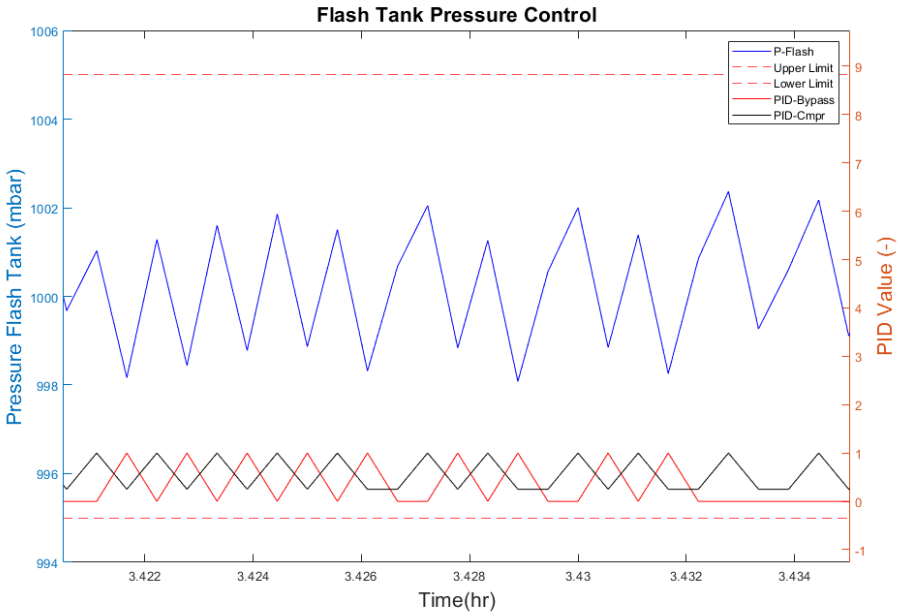

Figure B.8: Zoomed in version of Figure[B.7] showing pressure fluctuation. The PID controlled compressor and bypass valve operate in conjunction to keep pressure within desired limit value

C

Appendix: Relevant Theory

C.1. Maximum H_2O content for compression system:

C.1.1. Hydrate formation prevention:

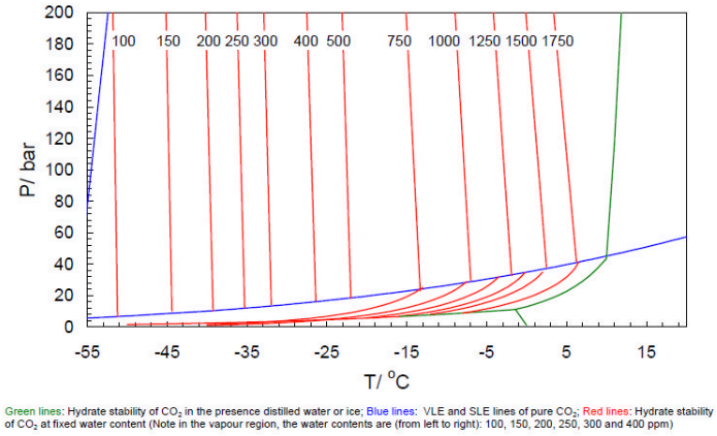

Figure C.1: CO_2 hydrate equilibrium at fixed water content [62]

C.2. System Performance Parameters:

C.2.1. DAC desorber pressure:

System pressure determines the VLE conditions in the desorber. Previous work at ZEF [57],[27], showed that by increasing the system pressure the top ratio and energy requirement of the DAC system can be improved at fixed desorber temperature. However, for as per ZEF's requirement the target is to operate the desorber at atmospheric pressure in-order to simplify the overall system and reduce the failure points in the system.

However, for ZEF DAC system, target is to operate at atmospheric pressure. Operating at atmospheric pressure simplifies the entire system as it eliminates the requirement of pumps and valves to maintain high pressure in the system; thereby reducing the failure points in the DAC system.

C.2.2. Desorber feed temperature:

Feed inlet temperature directly affects the reboiler power required to heat up the feed to desorption temperature C.3.

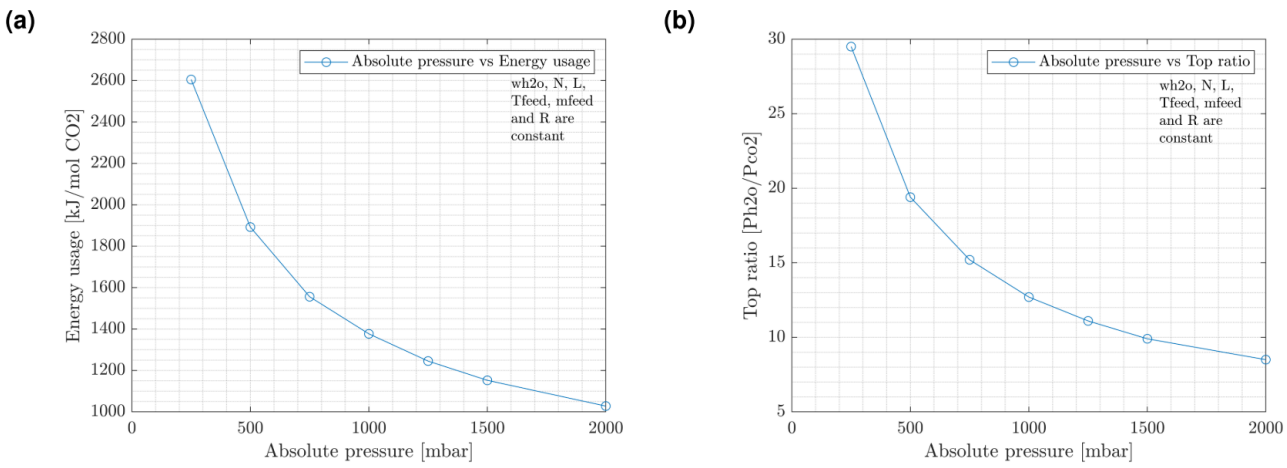

Figure C.2: Increasing the system pressure reduces the (a) energy requirement and improves the (b) Top ratio at the DAC outlet for fixed sorbent loading,feed flow and reflux [57]

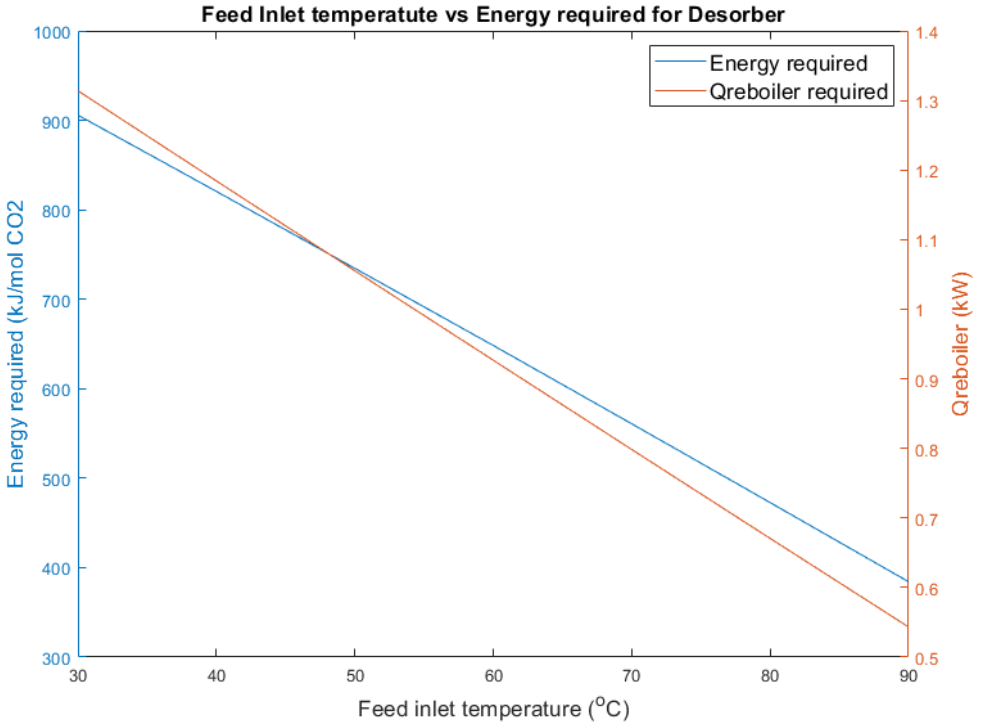

Figure C.3: As feed inlet temperature increases the reboiler power required to heat up the desorber to target temperature goes down

C.2.3. Desorber temperature:

Desorption of CO2 and H2O from the sorbent is favourable at higher temperatures. Previous work by Dubhashi et.al, [27] has showed that higher desorber temperatures, lower lean loadings are possible at lower holdup time.

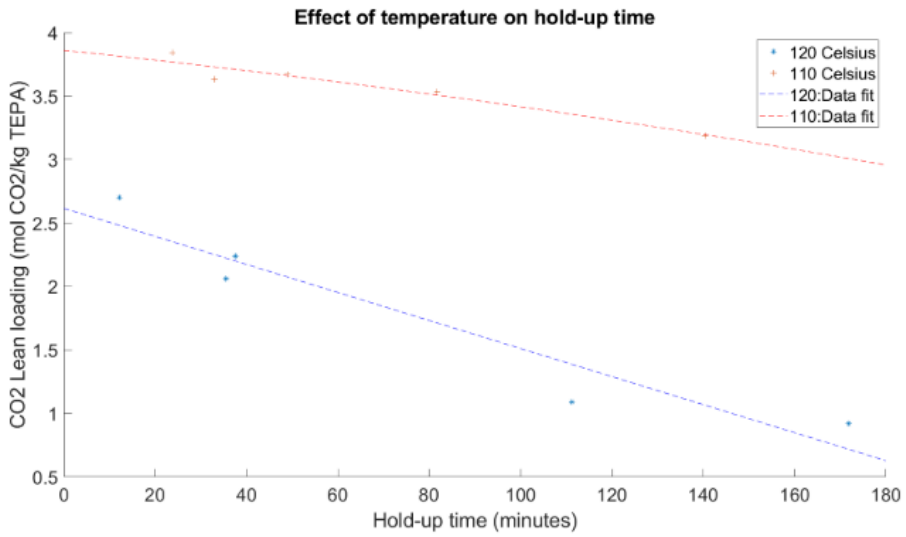

Figure C.4: Increasing the desorber temperature reduces the holdup time required to achieve particular lean loading in the desorber [27]

C.2.4. Flash tank volume:

Volume of flash tank is inversely related to the pressure fluctuation in flash tank, i.e., higher the volume lower the pressure fluctuation. Figure[C.5] shows the pressure fluctuation in the flash tank for same DAC output and flash tank pressure control with different flash tank volume.

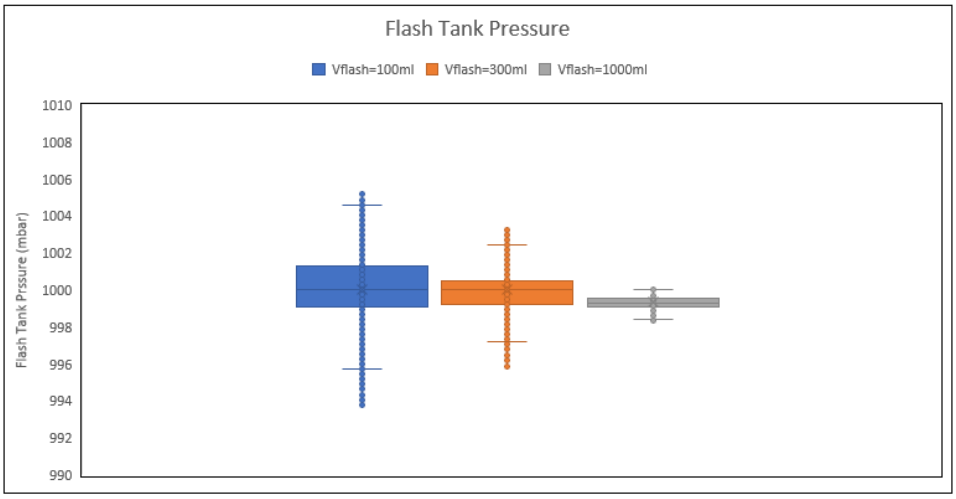

Figure C.5: Pressure fluctuation increases as for lower flash tank volume. The graph shows pressure fluctuation in flash tank with same DAC output and pressure control with only flash tank volume changed. For lowest Vflash=100ml, fluctuation observed is highest.

C.2.5. Flash tank temperature:

At higher temperature, the fraction of H2O in the vapour phase is higher and vice-versa.

C.3. Operational Scenarios:

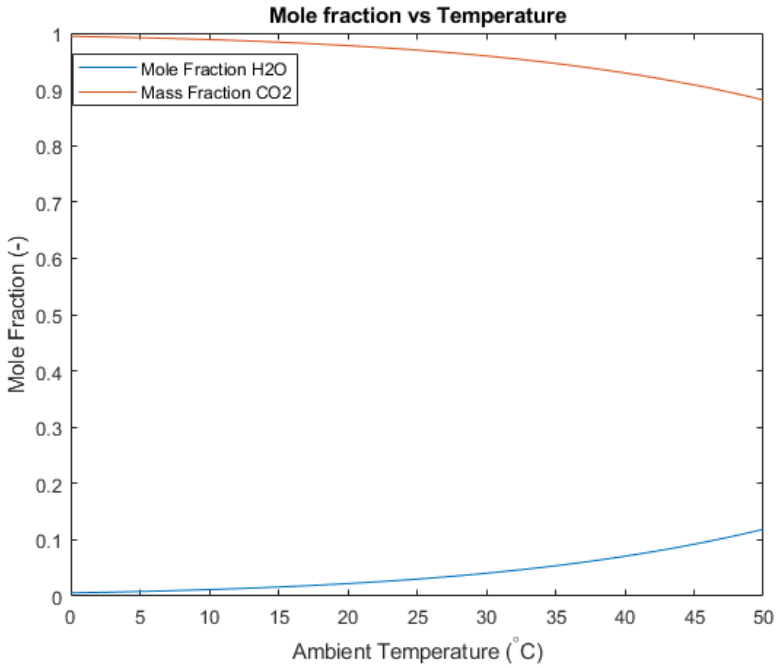

Figure C.6: Fraction of water in vapour phase in the flash tank increases with flash tank temperature and vice-versa

C.3.1. High Production/Ramp-up:

High output/ramp-up of DAC production can take place in case of following condition. The same is also shown in Figure[C.7]

- **High humidity:** With increase in absolute humidity, the H_2O loading in the sorbent increases (5.2). This will result in higher water output from the desorber.
- **Low ambient temperature:** At low ambient temperature, the CO_2 loading in the sorbent increases(5.1). This will result in higher CO_2 production from desorber.
- **High mass flow rate:** With desorber operating at constant temperature, increasing the feed flow to the desorber will increase the net production of CO_2 and H_2O from the desorber.
- **Desorber temperature/Heat Input:** Increase in heat input/desorber temperature at constant feed flow, will increase the desorption of CO_2 and H_2O and will increase the net production from the desorber.

C.3.2. Low Production/Ramp-down:

Low output/ramp-down of DAC production can take place in case of following condition. The same is also shown in Figure[C.8]

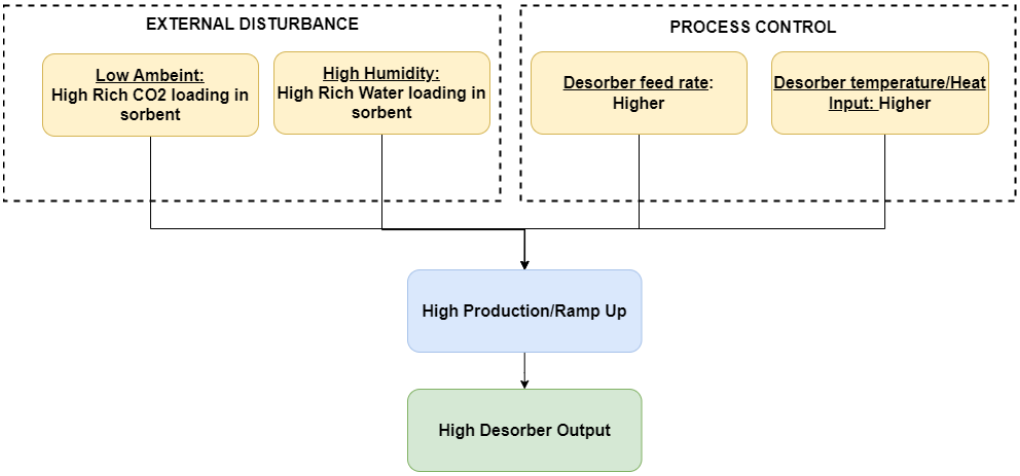

Figure C.7: External disturbance like High humidity, low ambient temperature will result in higher rich H_2O and CO_2 loading in the sorbent which will result in higher desorber output. Similarly, increase in sorbent feed to the desorber and/or heat input/desorber temperature will also increase the desorber output.

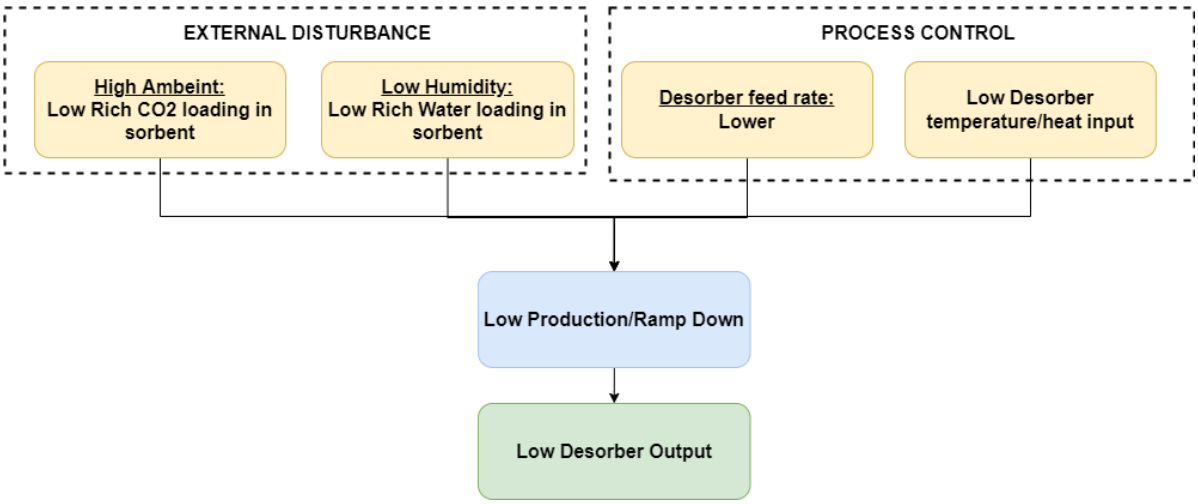

Figure C.8: External disturbance low humidity, high ambient temperature will result in lower rich H_2O and CO_2 loading in the sorbent which will result in lower desorber output. Similarly, lowering sorbent feed to the desorber and/or heat input/desorber temperature will also lower the desorber output.

C.4. Types of Controllers:

Different types of controls are available to maintain process variables at their target set points. Some of the most commonly used controllers are mentioned below [55]:

- **Proportional (P) Control:** It is the simplest form of control where the control action acting on the process/manipulated variable is proportional to the error signal. The major drawback of this type of controller is the its inability to achieve zero steady state error.

- **Proportional and Integral (PI) Control:** In addition to the proportional control, an additional integral control acts on the sum or integration of the error signal and reduces the steady state error. However, PI controllers are prone to induce oscillations in the system response.

- **Proportional, Integral and Derivative (PID) controller:** In addition of proportional and integral control and additional derivative controller is introduced. The derivative control acts on the rate of change of error signal and improves the transient response. PID controller gives the most stable control response, however they are more complicated to calibrate.

C.5. DAC Top Ratio Control:

As mentioned in 1.1, one of the requirements of DAC production is to have H_2O and CO_2 produced in the ratio 3:1. However as shown in Figure[7.1], even $\approx$ 10% change in water loading can result in $\approx$30% change in water production from DAC. Hence it becomes essential to control the top ratio (ratio of H_2O and CO_2) at DAC outlet.

For high water loadings, where top ratio exceeds the target of 3:1, the ratio can be varied by reducing the desorber temperature. This will reduce the vapour pressure of water and ensure that Top ratio of 3:1 is achieved.

For this a control scheme, which alters the reboiler temperature set point based on top ratio at DAC outlet was implemented and validated in the system model developed for this work. Figure[C.9] shows the effect of implementing the control on the DAC outlet for operation at humidity condition of $\approx$ 0.01 kg/m3 absolute humidity at water loading of 47.5mol H_2O/kg TEPA. With top ratio control, the ratio of H_2O and CO_2 at DAC outlet is maintained at $\approx$3, which is the target level.

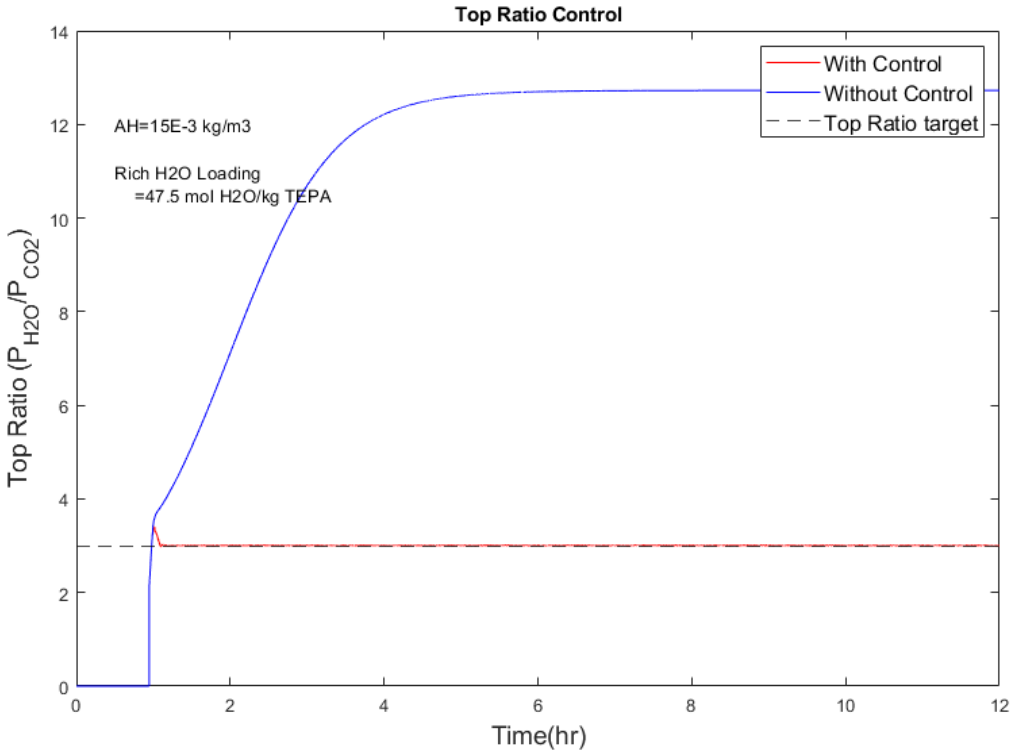

Figure C.9: With Top ratio control implemented, ratio of H_2O and CO_2 at DAC outlet is maintained at $\approx$3

Limitations: The current control has its limitation as well.

- Figure[C.10] shows the impact of top ratio control in humidity condition of 0.02kg/m3 and water loading of 79 mol H_2O/kg TEPA. Although top ratio control improves the outlet top ratio, it is still higher than target value.

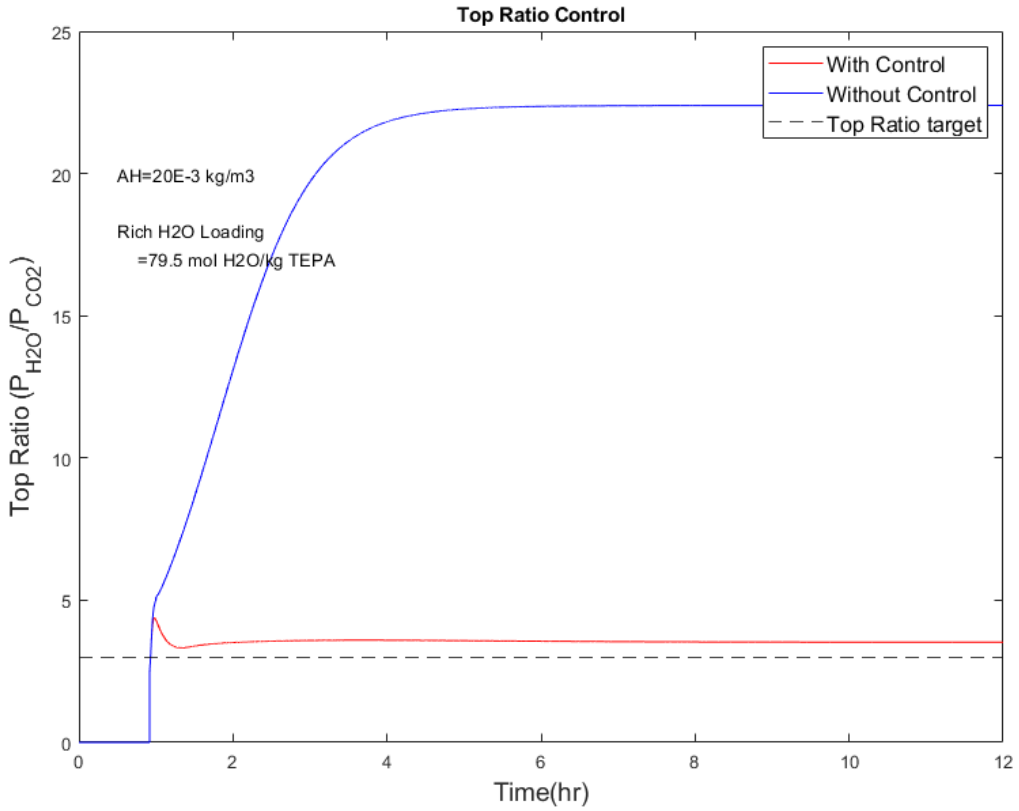

Figure C.10: With Top ratio control implemented, ratio of H_2O and CO_2 at DAC outlet is improved but is still higher than target value

- Figure[C.11] shows the DAC operation under low humidity (≈0.008kg/m3) and low water loading condition (14.56 mol H_2O/kg TEPA). As top ratio is lower than 3, the control scheme is not effective as maximum reboiler temperature set point is 120^{o}C, which is not sufficient to get top ratio of 3:1 at the given loading condition.

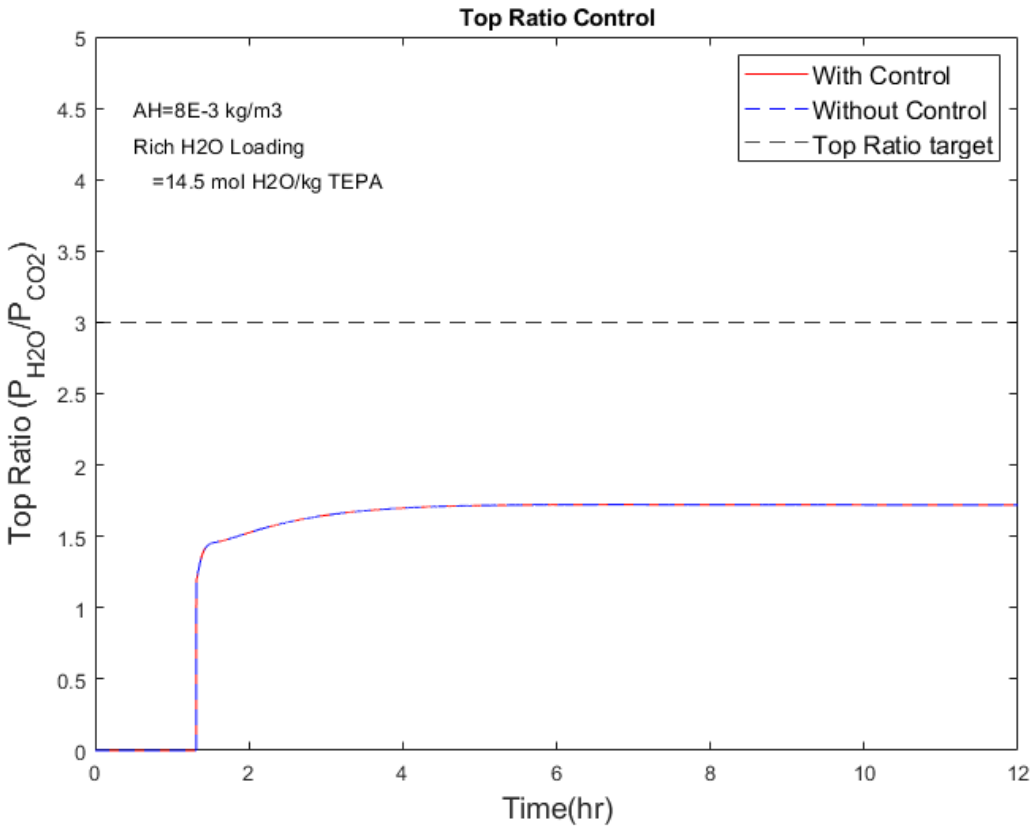

Figure C.11: Even with Top ratio control implemented, ratio of H_2O and CO_2 at DAC outlet is less than target as maximum reboiler temperature set point is 120^{o}C and at this temperature not sufficient H_2O is produced at low H_2O loading in the sorbent (14.56 mol H_2O/kg TEPA)

Delft University of Technology

Z E F

Zero emission fuels

TU Delft